Multi-Method Remote-Sensing Geophysical Investigation of Medieval Stone/Potsherd Pavements at Ita Yemoo, Ile-Ife, Southwestern Nigeria

Gérard Lucien, Francis Chouin, Adisa Ogunfolakan, M. O. Olorunfemi, A. G. Oni

IFE – SUNGBO ARCHAEOLOGICAL PROJECT

MULTI-METHOD REMOTE-SENSING GEOPHYSICAL INVESTIGATION OF MEDIEVAL STONE/POTSHERD PAVEMENTS AT ITA YEMOO, ILE-IFE, SOUTHWESTERN NIGERIA

FINAL REPORT

SUBMITTED BY

GERARD L. CHOUIN
HARRISON RUFFIN TYLER DEPARTMENT OF HISTORY
WILLIAM & MARY
VIRGINIA, USA
and
ADISA OGUNFOLAKAN
MUSEUM OF NATURAL HISTORY
OBAFEMI AWOLOWO UNIVERSITY
ILE-IFE, OSUN STATE
NIGERIA
and
THE ARCHAEOGEOPHYSICS GROUP
DEPARTMENT OF GEOLOGY
OBAFEMI AWOLOWO UNIVERSITY
ILE-IFE, OSUN STATE
NIGERIA

PROJECT TEAM

1. Prof. Gérard L. Chouin: PI
2. Prof. Adisa Ogunfolakan: Co-PI
3. Prof. M.O. Olorunfemi: Consultant Geophysicist (Fieldwork Co-ordinator)
4. Dr. A.G. Oni: Senior Geophysicist
5. Mr. T.K. Fadare (M.Sc.): Geophysicist
6. Mr. Emmanuel Ekpeyong: Trainee Geophysicist (Field Assistant)
7. Mr. Segun Oyetunji: Trainee Geophysicist (Field Assistant)
8. Mr. Temiloluwa Toromade: Field Assistant
9. Mr. Temola Ogundamisi: Field Assistant
10. Mr. Joseph Ayodokun: Finance officer

TABLE OF CONTENTS

LIST OF FIGURES

LIST OF TABLES

LIST OF PLATES

EXECUTIVE SUMMARY

I Project Definition, Objectives and Environment

An integrated geophysical investigation involving the magnetic, electrical resistivity and ground penetrating radar (GPR) methods was carried out within Ita Yemoo archaeological site at Ile-Ife, southwestern Nigeria.[1] This was with a view to assessing the potency of the geophysical methods to individually or collectively identify potsherd/stone pavement and map the spatial distribution of the archaeological feature to guide future excavation and minimize invasiveness. The study area is underlain by pegmatised schist characterised by clay/lateritic clay topsoil overlying a clayey weathered basement.

II. Field Design (Geometrics)

In order to generate potsherd/stone pavement geophysical characteristics (template) and assess the effectiveness of the geophysical methods adopted to map the archaeological feature and define its geometry, a pilot study was carried out over an outcropping potsherd pavement in front of the Heritage Multipurpose Hall and around a recently excavated portion of the main study area southeast of Yemoo Grove. The outcropping pavement was covered with twenty-one (21) main traverses (with inter-traverse spacing of 1 m) trending in approximately NW-SE direction each 10 m long and four (4) orthogonal traverses to the main traverses each 21 m long with inter-traverse separation of 2 m (Fig. 4). The pilot study at the main survey area engaged nineteen (19) approximately NW-SE trending in-line (main) traverses each 14 m long and fifteen (15) cross-line (orthogonal) traverses each 18 m long with inter-traverse and station interval of 1 m (Fig. 6b). The entire of the main survey area was covered with fourteen (14) main traverses trending NW-SE and ranging in length from 20 - 28 m with inter-traverse spacing of 2 m and station interval of 1 m and six (6) orthogonal traverses with lengths varying from 11-26 m and inter-traverse spacings of 4-6 m with station interval of 1 m. With inter –traverse spacing of 1 m for the GPR survey, the main

[1] Funding was provided by a Faculty Grant Fund Award, Faculty of Arts & Sciences, William & Mary, 2022. We thank Neil Norman and Tom Fitton for their methodological advices. We gratefully acknowledge MALA, Umea Sweden, through her Associate Product Manager, Dr. Andreas Viberg (PhD) and the Company's Subsidiary, Guideline Geo, for graciously granting us by the 14th of October, 2022, a free 3-month subscription of MALA Vision and by implication access to Mala Vision GeoGuidline software with upgraded 100 Gb of data storage space for the processing of the 2D configured MALA Ground Explorer (GX) GPR data.

traverses increased to twenty-seven (27) with orthogonal traverses increasing to seventeen (17) with inter-traverse separation of 2 m (Fig. 6a).

III. Methodologies

At both the pilot site and the main survey area, total field magnetic data were acquired along all the traverses - main (in-line) and orthogonal (cross-line) at 1 m station interval and at two sensor heights of 2.32 and 1.42 m. The magnetic data sets were corrected for diurnal variation and offset and the magnetic gradient data generated. The magnetic gradient data were subsequently reduced to the magnetic equator (RTE) to center the anomalies on respective causative targets. The RTE map was downward continued to estimate the depth of archaeological significance. The magnetic data were presented as maps and qualitatively interpreted. The resistivity survey involved 1D and 2D imaging techniques. The 1D Micro Vertical Electrical Sounding (Micro VES) technique adopted the Schlumberger array with half current-current electrode spacing (AB/2) of 0.075 m - 3.0 m and half potential-potential electrode spacing (MN/2) of 0.030 m - 0.25 m. The Micro VES data were presented as VES curves which were quantitatively interpreted and the results presented as geoelectric sections. The 2D imaging, involving the dipole-dipole array, was carried out along main (in-line) and orthogonal (cross-line) traverses with dipole lengths of 0.5 m and 1.0 m and expansion factor (n) varying from 1 to 5. The 2D dipole-dipole data were presented as pseudosections and subsequently inverted into 2D resistivity structures (images) from which true resistivity values were extracted at specific depth range levels for the preparation of resistivity depth slice maps. Apparent resistivity maps were also generated from the raw field data for different expansion factor (n). These maps were interpreted qualitatively for archaeological features. The GPR survey adopted the reflection profiling technique with twin antenna system whose transmitter was operated at 450 MHz and 750 MHz radar frequencies. The GPR data were processed with the MALA Vision GeoGuidline software. The raw data file was imported into the software which in-turn displayed the time-section raw data radargram for each of the profiled lines. Signal enhancing and processing filters including DC offset, De-banding through background (Bg) removal, automatic gain control (AGC) and exponential gain were applied to the raw data. The processed time-section radargrams were analysed for velocity of propagation of the radar wave to facilitate time-depth radargram conversion. By carrying out interpolation of all the processed 2D

radargrams, 3D cube was created from which depth slice maps were generated for spatial delimitation of anomalous radar reflections.

IV. Results and Conclusions

(i) Potency Assessment

The magnetic method revealed that potsherd/stone pavements are weakly magnetic with intensities overlapping significantly with that of the also weakly magnetic basement derived clayey weathered host materials. The results from the present study show that the pavements are majorly associated with classified intermediate (0 to 15 nT/m (pilot site) and 0 to 40 nT/m (main study area)) magnetic intensities. The archaeological feature was also identified within zones with classified low (0 to -28 nT/m (pilot site) and 0 to -318 nT/m (main study area)) and high (15 to 28 nT/m (pilot site) and 40 to 327 (main study area)) magnetic intensities. In essence, pavements are associated with virtually the entire magnetic spectrum. This limitation does not make the magnetic method an index geophysical method in pavement mapping. The method however, has its relevance in the estimation of depth of archaeological significance required in field design.

The 1D Micro VES technique of the electrical resistivity method is effective for the mapping of potsherd pavement only at shallow depth, most especially when it outcrops at the surface or located under very thin soil cover when both the layer resistivities (91-244 ohm-m (pilot site)) and thicknesses (0.03-0.04 m (pilot site)) can be effectively estimated. We found estimates of the layer resistivity values useful in the interpretation of 2D resistivity maps. Due to the very thin thicknesses of the pavements, the delineation of the archaeological feature was virtually impossible at depth due to suppression, as experienced at the main study area. This technique has limited application and only where the feature is near-surface or outcropping. The 2D resistivity data were presented as 2D apparent resistivity maps and 2D resistivity depth slice maps. The former are depth specific 2D resistivity maps generated for specific expansion factor (n) and depth while the latter are maps generated for different depth level ranges of the inverted 2D resistivity structures. At the pilot site, the 2D apparent resistivity maps at expansion factors, n=1-3 (at depth levels of 0.29 m, 0.39 m and 0.49 m) delineate the exposed potsherd pavement within resistivity ranges of 80-185 ohm-m, 115-226 ohm-m and 115-220 ohm-m respectively. The equivalent 2D resistivity depth

slice maps at depth levels of 0-0.25 m and 0.25-0.50 m delineate the exposed potsherd pavement within resistivity ranges of 55-115 ohm-m and 100-200 ohm-m respectively. These resistivity ranges (most especially those established from the apparent resistivity maps) correlate significantly well with the Micro VES derived resistivity range of 91-244 ohm-m for the exposed pavement. The depth specific 2D apparent resistivity maps were more diagnostic in terms of better definition of the geometry of the exposed potsherd pavement. However, the 2D vertical resistivity images (sections) did not resolve the pavement possibly due to the scale of presentation of the images (the potsherd pavement is very thin – 0.03-0.04 m) or outright suppression.

The GPR radargrams map the planar potsherd/stone pavements as high amplitude, bright coloured (yellow/red) radar reflections and significantly continuous and traceable radar signals characteristic of high dielectric contrasting feature. The radargrams also enabled estimation of pavement depths of occurrence and lateral extent. In this regard, the GPR radargrams are superior to 2D resistivity vertical images (sections). The depth specific 2D GPR depth slice maps were also effective in directly mapping the pavements (within the excavated portion of the main survey area) and establishing the spatial distribution within and outside the excavated area. The GPR method however, has the limitation of shallow depth of investigation. Strong GPR signals were rarely recorded at depths greater than 1.0 m except for diffracted signals. Resistivity images were still very diagnostic far beyond this threshold depth for the GPR. For this study though, the effective depth of archaeological relevance is about 1 m.

Based on the results from this study, the GPR method is the most potent geophysical method for pavement mapping at relatively shallow depth (of up to 1.0 m or there about) using radargrams and depth slice maps attributes. The electrical resistivity method is next in potency using 2D dipole-dipole data derived and depth specific 2D apparent resistivity maps as diagnostic attributes. This method has the limitation of suppression of the archaeological feature due to its thin nature and overlapping resistivity values with the host materials. The 1D Micro VES has very limited but useful application in the estimation of pavement resistivities and thicknesses of outcropping pavements. These geoelectrical parameters are needed to constrain the interpretation of both 2D resistivity sections and maps. The magnetic method has the least potency because of the overlapping magnetic effects of the weakly magnetic potsherd/stone pavement and the equally

weakly magnetic weathered basement derived host materials. The method is however useful in the estimation of depth of archaeological relevance which is needed in field design.

With the benefit of the above, we would also observe as follows that:

(i)The planar nature of the potsherd/stone pavement demands depth specific (not depth range) geophysical attributes for its delineation. The mapping of pavements is essentially an interface problem.

(ii)For potsherd/stone pavement to be effectively mapped, some background information on its characteristic features such as thickness, resistivity range, depth(s) of occurrence, the environment of existence and the subsurface stratigraphy are useful for field design and to constrain interpretation of geophysical attributes.

(iii)While this study rates the GPR method highest in potency followed by the resistivity method and the magnetic method as the least potent in potsherd/stone pavement mapping, there is always the need to integrate several relevant geophysical methods if ambiguities associated with individual geophysical method are to be minimized or resolved and the quality of results and subsequent prediction are to be enhanced.

(ii) Archaeology

An archaeological map (Fig. 36) was developed for the study area from stacked composite apparent resistivity and GPR derived archaeological prospect maps. The composite resistivity thematic map was developed from stacked prospect maps at depth levels of 0.59 m, 0.78 m and 0.98 m while the composite GPR thematic map was generated from stacked prospect maps at depth ranges of 0 – 0.25 m, 0.25 – 0.50 m and 0.50 – 0.85 m.

Prospective archaeological zones are associated with the recently excavated Pits 1-3; the cement concrete slab (III); mounds M1 and M2 and adjoining areas from correlated resistivity and GPR thematic maps. Two other prospective archaeological zones A1 and A2 emerged from correlated coincident resistivity and magnetic thematic maps while zone A3 was developed from correlated resistivity, magnetic and GPR (3D) thematic maps.

The most prominent archaeological zone is associated with the excavated Pits 1-3 with potsherd/stone pavements as the archaeological feature (see Figs. 22a-h). The pavements occur at

varying depths from 0 m (ground level) to up to 0.85 m. The presently barren segments of Pit 1 and Pit 2 and Pit 3 with trace of pavement are prospective at deep depths of 0.25 – 0.85 m while the stone pavement extends westward from Pits 1/2.

The prospective zone associated with cement concrete slab (III) displays GPR radargrams with high amplitude radar reflections (see Fig. 22d) typical of pavements. This zone is suspected to host pavements.

The prospective archaeological zones associated with mounds M1 and M2 with its southeastern extension display hyperbolic diffracted radar reflections which are sometimes chaotic (see Figs. 22e; 23a&b). These characteristics are not typical of potsherd/stone pavements but typical of buried archaeological features such as ritual pots, pieces of potsherds, ancient vessels etc. The mounds display relatively high resistivity with coincident negative polarity magnetic intensity which are characteristics of the aforementioned archaeological features.

We are not sure if the referenced mounds are natural or whether they are dumped soil materials excavated from the Yemoo Grove potsherd pavement or excavated soil materials from the old Pit 4. However, the archaeology map (Fig. 36) shows that archaeological features beneath and around the mounds could extend from 0.25 m to about 0.85 m depth level.

Prospective archaeological zones A1 and A2 display no GPR characteristics but show coincident intermediate resistivity and negative polarity magnetic intensity typical of pottery related archaeological features. Zone A3 has correlated resistivity, magnetic and GPR attributes which could be indicative of pavement or pottery related artefacts. The depth of archaeological relevance could vary from 0.25 – 0.85 m.

The summary of the archaeology of the study area is contained in the table below.

S/N	Prospective Zone	Geophysical Attributes	Suspected Archaeological Artefacts	Depth of Archaeol. Relevance
1	Premises of Excavated Pits 1-3	Intermediate resistivity (120-350 ohm-m) and high amplitude radar reflections.	Potsherd/Stone Pavement	0.0-0.85 m

2	Cement Concrete Slab (III)	High amplitude radar reflections	Pavement	0.25-0.85 m
3	Mounds M1 and M2	Hyperbolic diffracted radar reflections, sometime chaotic; intermediate resistivity and negative polarity magnetic intensity	Pottery related archaeological features	0.25-0.85 m
4	Zones A1 and A2	Intermediate resistivity and negative polarity magnetic intensity	Pottery related archaeological features	0.25-0.85 m
5	Zone A3	Intermediate resistivity, high amplitude radar reflections and negative polarity magnetic intensity.	Pavement/pottery related archaeological features	0.25-0.85 m

The reference co-ordinate for this study site is 0673123, 0828699 (UTM Minna Zone 31 Datum) defining the point of intersection of Traverse TR 6a and TR 19.

1.0 INTRODUCTION

1.1 Preamble

Ita Yemoo, Ile-Ife, southwestern Nigeria (Fig. 1), is a renown archaeological site under the National Commission for Museum and Monuments (NCMM) of the Federal Ministry of Culture and Tourism. The earliest recorded archaeological excavation work at this site was carried out by Frank Willett in 1957 and between 1962 and 1963. This was followed by another excavation by M.O. Adesina in 2008. These excavations led to the recovery of several artefacts including a complete bronze figure of an Ooni, fine terracotta heads with elaborate head dresses, ancient vessels and several pieces of potsherds (Willett, 1959). One of the potsherd pavements housed by Yemoo Grove shed was dated between 13th and 15th centuries. Between 2015 and 2017, the Ife-Sungbo Archaeological Project directed by Chouin and Ogunfolakan with their team of archaeologists and geophysicists carried out further archaeological excavation at Ita Yemoo with focus on a segment of an ancient embankment system (trench) of the old city of Ile-Ife. This led to the development of a complete stratigraphic profile of the embankment and the identification of another small potsherd pavement suspected to be a continuation of an earlier discovery by Willett. During the referenced project, several fragments of exposed potsherd pavements were identified within the premises of Ita Yemoo and most prominently at the frontage of the Heritage Multipurpose Hall (Fig.1). According to Willett (2004), fragments of potsherd pavement were found within a radius of 6 km from the city center of Ile-Ife. Apart from Ile-Ife, potsherd pavements have been identified in several other towns in the southwestern Nigeria including Imesi-Ile (Siyanbola, 1988), Ila – Orangun (Ogunfolakan, 1994), Itagunmodi (Agbaje-William, 1995), Ilare-Ijesa (Ogundiran, 2000), Ope-Odu, Ibadan (Orijemie and Ogiogwa, 2016) and other localities along the trade and migration route of the Yorubas of southwestern Nigeria up to the Republic of Benin (Ige *et al.,* 2009)

Aguigah (1995) opined that potsherd pavements are expressions of the ways urban spaces were organized and built in Yorubaland. The submission of Chouin and Ogunfolakan (2015) that the existence and locations of potsherd pavements should be documented is therefore understandable judging from the point of view of their fast disappearance from the urban landscape and the fact that they could become effective chronological indicators of urbanization in Yorubaland and in the West African sub region.

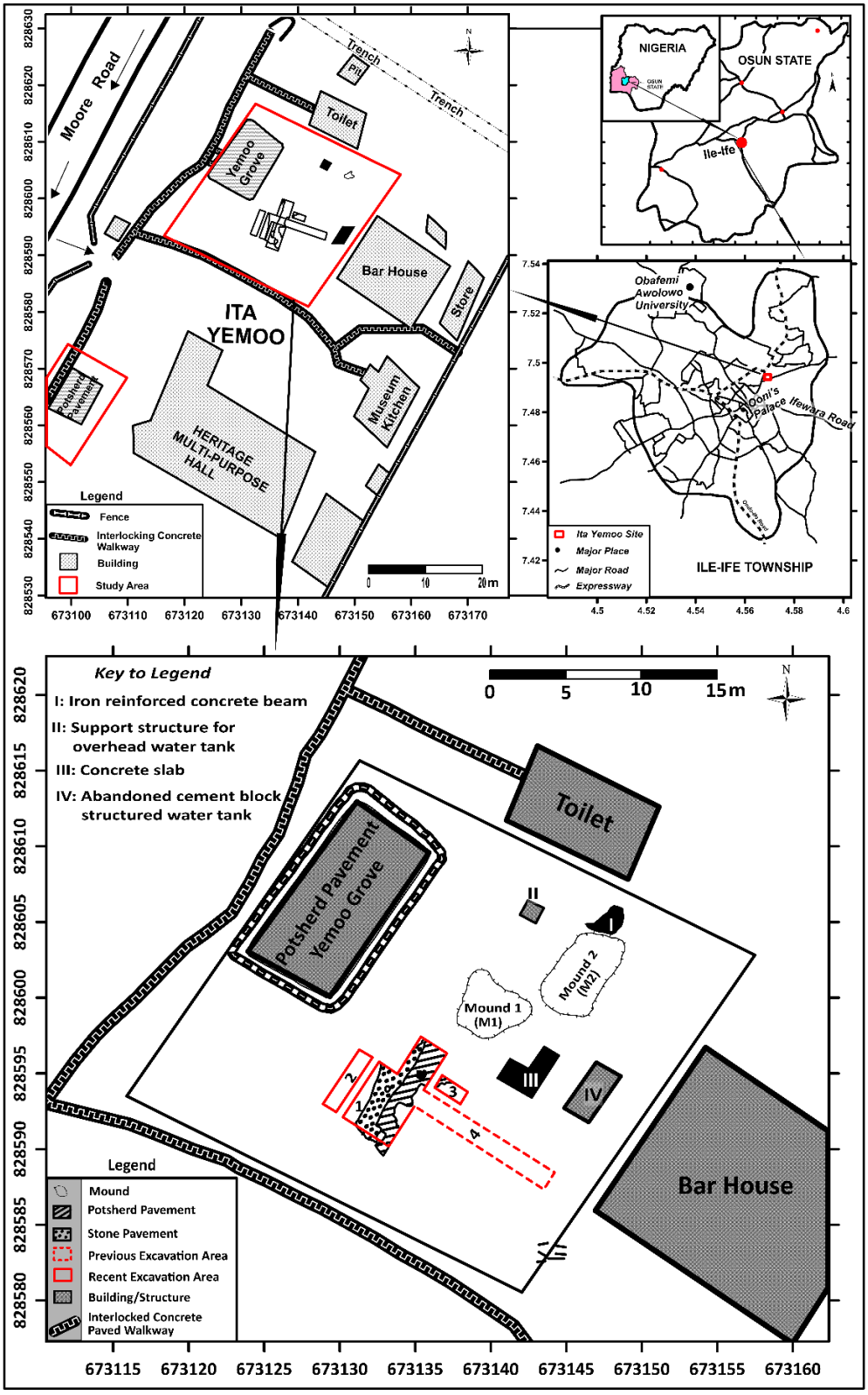

Fig. 1a: Location map showing the Ita Yemoo archaeological site (Inset: map of Nigeria, Osun State, Ile-Ife township and main survey site)

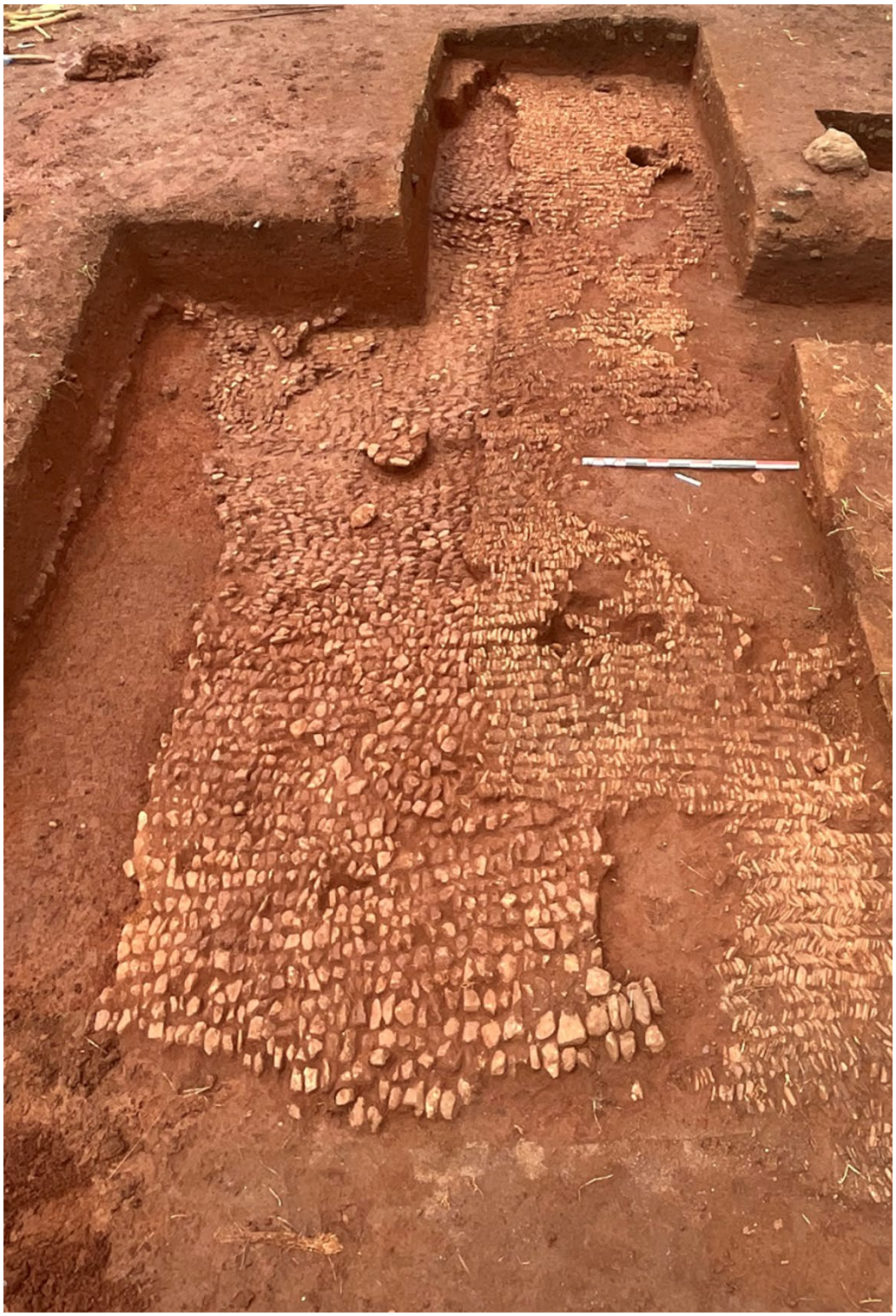

Fig. 1b: Portion of pavement excavated at Ita Yemoo during the 2022 Season of the Ife Sungbo Archaeological project (Photograph: Gérard L. Chouin, Ife Sungbo Archaeological Project 2022).

Potsherd pavements are associated with walkways (roads) (Ogundiran, 2000; Adeyemo *et al.,* 2021); ritual storage (sometimes containing ritual pot at its center) (Ogunfolakan, 1994; Ogundiran, 2000; Ige *et al.,* 2009; Orijemie and Ogiogwa, 2016 and Adeyemo *et al.,* 2021); element of cultural, tourist (Adeyemo *et al.,* 2021) and historical value (can be used to classify Ife history into pre-pavement (pre 12^{th} century), pavement (12^{th} – 16^{th} century) and post-pavement (post 16^{th} century) phases) (Eyo, 1974; Ogundiran, 2000 and Adeyemo *et al.,* 2021).

The 2022 Ife-Sungbo archaeological excavation project at Ita Yemoo, Ile-Ife (Fig. 1) was focused on generating more information on the stratigraphy, topography and the chronology of the Ita Yemoo potsherd pavement. Roth *et al*. (2021) inferred, from existing Willett documentation, two stratigraphic units of potsherd pavements. The first is exposed (outcropping) or situated near-surface with overlying thin humus-like soil while the second is located at relatively deep depth below the ground level and covered by clayey and reddish-brown lateritic soil. The second pavement is stratigraphically older in age which implies that such pavements have chronological implication. The recent (2022) excavation may have confirmed the above inference from the old Willett records. Apart from this, it was also discovered that a stone pavement exists, at this excavation site, side by side with a potsherd pavement (Pit 1) (Fig. 1) with depths to the pavements ranging from near zero to close to 1 m. Some of the pits excavated have little (Pit 3) or no find (Pit 2) which implies that the pavements are spatially limited in distribution.

The need to establish the spatial distribution of both the potsherd and the stone pavement informed the request by the project for a multi-method geophysical investigation of a portion of Ita Yemoo (south/southeast of Yemoo Grove shed) that covers the current excavation site (Fig.1a and 1b)

1.2 Characteristics of Stone/Potsherd Pavements

Stone/Potsherd pavements are beautifully patterned (herringbone for Ife potsherd pavements) potsherds (ceramic) or stone materials the technology of which was linked to Queen Lunwo, the first female Ooni of Ife (Adeyemo *et al.,* 2021). This may have led to the insinuation that the technology of production of potsherd pavements could have been transferred through migrants from Ile-Ife (Ige *et al.,* 2009). Researches into the physical and chemical characteristics of the pavements are very limited so also the relevant literature. Microscopic analysis carried out by Ige *et al*. (2009) showed that potsherd pavements are composed of quartz, micas, plagioclase, tourmaline, amphibole and ferruginous grains typical of granitic basement derived regolith

(weathered basement). The sample sites were located within the basement complex underlain southwestern Nigeria. Orijemie and Ogiogwa (2016) also observed that pottery samples from Ope-Odu, Ibadan contain kaolinite, quartz, feldspar, mica and some heavy minerals. The stone pavement is composed of dioxide of silicon (silica or quartz).

Chouin and Ogunfolakan (2015) established that potsherd pavements are hard, compact and resistant to erosion. The hard and compact nature must have derived from firing (baking) when soil mixed with palm-oil were combusted on the well prepared pavements (Ige *et al*., 2009). Because baked potsherd pavements are compact and the porosity and moisture contents are low, the layer resistivity values are expected to be relatively high as illustrated in Achie (1942) equation.

$$\rho = a\phi^{-m}\rho_w S_w^{-n}$$

where ρ = formation resistivity, ϕ = porosity, ρ_w = resistivity of formation water, S_w = water saturation and a (proportionality constant), m (cementation factor) and n (saturation exponent) are empirical constants.

Quartz composed stone pavements with very low porosity (less than that of potsherd) should also display high resistivity or low conductivity values. This makes both stone and potsherd pavements amenable to delineation using the electrical resistivity and electromagnetic (including ground penetrating radar, GPR) methods, all other factors being equal.

Quartz has an average magnetic susceptibility of -0.01 x 10^{-3} (SI) which makes it diamagnetic (Telford *et al.,*1991). Stone pavement made up of assemblages of quartz is therefore not expected to display significant anomalous magnetic response. However, during the cooling process of the baked pavements, the potsherds might have acquired thermo-remanent magnetization in the presence of the existing earth's field with enhanced magnetic susceptibility. The baking process also enhances electric resistivity (decreases conductivity) by reducing the moisture content. These effects make fired clay furnaces, pottery kilns and potsherd pavements amenable to magnetic survey delineation (Leute, 1987; Powell *et al.,* 2002; Fagan and Durrani, 2004; Olorunfemi *et al.,* 2019; Oni *et al*., 2022 and Olorunfemi *et al.,* 2022). The above informed the adoption of the magnetic, resistivity and ground penetrating radar (GPR) geophysical methods in the present study.

1.3. Statement of Problem and Objectives

Recent archaeological excavation at Ita Yemoo, Ile-Ife, archaeological site identified contiguous stone and potsherd pavements in one of the pits (Pit 1), a minor find in another (Pit 3) and barrenness in the third (Pit 2) (Fig. 1). This implies that the archaeological features are spatially limited. There is the need therefore, to establish the spatial distribution of the features so as to guide future excavation and minimise invasiveness. The study is also required to assess the potency of the three adopted geophysical methods (magnetic, electrical resistivity and ground penetrating radar) to individually or collectively identify potsherd and stone pavements within the survey area.

1.4 Description of the Project Environment

1.4.1 Geographic Location

The Ita Yemoo archaeological site is located in the ancient city of Ile-Ife in Ife East Local Government Area (LGA) of Osun State, southwestern Nigeria (Fig. 1). The survey area is situated within Universal Traverse Mercator (UTM) geographic coordinates of Northings 828530 – 828630 mN and Eastings 673090 – 673170 mE, Zone 31 Minna Datum (Fig. 1).

1.4.2 Relief, Climate and Vegetation

Ita Yemoo archaeological site is located on a relatively flat topography with elevations ranging from 268 – 271 m asl and a relief of about 3 m (Fig. 2). The climate is the tropical rainforest type characterised by short dry season (November-March) and a long wet season (April-October) with mean annual rainfall ranging between 1000 and 2000 mm (Iloeje, 1981). The annual mean temperature is between 24^{o}C and 27^{o}C. The high rainfall and the relatively high temperature regimes promote rock weathering and laterisation of the weathered column. Although the site is located within a developed area, relics of the tropical forest in tap rooted trees and bananas are evident along an ancient trench.

1.4.3 Local Geology

The Ife-Ilesha area, in southwest Nigeria, is located within the Ilesha Schist Belt that is composed of amphibolite schists, politic schists, granite, gneiss, pegmatite, quartz schist,

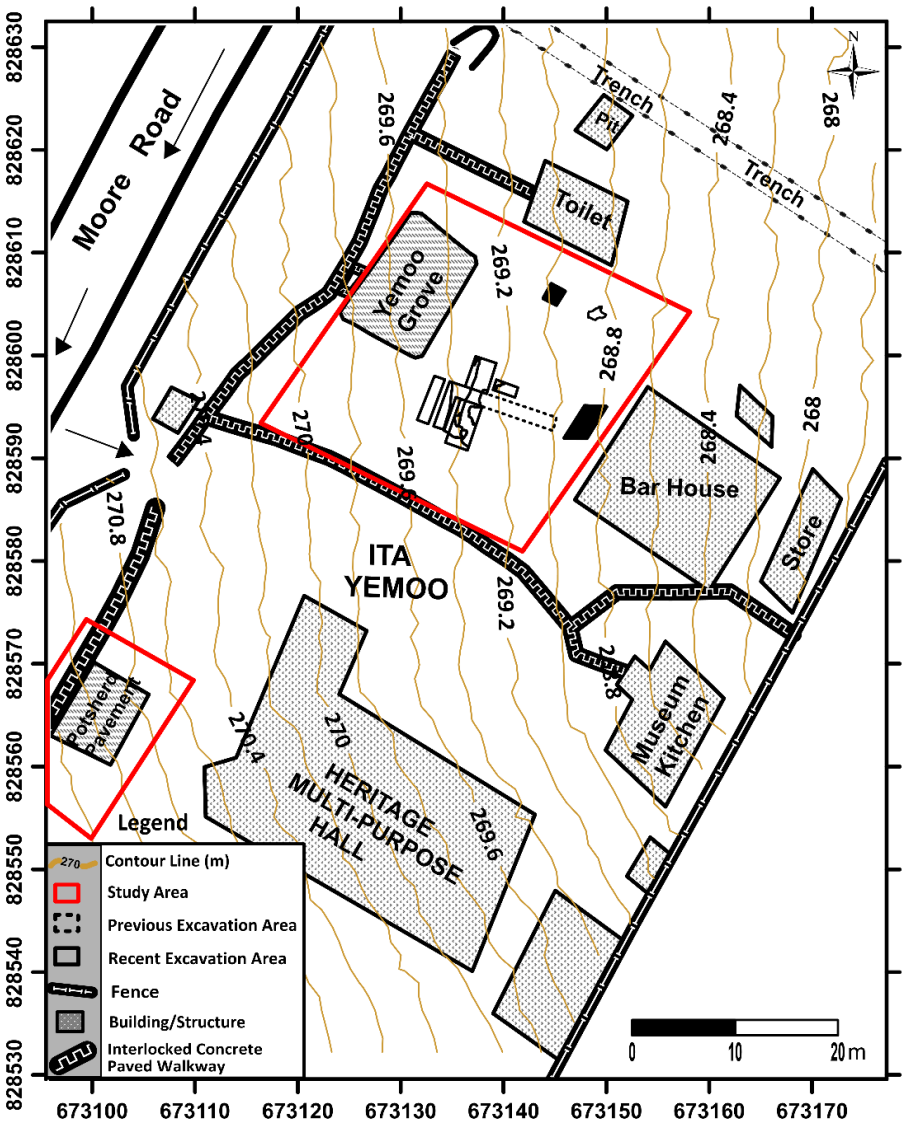

Fig. 2: Topographical map of Ita Yemoo site

quartzo-feldspathic gneiss and quartzites (Turner, 1989). The area around Ile-Ife is underlain by granite gneiss, pegmatised schist, migmatite, quartzite and intrusive pegmatite (Fig. 3). The Ita Yemoo study area is underlain by pegmatised schist. The schist is characterised by clay/lateritic clay topsoil overlying a clayey weathered basement rock. The basement rock is concealed within the study area by a variably thick overburden.

1.5 Project Assumptions

The field design of this project was based on the following assumptions that

(i) a potsherd/stone pavement is an approximation of a planar 2D feature with significant lateral extents (in the x and y directions) but limited in the depth (thickness) extent (in the z direction). Field check and a pilot study actually showed thicknesses of pavements in the range of 3 - 4 cm (0.03 – 0.04 m) and outcropping areal extent of maximum of 5 x 2.5 m;

(ii) arising from (i), the archaeological feature can be treated as a stratigraphic unit;

(iii) both stone and potsherd pavements are of relatively high resistivity and high magnetic susceptibility (for potsherd) with respect to the host layers;

(iv) the resistivity (or conductivity) and magnetic susceptibility contrasts are significant enough to give discernable geophysical (resistivity, magnetic and GPR) anomalies;

(v) the planar nature of the pavements will require a field design involving 1D, 2D/3D data gathering. We are however, not oblivious of the problem of suppression of a thin layer that is overlain by a significantly thick overburden. The 2D/3D data gathering will enable data presentation in 2D plan and 3D volume, if necessary;

(vi) even with the 2D/3D imaging, we also are not oblivious of the suppression phenomenon;

(vii) the anomalies of the pavements are not subsumed within or overlap significantly with that of the geologic environment and or urban interferences (noise);

(viii) the pavements occur at relatively shallow depth of not more than 1 – 1.5 m below the ground level. There are field evidences of depths of between 0.4 and 1.0 m aside from the outcropping or near-surface upper pavement; and

(ix) there may be prospects for the identification of other archaeological features that our field design should accommodate and resolve.

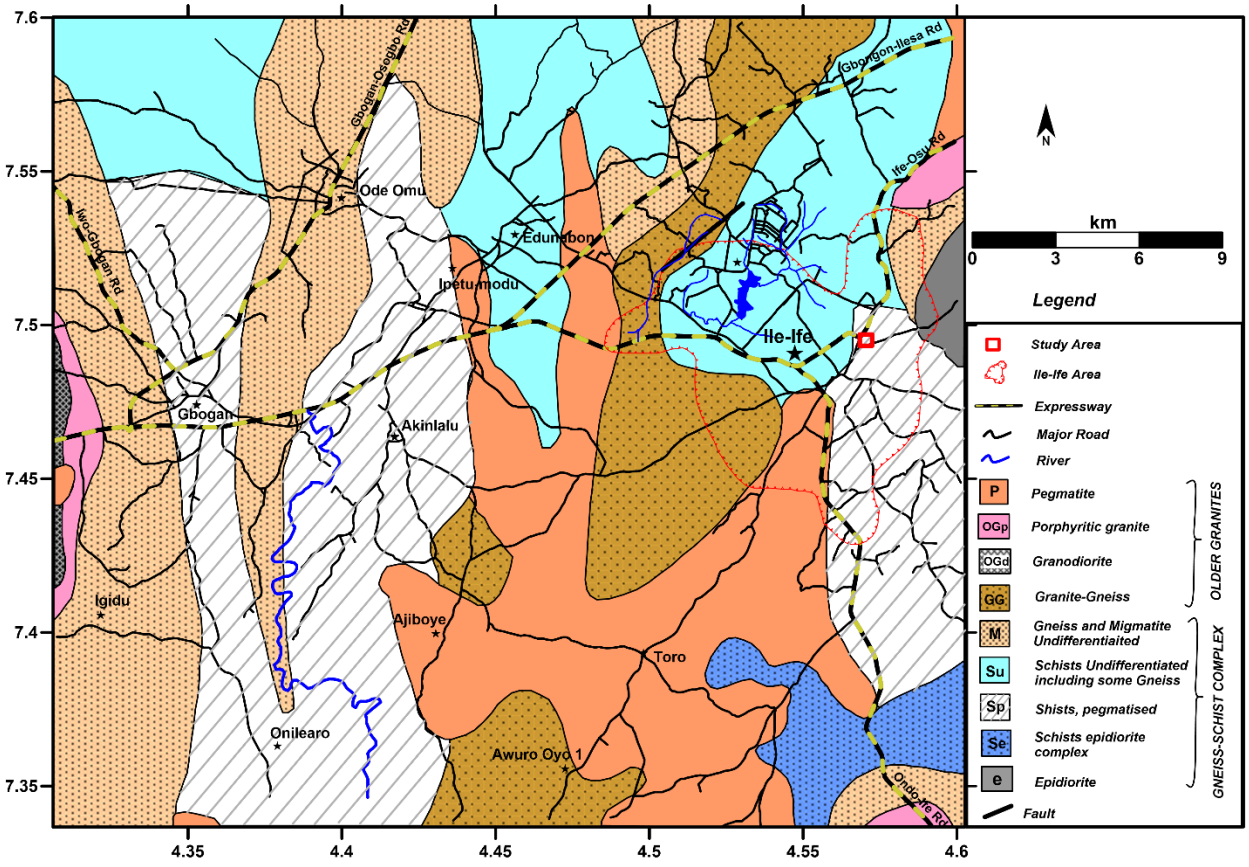

Fig. 3: Geological map of the area around Ile-Ife (Courtesy of Directorate of Oversea Surveys, the British Government's Ministry of Oversea Development, 1966)

2.0 FIELD DESIGN AND METHODOLOGY

The field work was carried out between 9th – 16th and 21st – 28th August, 2022.

2.1 Field Design

The field work was executed in two phases. The first phase involved a pilot study of two geophysical methods (magnetic and electrical resistivity) and several techniques on a concrete block enclosed outcropping potsherd pavement in front of the Heritage Multipurpose Hall within Ita Yemoo (Fig. 1). This was with a view to generating the pavement geophysical characteristics and assess the effectiveness of the methods to map the pavement and possibly define its geometry. It was also with an intent to develop a template that will assist the interpretation of similarly generated anomalies within the main study area, where the archaeological feature is concealed. The results from the pilot study served as control for the main study area.

The second phase involved the adoption of the above mentioned geophysical methods and the Ground Penetrating Radar (GPR) method at the main study area. The GPR was not engaged in the pilot study because the equipment was not available when the study was carried out.

2.2 Pilot Study

2.2.1 Geometrics

Where the pavement outcrops, we dug through at three of its edges to determine the thicknesses which we measured as 3.5 – 4.0 cm (0.035 – 0.04 m). The areal extent of the outcrop is about 5 x 2.5 m. The pavement is elongated in an approximately NE – SW direction. For the magnetic survey, twenty-one (21) (main) traverses (TR 1 – 21) trending approximately NW – SE direction were established each 10 m long with traverse – traverse and station interval of 1 m. In addition, four (4) orthogonal traverses (TR 22 – 25) to the main traverses each 21 m long, were established with inter-traverse separation of 2 m in an approximately NE - SW direction. A station interval of 1 m was adopted. For the resistivity survey, the coverage was reduced to 7 x 13 m (from 10 x 21 m) which necessitated four (4) main traverses (TR 4, 9, 11 and 17) at 2 – 6 m interval and four (4) orthogonal traverses (TR 22, 23, 23.5 and 24.5) at 1 – 2 m interval. A station interval of 0.5 m was adopted. However, one of the orthogonal traverses (TR 23) was additionally traversed at a station interval of 1.0 m (Fig. 4) for comparison and assessment of target resolution.

One of our research assumptions was that the investigated pavement can be treated as a stratigraphic layer. This planar structure favours the adoption of Vertical Electrical Sounding

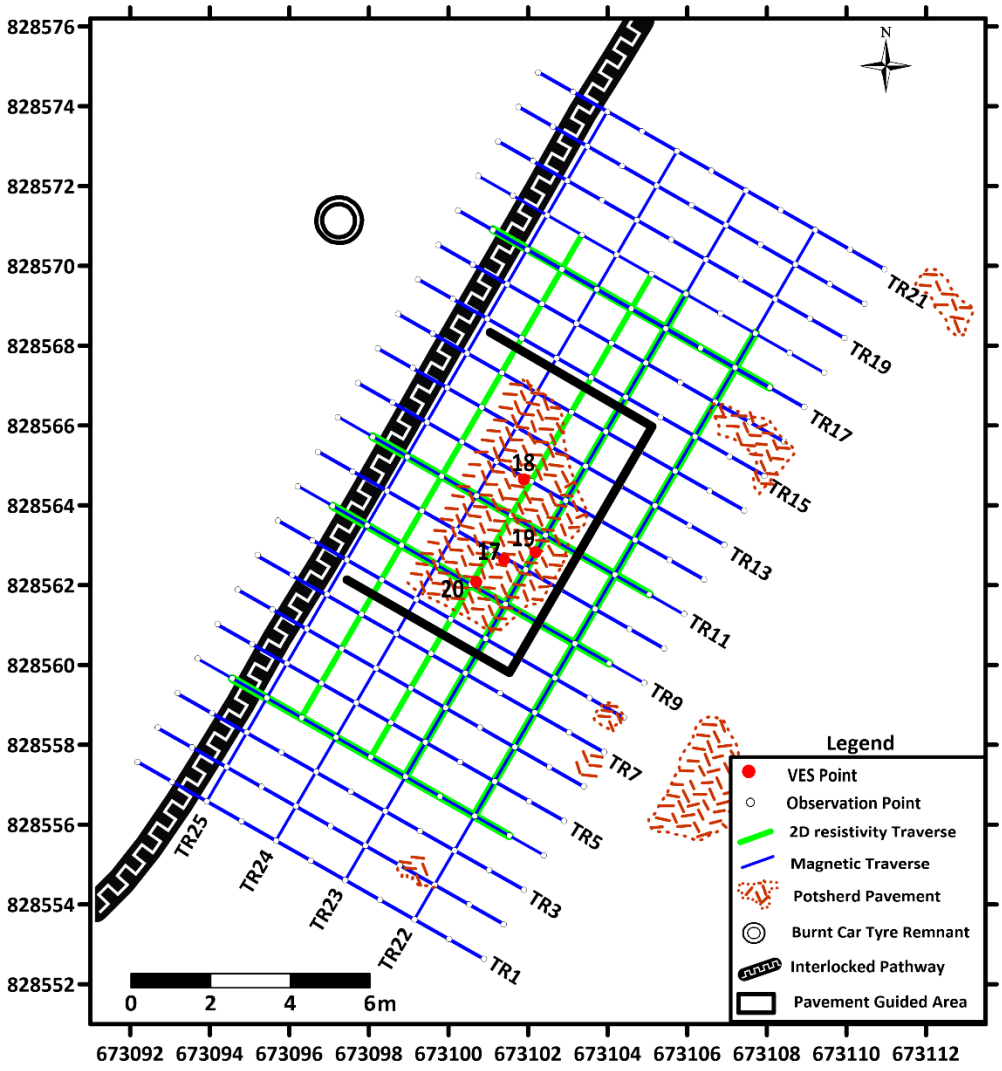

Fig. 4: Data acquisition map over the outcropped potsherd pavement at the pilot site

(VES) 1D technique. The very thin nature of the pavement (0.035 – 0.04 m thick) necessitated a micro VES design adopting a Schlumberger array with half current – current electrode (AB/2) separation varying from 0.075 - 3.0 m and half potential – potential electrode (MN/2) separation of 0.03 – 0.25 m

2.2.2 Methodology

2.2.2.1 Magnetic Survey

The magnetic survey involved profiling. Data were acquired with a Proton Precession Magnetometer (GEM 19T) that measured the earth's total magnetic field intensity. The data acquisition followed the standard procedures and measurements were made at two sensor heights of 2.32 m and 1.42 m. Two magnetic measurements were made at 1 m station interval along all the traverses (main and orthogonal) and the time of measurement recorded. A base station was established in a magnetically quite location within the premises of the pilot study site where four (4) sets of measurements were made before and at the close of each traverse line. This was to enable the monitoring of the diurnal variation of the earth's magnetic field and also allowed the correction of each set of the field data for diurnal variation and offset. The corrected magnetic field data at the upper sensor height were subtracted from the corrected magnetic field data at lower sensor height and the difference divided by the sensor height difference (of 0.90 m) to obtain the magnetic gradient. Magnetic gradient data have the advantage of better resolution of small near-surface features (Liritzis *et al.,* 2020) and attenuation of cultural noise. The current survey site is within a developed area with several sources of cultural noise. It also adjoins a highly trafficked Moore Road.

The magnetic gradient data were subsequently reduced to the magnetic equator (RTE) to center the anomalies on respective causative targets. The RTE map was downward continued to estimate the depth of significance of the near-surface targets. The magnetic data were finally presented as maps.

2.2.2.2 Resistivity Survey

In the resistivity survey, the ground resistance was measured by injecting a DC or low frequency AC current into the ground through two current electrodes while the resulting potential was measured across another pair of potential electrodes that were located within (for Schlumberger array) or outside (for dipole-dipole array) the current electrode pair. The apparent resistivity (ρ_a)

was computed from the product of the resistance and the geometric factor of the electrode array. The ground resistance data were acquired with the PASI (16gl) Digital Resistivity Meter. This study involved 2D imaging with the dipole-dipole array (Fig. 5b) and 1D Vertical Electrical Sounding (VES) with the Schlumberger array (Fig. 5a). 2D dipole-dipole profiling was carried out along the main and orthogonal traverses at station interval of 0.50 m (the dipole length) with an expansion factor, n, varying from n = 1 to 5. However, one of the orthogonal traverses (TR 23) was reoccupied at station interval of 1.0 m for comparison and assessment of quality of resolution.

The apparent resistivity (ρ_a) data were computed from the equation:

$$\rho_a = \pi \text{Ra } n(n+1)(n+2)$$

where R is the measured resistance

a is the dipole length

n is the expansion factor (1 – 5)

and π is a constant (3.142).

The theoretical depth of investigation (D) of this array is given by the equation:

D = 0.195 AN (Roy and Apparao, 1971)

where AN is the total length of the array

For a = 0.5 m and n varying from 1 – 5, the theoretical depth of investigation for the pilot study became 0.29, 0.39, 0.49, 0.59 and 0.68 m for the different values of n; and 0.59, 0.78, 0.98, 1.17 and 1.37 m for a dipole length of 1 m.

The dipole-dipole data were presented as pseudosections and inverted into 2D resistivity structures (images) from which true resistivity values were extracted at specific depth levels for the preparation of resistivity depth slice maps. Apparent resistivity maps were also generated from the raw field dipole-dipole data for different expansion factor (n). These maps were correlated with the known images of the outcropping pavements for the assessment of the potency of the maps in effectively mapping the pavement and defining the geometry.

1D Micro Vertical Electrical Resistivity Sounding (VES) was carried out by gradually expanding the electrode spacing about the center of the array. The Schlumberger array (Fig. 5a) was adopted with half current-current electrode spacing (AB/2) varying from 0.075 m to 3.0 m and half

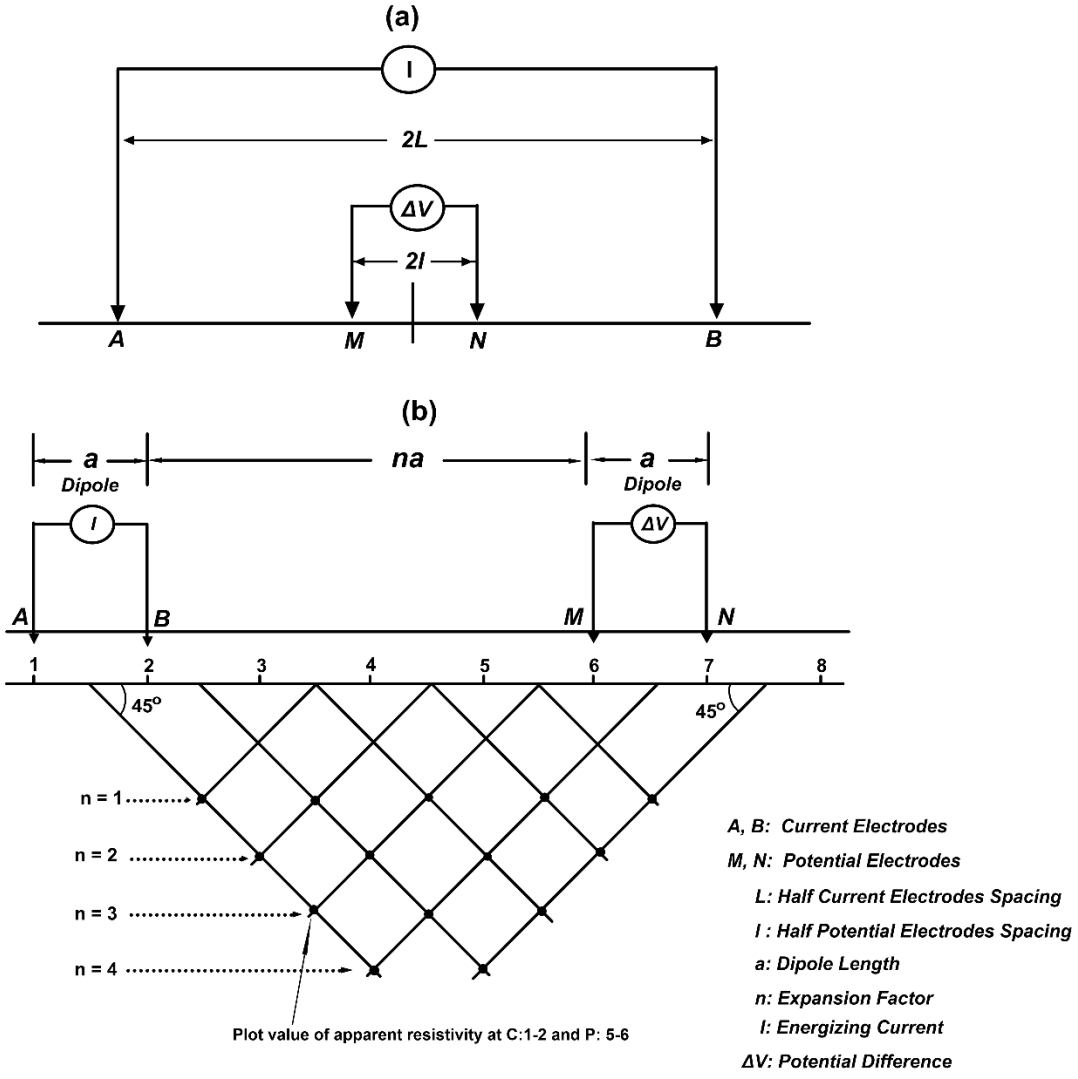

Fig. 5: Electrode arrays (a) Schlumberger and (b) Dipole-Dipole

potential-potential electrode spacing (MN/2) ranging from 0.030 m to 0.25 m. This micro VES enabled the mapping of the pavement as a geoelectric layer.

The apparent resistivity (ρ_a) equation is defined as:

$$\rho_a = \frac{\pi R L^2}{2l}$$

where R is the measured ground resistance

L is half the current - current electrode spacing

l is half the potential – potential electrode spacing

and π is a constant (3.142)

The theoretical depth of investigation (D) of this array is given by the equation

D = 0.125 AB (Roy and Apparao, 1971)

where AB is the current-current electrode spacing

For this field design (with maximum AB of 6.0 m), the theoretical depth of investigation is 0.75 m. The effective depth could be greater if the subsoil is resistive as observed in this study. The micro VES data were presented as VES curves. Four (4) micro VES stations (VES 17-20) were occupied.

2.3 Main Survey Area

2.3.1 Geomatics

For the magnetic and resistivity surveys at the main survey area (premises of Yemoo Grove) (Fig. 6a), fourteen (14) main traverses (TR 1 – 14) trending approximately NW – SE and ranging in length from 20 - 28 m, with inter-traverse spacing of 2 m and station interval of 1 m were established. In addition, six (6) orthogonal traverses (TR 15 – 20) with lengths ranging from 11 to 26 m and traverse – traverse intervals of 4 – 6 m and station interval of 1 m were also established in an approximately NE – SW direction. Additional orthogonal traverse (TR 17b) was established later to cross-check a suspected geophysical anomaly. In essence, twenty-one traverses were established at this site (Fig. 6a).

For the ground penetrating radar (GPR) survey, a much denser coverage was adopted. The inter-traverse separation of the earlier main traverses was reduced to 1 m thereby doubling the number to twenty- seven (27) while still maintaining the traverse coding with the intermediate traverses carrying subset codes such as TR1b, TR7b, TR7c etc. The orthogonal lines were established at a

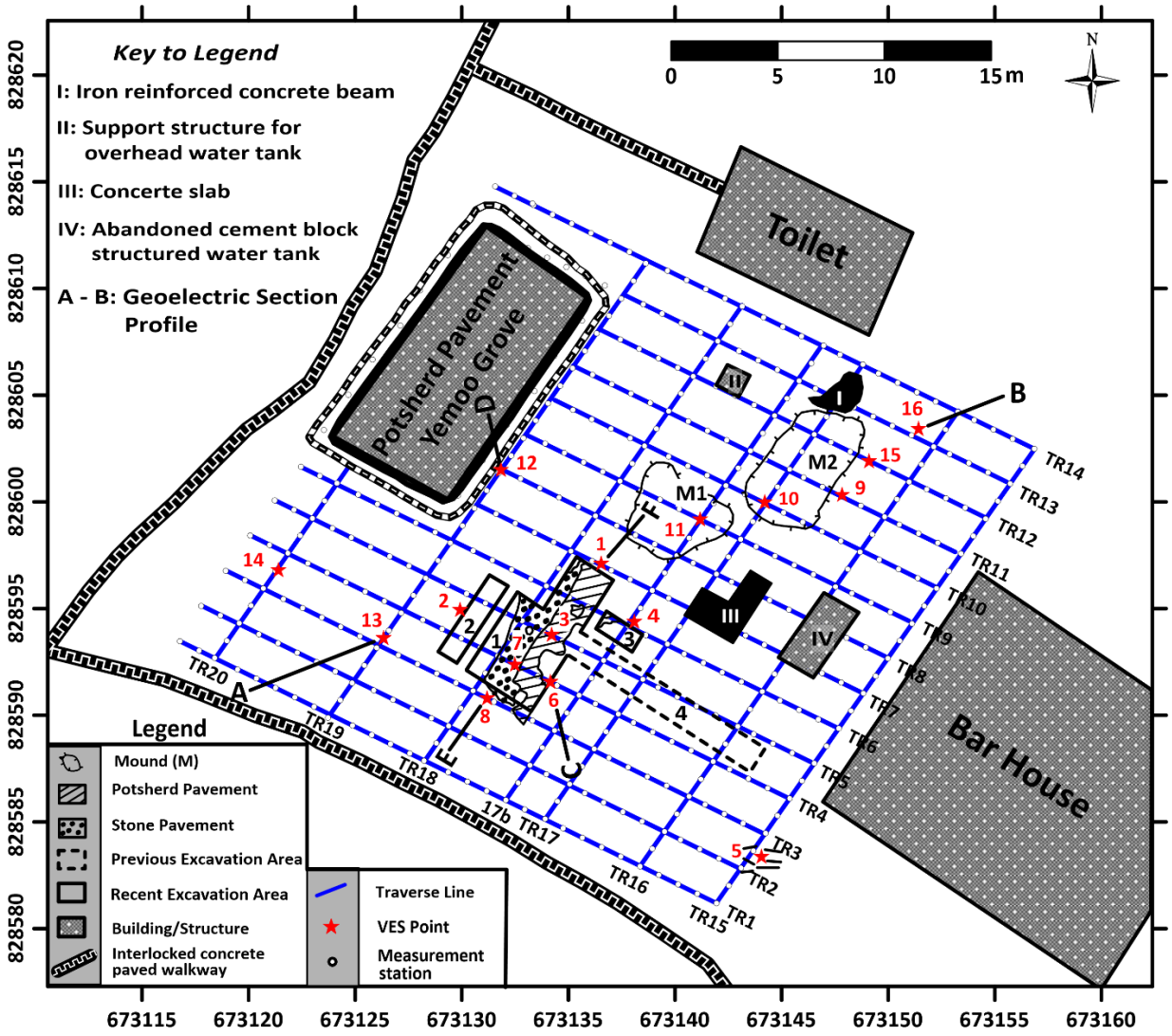

Fig. 6a: Data acquisition map for magnetic and resistivity surveys at the main survey area

regular interval of 2 m while retaining the initial traverse coding but numbering the newly established relative to the earlier ones (see Fig. 6b). There were seventeen (17) orthogonal traverses established. The above described field layout was for a 2D coverage at 1x2 m grid network. We executed a 3D denser coverage with 1x1 m grid network to cover the excavated site and two suspected mounds. This 14 x 18 m block was covered with nineteen (19) main and fifteen (15) orthogonal traverses (Fig. 6b).

2.3.2 Methodology

2.3.2.1 Magnetic Survey

The field procedures are exactly as reported in section 2.2.2.1. The magnetic profiling was also done at 1 m station interval.

2.3.2.2 Resistivity Survey

The field procedures are essentially as reported in section 2.2.2.2 except that the 2D imaging was carried out with a station interval (dipole length) of 1 m while repeat coverage was carried out with a station interval of 0.5 m along traverses TR7 and TR10 for comparison and quality check.

The sixteen (16) micro soundings carried out within this site were located within and around the recently excavated pits, suspected mounds (Figs. 1&6) and to check specific geophysical anomalous zones.

2.3.2.3 Ground Penetrating Radar Survey

The ground penetrating radar (GPR) images the subsurface at high resolution using short electromagnetic radar pulse in the frequency band of 10 – 3000 MHz from a transmitting (Tx) antenna. Part of the radar pulse is reflected by an interface with contrast in dielectric or conductivity properties and recorded by a receiving (Rx) antenna.

In the present study, the roll/push along MALA Ground Explorer (GX) GPR equipment was adopted. The twin antenna system was operated at 450 and 750 MHz frequencies with an estimated 5.0 and 2.7 m depth of investigation for the 2D data coverage and 450 MHz frequency with about 5.0 m depth of exploration for the 3D data coverage. The reflection profiling technique (with fixed $T_x - R_x$ spacing) was adopted. The returned radar signals were amplified, digitized, recorded and displayed on the recorded screen as a radargram.

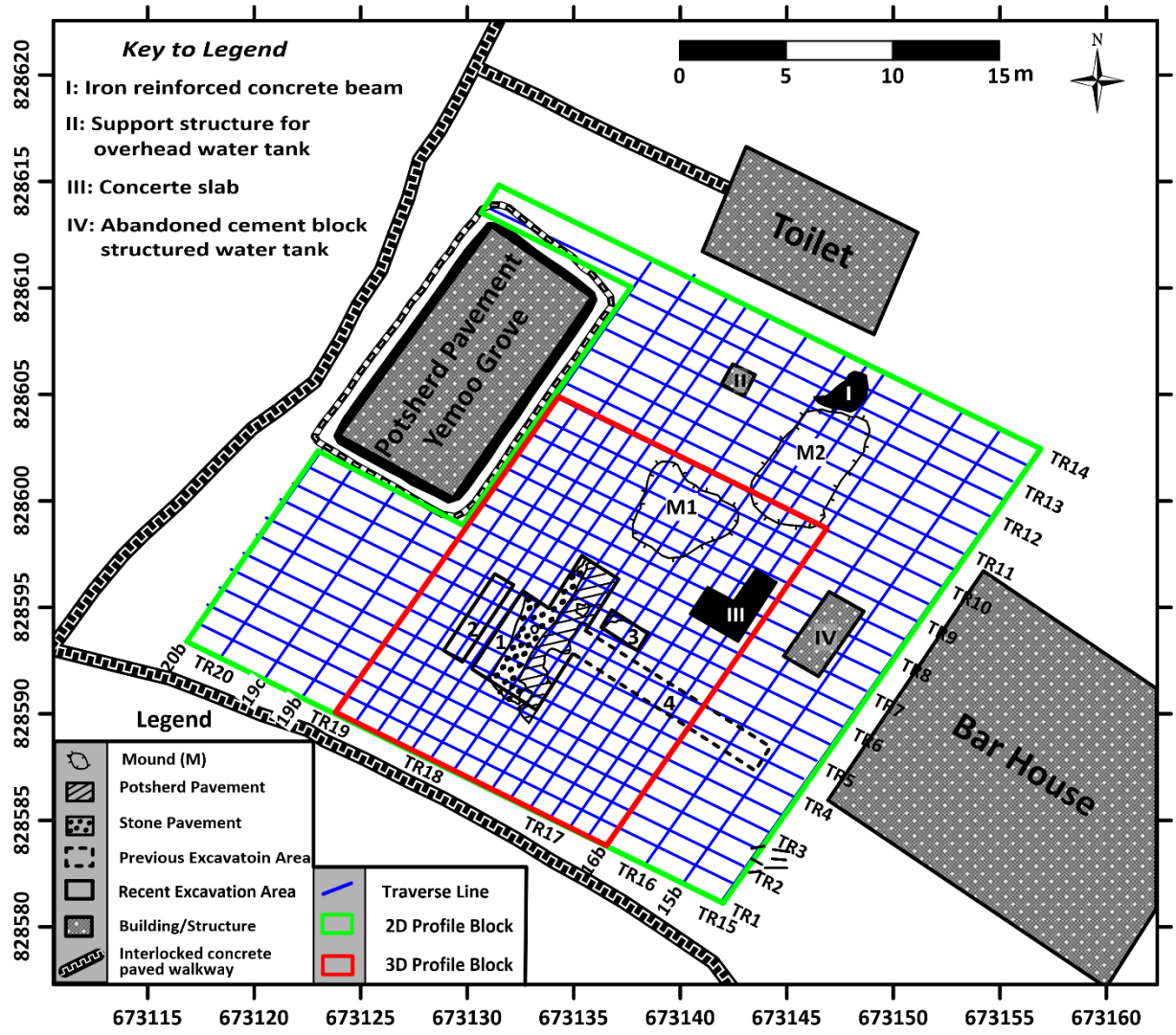

Fig. 6b: Data acquisition map showing 2D (1×2 m) and 3D (1×1 m) grid network for GPR survey at the main survey area

The GPR data processing was carried out using the MALA Vision GeoGuidline software. This cloud-based software utilized powerful computing and unique artificial intelligence across its processing phases. The field observed (raw) data file was first imported into the software which in-turn displayed the time-section raw data radargram (Fig. 6c) for each of the profiled lines. Signal enhancing and processing filters including DC offset, De-banding through background (Bg) removal, automatic gain control (AGC) and exponential gain were applied to the raw data. The processed radargrams (still in time section) were analyzed for velocity of propagation of the radar wave to facilitate time-depth radargram conversion. One way of determining the radar velocity at a survey area is by using known depth (through excavation or depth probing) to a desired reflector (in this case a potsherd/stone pavement) and measured reflection time to calculate the velocity (Jol and Bristow, 2003). Alternatively, where such exact depth information for specific locations are not available (as in the present case where we only have information on a range of depths) existing propagation velocity of radar waves in similar geological materials could be adopted.

The present survey area is underlain by clay and lateritic clay subsoils (Fig. 15). The clayey formation can be considered wet (this investigation was carried out in August, 2022, at about the middle and peak of the raining season) for which recorded radar wave velocities in the literature are: 80-110 mm/ns (Sharma, 1997); 86-110 mm/ns (Reynolds, 1997, Hui and Haita, 2011); 120 mm/ns (Zeng and McMechen, 1997) and 95 mm/ns (Robinson *et al.,* 2013) with a general range of 80-120 mm/ns. For this study, we applied a median radar velocity value of 100 mm/ns. Depth checks on a radargram high amplitude radar reflections suspected to be pavement correlated well with image from 2D resistivity structure and are within the depth range at the excavated site. Other processing operation was to mute (cut-off) section of air column between the GPR sensors and the ground level for depth normalization.

By carrying out linear interpolation of all the processed 2D radargrams, 3D cube (volume map) was created to facilitate depth (z) slice map or cartesian plane (x,y) sections for easy spatial delimitation of anomalous reflections. Targets of interest manifested as linear high amplitude reflection zones and hyperbolic (diffraction) features on the processed radargram depicting layered medium or artefact of contrasting elastic property relative to the immediate environment.

Plates 1-3 are recorded images of the field operations.

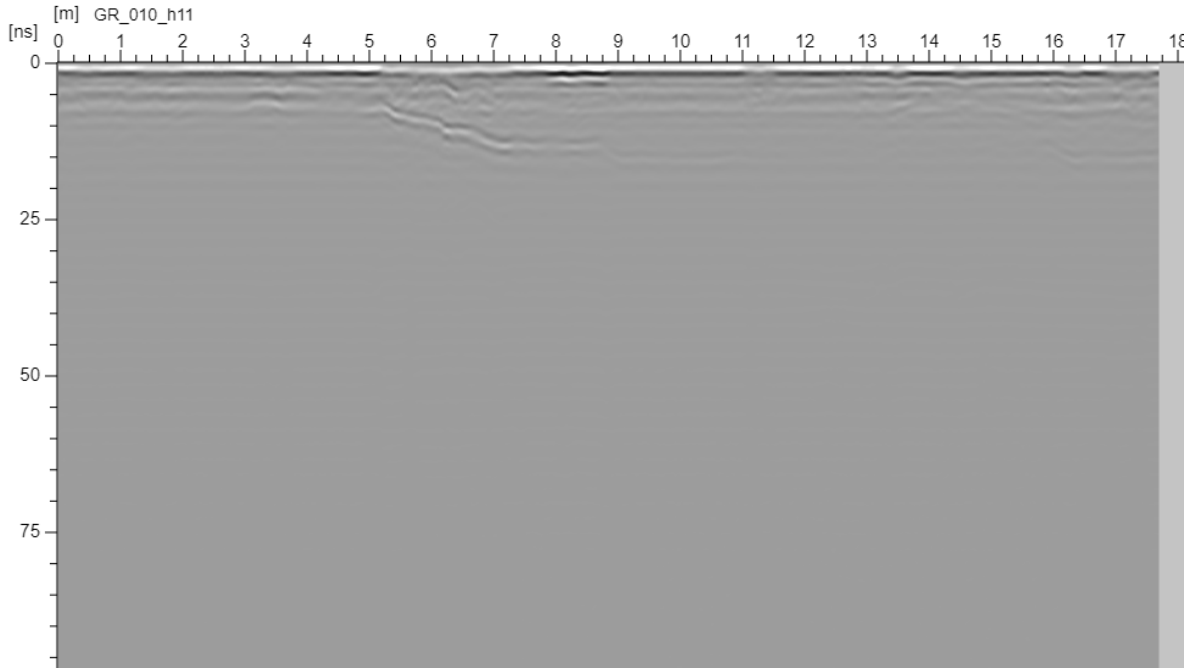

Fig. 6c: Raw GPR data radargram along cross-line 11 (Fig. 21) (TR 18c on Fig. 6b)

Plate 1: Photographs of magnetic survey at the Ita Yemoo project site while adopting low (a &b) and high (c &d) sensor heights for gradiometry magnetic survey

Plate 2: Photographs of Ground Penetrating Radar (GPR) survey at the Ita Yemoo site (a) setting-up of the radar (b &c) data acquisition in progress and (d) geometry and field parameters recording at the termination of a traverse measurement

Plate 3: Photographs of resistivity survey at the Ita Yemoo site (a-c) data acquisition in progress at the main site and (d) at the outcropped potsherd pavement site

2.4 Field Operational Problems

Ita Yemoo archaeological site is located within an urban Ile-Ife. The site contains various infrastructures which include the Heritage Multipurpose Hall, Art Museum Building, Yemoo Grove, Museum Kitchen, Bar House, several electric current carrying overhead cables, a demarcating wall with 33metal structure and an adjoining heavily trafficked Moore Road. The site receives visitors particularly in the afternoons/evenings with vehicles moving in and out of the premises. The cultural noise level is very high most especially for magnetic survey. The metal/aluminum roofing sheets of the adjoining buildings (Heritage Multipurpose Hall, Art Museum House, Museum Kitchen and the Bar House) and the metal carrying cement block fence that enclosed the main survey site are also problematic for magnetic data gathering. We had to come very early when traffic was light and stood-by assistants to direct traffic. We envisaged the magnetic gradient data option will correct for cultural noise to some extent. However, the roofing sheets were problematic for the high sensor height which puts the magnetic sensor close to the sheets. We therefore envisaged spurious magnetic effects at the edges of the plot. Also, there are within the survey area, a metal rod reinforced concrete beam and a suspected waste chamber with metal rod reinforced concrete lid at the southwestern edge of the toilet building. These in addition to a suspected iron rod reinforced platform of a cement block structure support for a water tank servicing the toilet are sources of cultural magnetic noise. It is also not clear what effect the diamagnetic polyethylene nylon liner (with negative permeability of -9.67×10^{-6}) within the excavated pit would have on the magnetic effect of the underlying potsherd pavement. For the resistivity survey, occasionally some of our traverses cut across concrete interlocking pavement which create high contact resistance at the current electrode positions. We had to drive the electrodes down beyond the pavement to ensure appreciable current input into the ground for measureable potential.

At the main study area, the recently excavated site was back filled with weathered/excavated soils after lining the exposed pavements with an impermeable black polyethylene nylon. The impermeable nature of the liner may have inhibited infiltration of rain water causing the fill to be water logged. The high water saturation in the fill created artificially low resistivity zone over the excavated site at shallow depth practically obscuring the true resistivity responses of the overlying fill and perhaps the underlying pavements.

2.5 Data Interpretation

2.5.1 Magnetic Survey

The interpretation of the magnetic maps is essentially qualitative and this involved inspection of such maps for signature typical of potsherd pavement using the template developed on the exposed pavement at the pilot site as control. Previous archaeological investigations (e.g. Olorunfemi *et al.,* 2022 and Oni *et al.,* 2021) have also shown that coincidence of magnetic lows (negative polarity) and high resistivity is characteristics of fired pottery related artefacts.

2.5.2 Resistivity Survey

2.5.2.1 Micro VES

The interpretation of micro VES data is quantitative and this involved partial curve matching with model two layer curves and the auxiliary curves. The preliminary geoelectric data (layer resistivity and thickness) derived are further refined by a technique involving 1-D forward modelling with W.Geosoft/WinSev 5.1 software. The interpretation results were used to generate a geoelectric section which imaged the subsurface stratigraphy at shallow depth.

2.5.2.2 2D Imaging

The 2D dipole-dipole data were inverted into 2D resistivity structures (images) which are migrated version of the raw pseudosection. True resistivity data were subsequently extracted from the 2D structures at different depth levels of 0 – 0.25 m; 0.25 – 0.5 m; 0.5 – 1.0 m and 1.0 – 1.5 m for the 0.5 station interval and 0 – 0.5 m, 0.5 – 1 m, 1 – 2 m and 2 – 3 m for 1.0 m station interval and prepared into various depth slice maps. Also, field observed apparent resistivity data for expansion factors (n = 1 – 5) were used to generate resistivity maps also at different depth levels of 0.29, 0.39, 0.49, 0.59 and 0.68 m for dipole length of 0.5 m and 0.59, 0.78, 0.98, 1.17 and 1.37 m for 1 m dipole length.

These maps were qualitatively interpreted based on the template developed from the pilot study and also relying on our previous experiences (e.g. Fadare *et al*., 2020, Olorunfemi *et al.,* 2019, Oni *et al.,* 2022 and Olorunfemi *et al.,* 2022). The maps were visually inspected for characteristic signatures typical of archaeological artefacts and the project assumptions detailed in section 1.5.

2.5.3 Ground Penetrating Radar (GPR)

The interpretation of GPR radargram or profile is commonly performed by interface mapping where:

(i) zone of high impedance reflection or zone of low attenuation is attributed to resistive (high resistivity) materials including potsherd pavements

(ii) zone of low impedance reflection or high attenuation is associated with conductive materials such as clay; and

(iii) hyperbolic diffraction patterns are associated with buried features such as ritual pots, buried channels, cavities, ground subsidence, drums and pipes.

2.6 Interpretation Limitation

2.6.1 Magnetic Survey

Except metallic objects, most archaeological artefacts generate weak magnetic effects which can easily be subsumed within relatively higher magnetic responses of host materials and environment. This is normally the case when a magnetic survey is carried out within a developed area like the present study area. The magnetic responses of several artefacts could overlap significantly (e.g. potsherd, ritual pot, fired clay etc.) making their differentiation difficult unless due cognissance is paid to the anomaly pattern or one has background information on the archaeological history of such a site.

2.6.2 Resistivity Survey

The stone/potsherd pavement, which is the principal target in this study, is a very thin stratigraphic layer (0.035 – 0.04 m thick). Although, the layer resistivity is relatively high, it has the tendency of being suppressed, most especially when it is buried under a much thicker overburden (of 0.4 – 1.0 m) as it is the case with the lower stone/potsherd pavement where the difference in thickness is more than one order of magnitude. Suppression is envisaged on the VES curve and 2D images. Even where the pavement outcrops, as it is the case at some locations within Ita Yemoo, the electrode array must be configured to measure apparent resistivity at very small (micro) current electrode spacing (AB/2) (as small as 0.075m) as it is the case in this study.

Again, it becomes difficult to identify the pavement when it is juxtapositioned with or resting on a layer with overlapping resistivity, Excavation works and our preliminary study have shown such pavements resting on lateritic layer with overlapping resistivity value.

2D modelling of traverses done directly on outcropping potsherd pavement could not delineate the pavement because of the very thin configuration and the scale of the image presentation. If this happens at shallow depth, it may be difficult to image same at deep depth where there is the

tendency it will be suppressed. There is also the non-uniqueness in the modelling of resistivity data (1D VES forward and 2D inversion models). This was why we carried out a pilot study on an outcropping potsherd pavement and pitted same to obtain information that will enable us constrain our modelling and data interpretation.

2.6.3 Ground Penetrating Radar (GPR) Survey

Most archaeological features (potsherd pavements, ritual pots, pottery, tuyere etc.) are compact, hard, of low moisture content and hence of relatively high resistivity values. Such features will display similarly high impedance reflections that could make their differentiation difficult except the anomaly pattern display distinctive geometries.

3.0 RESULTS AND DISCUSSION

3.1 The Pilot Study Area

3.1.1 Magnetic Survey

The magnetic anomaly maps for low (1.42 m) and high (2.32 m) sensor heights (Figs. 7a&b) respectively display magnetic intensities in the range of – 108 to 184 nT and -69 to 191 nT. The anomaly contours significantly trend approximately NW – SE over the major potsherd outcrop. The isolated anomalously low (negative) magnetic intensity in the northwestern corner is suspected to have been created by metal wire rings embedded in a nearby burnt car tyre (Fig. 7). Both maps do not seem diagnostic of the potsherd pavements having been located on or close to virtually the entire spectrum (-60 to 190 nT) of the magnetic anomaly. The magnetic gradient map (Fig. 7c) and the Reduced to the Equator (RTE) equivalent (Fig. 7d) with magnetic intensities of -44 to 25 nT/m and -28 to 27 nT/m respectively display identifiable anomaly closures. The RTE magnetic gradient map (Fig. 7d) centers anomalies on causative bodies and hence will be used to assess the potency of the magnetic method in identifying the exposed potsherd pavement.

Based on anomaly closures and colour bands, the RTE map (Fig. 7d) can be classified into three magnetic zones – A (0 to -28 nT/m in blue/green colour band), B (0 to 15 nT/m in light brown/yellow colour band) and C (15 to 28 nT/m in deep brown colour). Exposed potsherd pavements within this pilot site are majorly located within zone B (0 to 15 nT/m) but are also found within zone A (0 to -10 nT/m) and in the proximity of zone C (> 15 nT) (enclosed pavement and outcropping pavement at the northeast corner). In essence, the potsherd pavements are associated with virtually the entire magnetic anomaly spectrum.

The following deductions can be made from the present results

(i) That potsherd pavements are weakly magnetic and hence the magnetic responses could overlap significantly with that of the immediate surrounding or host materials

(ii) Although potsherd pavements are majorly associated with intermediate range (0 to 15nT/m) of magnetic anomalies, some are located within or close to low (0 to -28 nT/m) and relatively high (15 – 27 nT/m) magnetic zone.

(iii) It may be difficult therefore, to use the magnetic method alone to map potsherd pavement. It seems good enough as a reconnaissance tool.

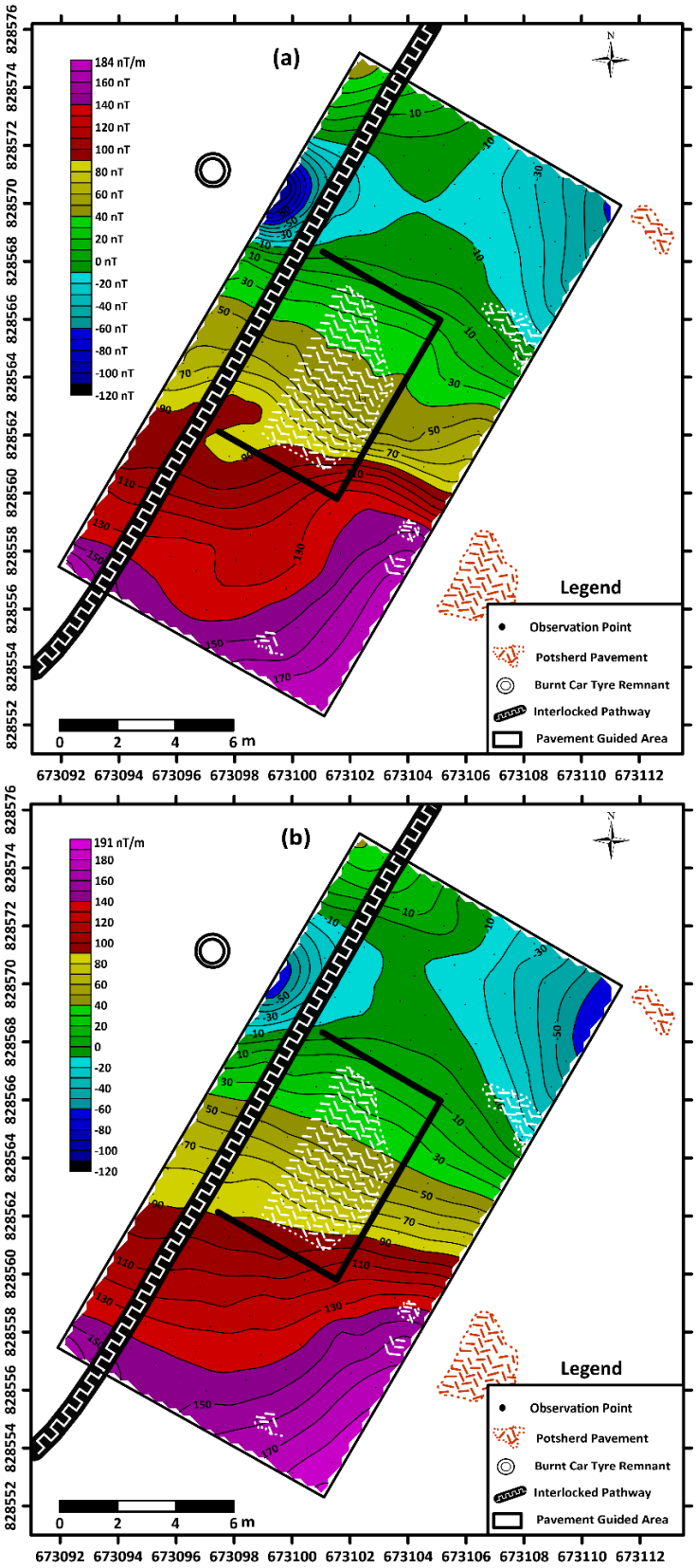

Fig. 7: Magnetic anomaly maps at (a) low (1.42 m) and (b) high (2.32 m) sensor heights

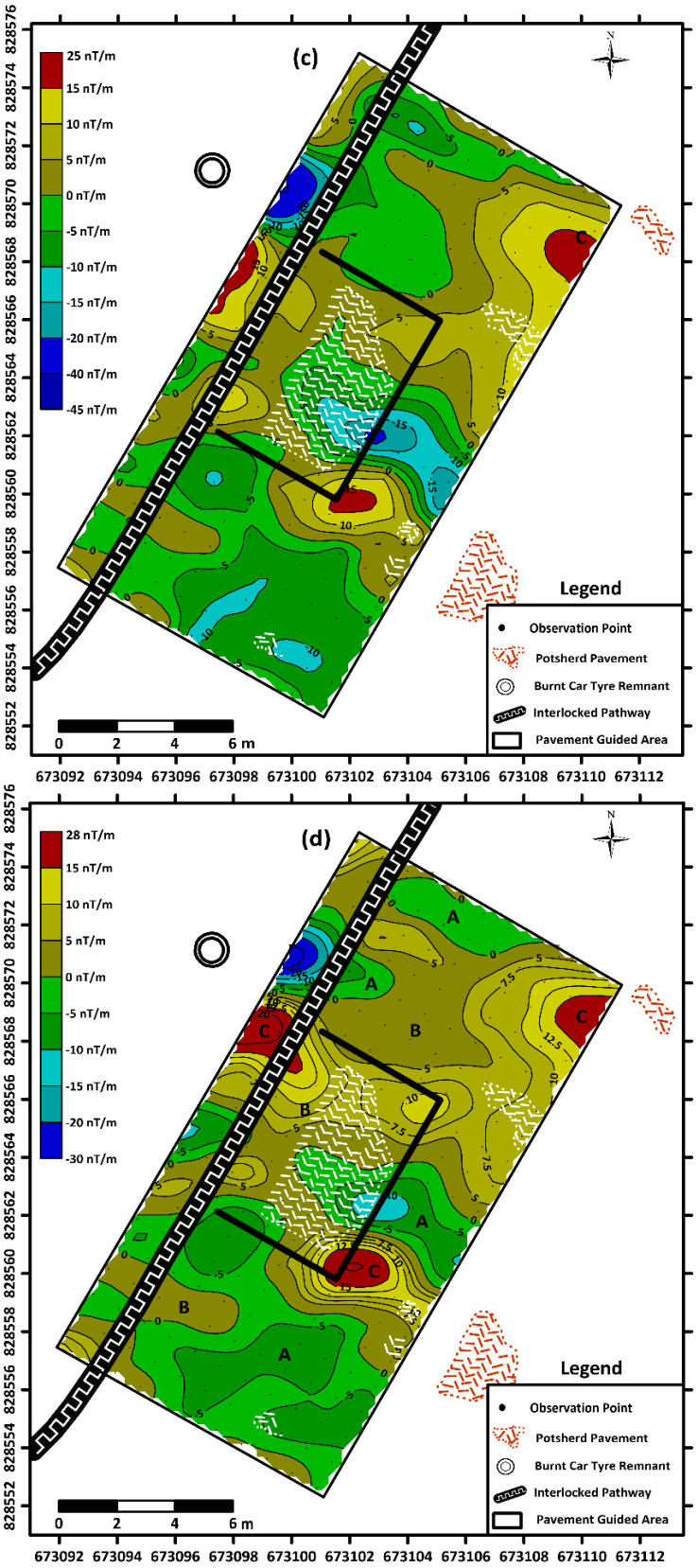

Fig. 7:(c) Magnetic gradient and (d) Reduced to the Equator (RTE) magnetic gradient anomaly maps

3.1.1.1 Estimation of Depth of Archaeological Relevance

In order to estimate the depth of archaeological significance, the RTE magnetic gradient map was downward continued at a step of 0.25 m and up to 1.0 m depth level (Fig. 8a-d). The maps retain their characteristics only up to 0.50 m depth level (Figs. 8a&b) beyond which they are completely distorted (Figs. 8c&d)). This indicates that the depth of relevance of the causative bodies is shallow (near-surface) and is maximum of 0.5 m.

3.1.2 Resistivity Survey

3.1.2.1 Micro Vertical Electrical Sounding (Micro VES)

Four (4) micro-vertical electrical soundings were carried out to image the subsurface stratigraphy at shallow depth and also investigate the potency of the technique in estimating the thicknesses and layer resistivity values of the potsherd pavement. The subsurface image so generated will assist the interpretation of 2D resistivity images that will subsequently be inverted from the observed 2D data.

Within the limits of the electrode spread (AB = 6 m), the VES curves are the H type (Fig. 9a). The geoelectric section generated from the interpretation results contained in Table 1, is displayed in Figure 9b.

Table 1. Micro VES Interpretation Results at the Pilot Study Area

VES NO.	DEPTH (m) $d_1/d_2/d_3/\ldots.d_{n-1}$	RESISTIVITY ($\boldsymbol{\Omega}$m) $\rho_1/\rho_2/\rho_3\ldots..\rho_n$	RESISTIVITY TYPE CURVE
17	0.04/0.25	244/100/284	H
18	0.04/0.40	150/122/259	H
19	0.03/0.17	157/89/235	H
20	0.03/0.21	91/51/312	H

Figure 9b delineates three subsurface layers as detailed below.

1st Layer: Potsherd Pavement (as topsoil)

Resistivity: 91-244 ohm-m; Thickness; 0.030 – 0.04 m

2nd Layer: Clay/Sandy Clay Fill?

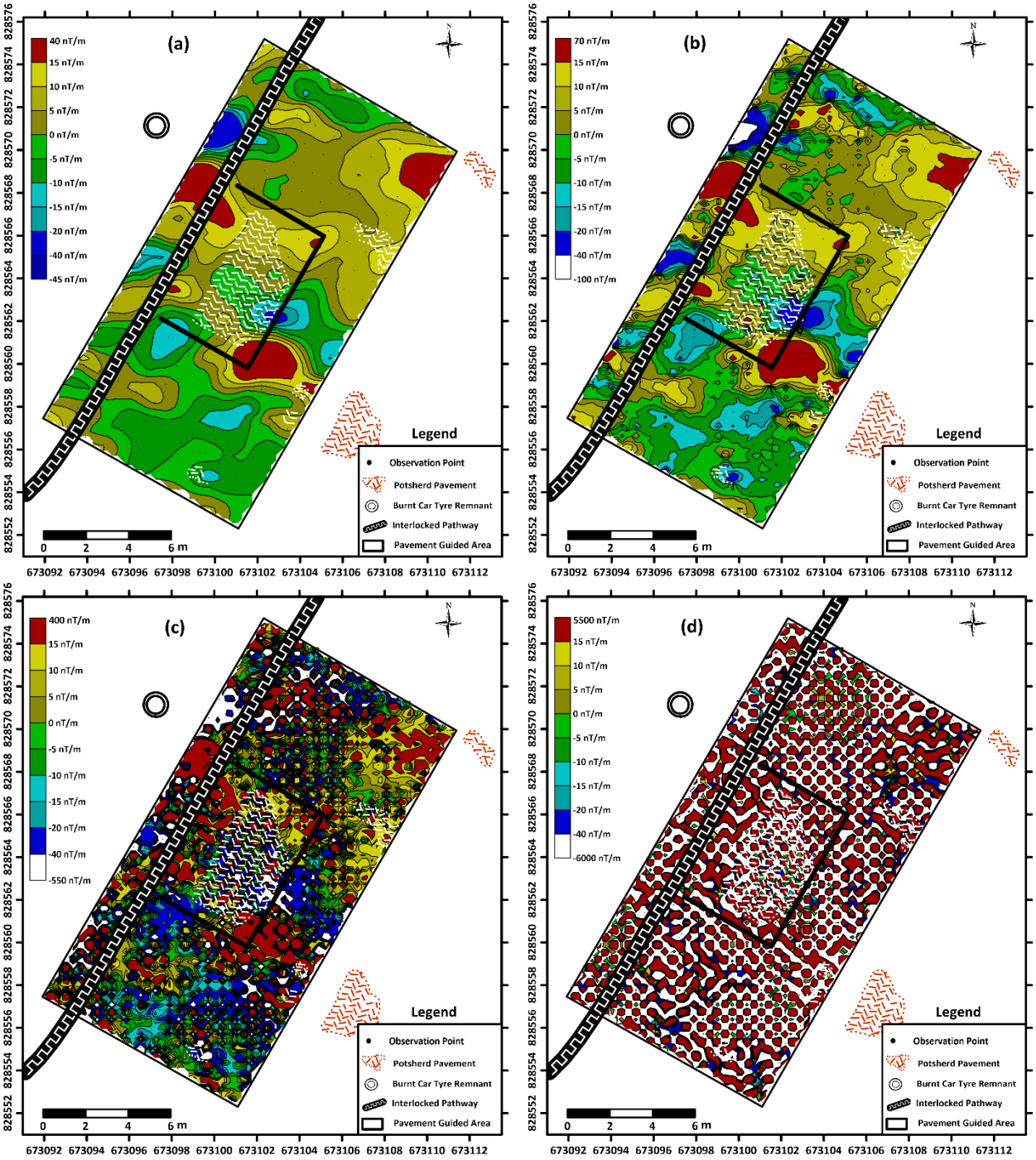

Fig. 8: Downward continued RTE magnetic gradient maps at (a) 0.25 m (b) 0.5 m (c) 0.75 m and (d) 1 m depth levels

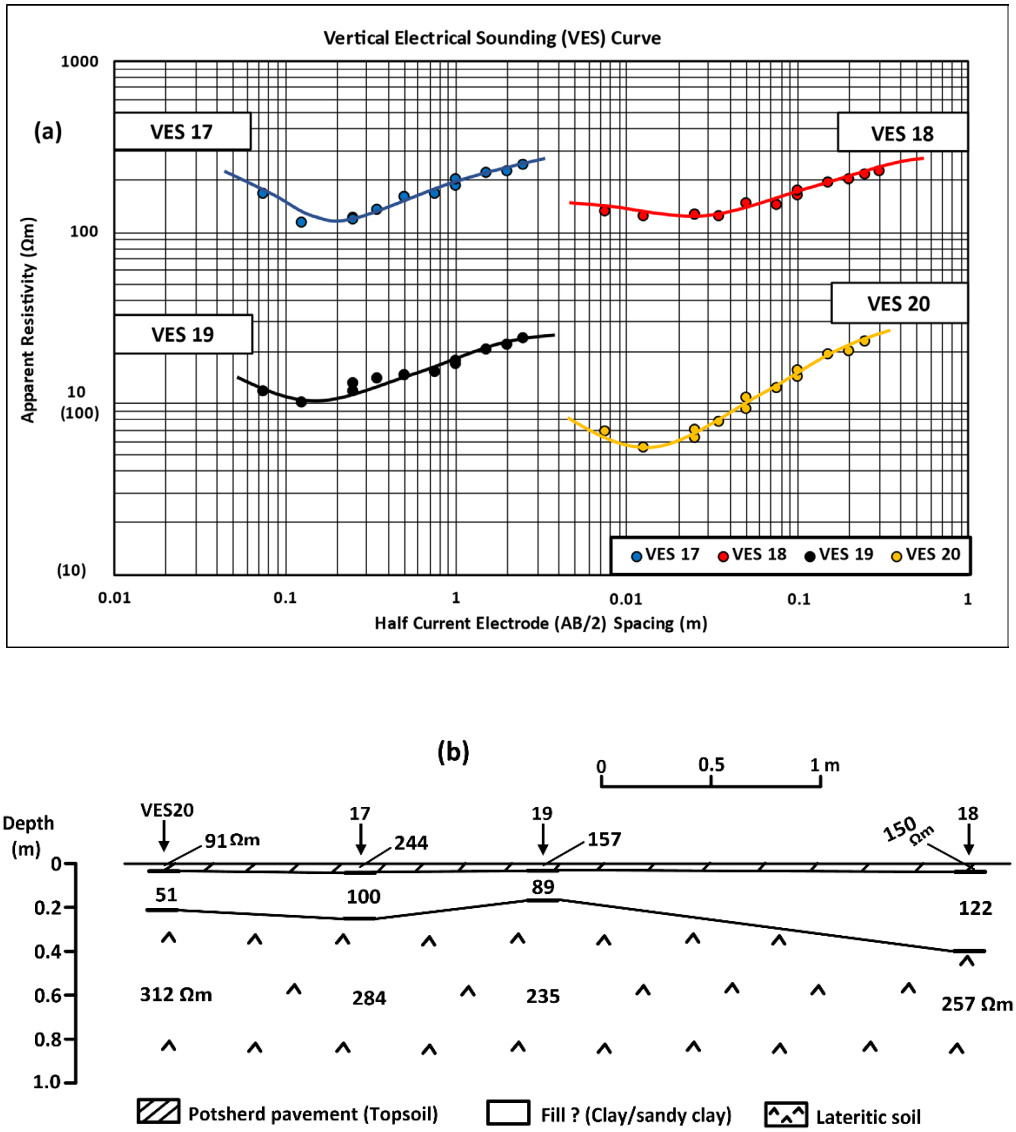

Fig. 9(a) Typical VES curves and (b) geoelectric section at the pilot study site, Ita Yemoo, Ile-Ife

Resistivity: 51-122 ohm-m; Thickness; 0.14 – 0.36 m

3rd Layer: Lateritic Clay

Resistivity: 235 – 312 ohm-m; Rockhead at 0.17 - 0.40 m.

Deductions

(i) The estimated thicknesses of the potsherd pavement (0.03 – 0.04 m) compare with the 0.035 – 0.04 m obtained from pitting. This confirms that the potsherd pavement could be treated as a stratigraphic layer (unit).

(ii) The estimated layer resistivity values for the pavement range from 91 – 244 ohm-m. This shows that the layer resistivity values could vary depending on the physical state (whether dry, weathered or water saturated) of the pavement.

(iii) The estimated layer resistivity values overlap to some extent with that of the underlying layer (fill ?) and on the high resistivity spectrum, with the basal lateritic layer (which is suspected to be a palaeosoil).

(iv) At shallow depth, the potsherd pavement could be delineated through micro sounding. The prospect at deep depth cannot be assessed with the present field design. However, the small thickness of the pavement makes it highly susceptible to suppression at deep depth (where the thickness of the overlying layer is multiple times larger than the pavement itself).

3.1.2.2 2D Dipole-Dipole Imaging

The 2D dipole-dipole data are presented in 2D modes as apparent resistivity maps developed for different expansion factors (n=1-5) using the observed field data and as resistivity depth slice maps generated from the extracted true resistivity values from the inverted 2D images between some depth intervals. The former is equivalent to resistivity depth slice maps at specific depth levels for the different expansion factor (n) as defined by Roy and Apparao (1971) (see section 2.1.1.1b). The resistivity data for these maps were generated from four (4) main and four (4) orthogonal traverses (Fig. 4).

(i) Apparent Resistivity Maps

The apparent resistivity maps (Figs. 10a-e) were generated for expansion factors n=1-5 and specific theoretical depths of 0.29, 0.39, 0.49, 0.59 and 0.68 m. The potsherd pavement investigated at this pilot site outcrops or occurs very close to the ground surface and varied in

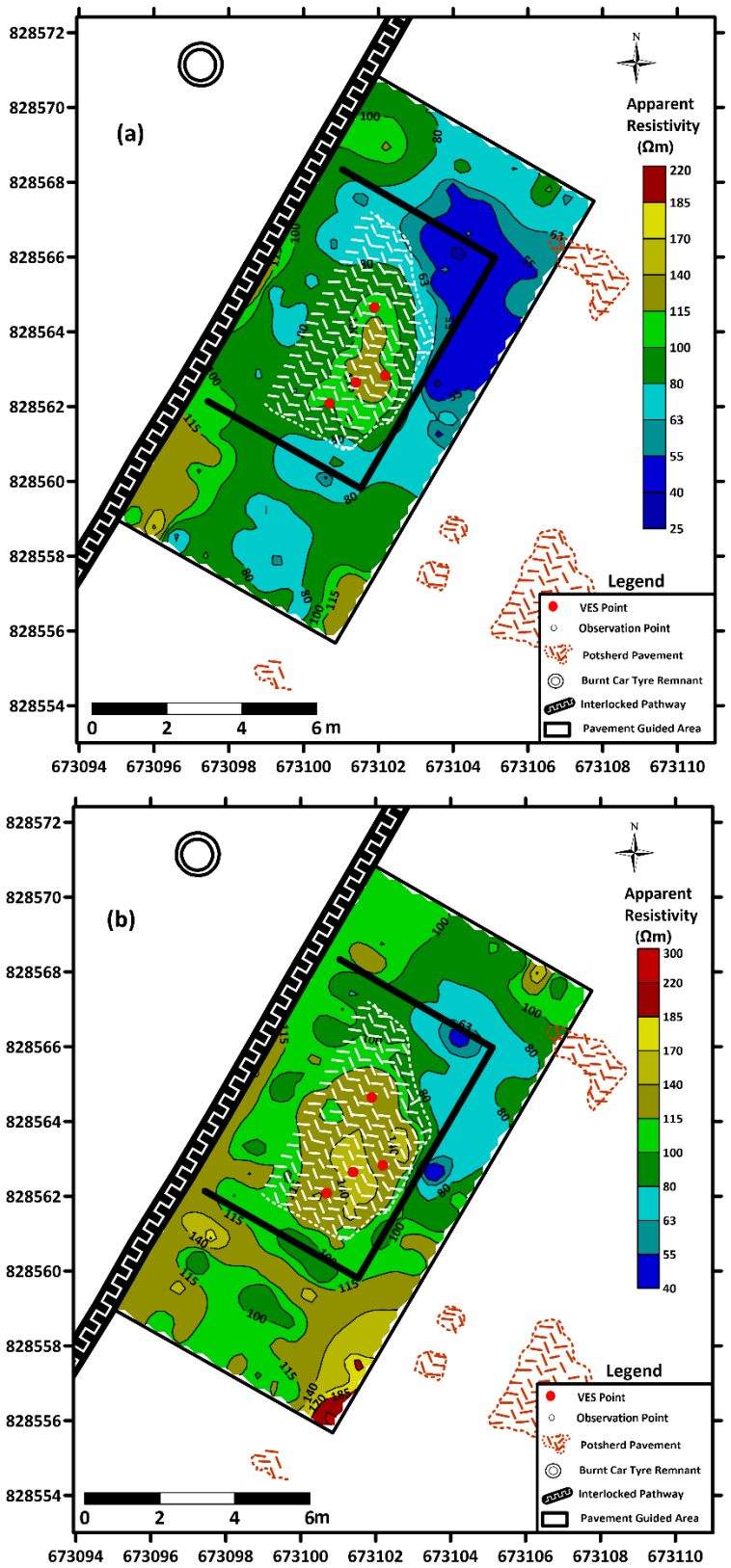

Fig. 10: Apparent resistivity maps at (a) expansion factor (n) of 1 and theoretical depth of 0.29 m and (b) expansion factor (n) of 2 and theoretical depth of 0.39 m

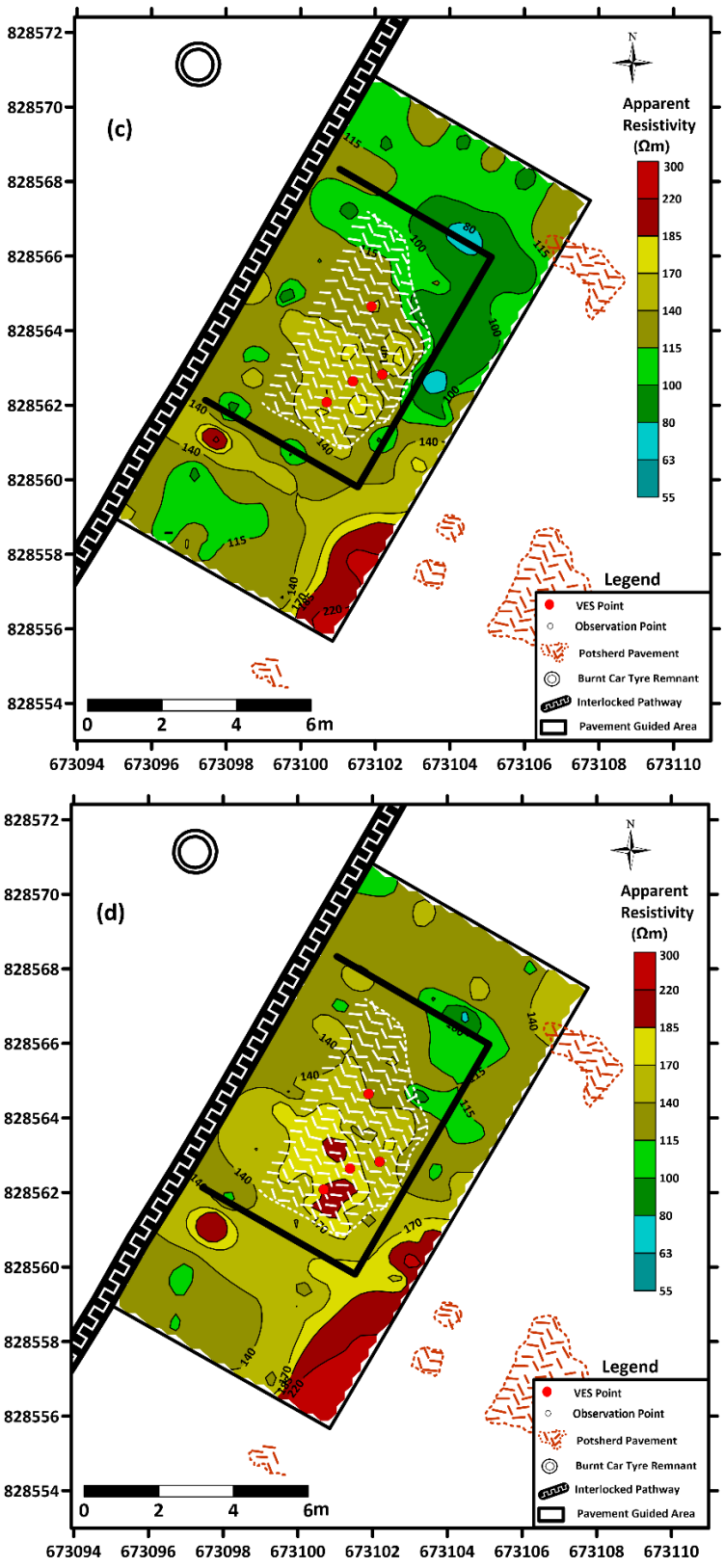

Fig. 10: Apparent resistivity maps at (c) expansion factor (n) of 3 and theoretical depth of 0.49 m and (d) expansion factor (n) of 4 and theoretical depth of 0.59 m

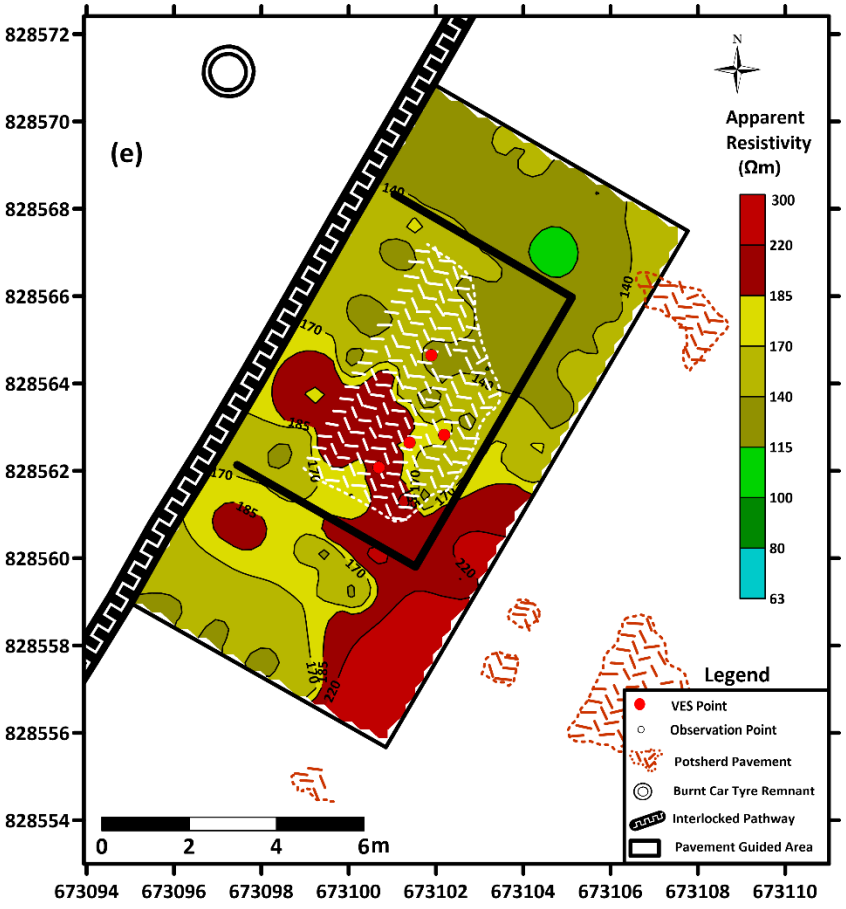

Fig. 10e: Apparent resistivity map at expansion factor (n) of 5 and theoretical depth of 0.68 m

thicknesses from 0.03 to 0.04 m. The relatively high resistivity (91 – 244 ohm-m from Micro VES) pavement is underlain by relatively low resistivity (51 – 122 ohm-m) thin (0.14 – 0.36 m) layer suspected to be a fill? overlying a relatively high resistivity basal lateritic clay layer at depths ranging from 0.17 – 0.40 m. In essence, apparent resistivity maps generated for n = 1 (0.29 m), n = 2 (0.35 m) and possibly n = 3 (0.49 m) should be relevant for the mapping of the outcropping pavement. Maps generated for n = 4 to 5 (for depths 0.59 and 0.68 m) may be too deep and reflective of the deeper lateritic layer

Figure 10a presents the resistivity map for n=1 at a theoretical depth level of 0.29 m. The recorded apparent resistivity values range from 31 – 189 ohm-m. The exposed potsherd pavement falls significantly within resistivity range of 80 – 185 ohm-m (recall 91 – 244 ohm-m from micro VES) with its edges significantly well defined by the 80 ohm-m contour at the southwest, southeast/east, northeast edge and mirrors the boundary in the north. The lower resistivity (63 – 80 ohm-m) of the pavement at the northern edge may be due to water saturation from the water logged northeastern corner of the cement block enclosure. The water logged area is mapped in deep blue colour as the very low resistivity (25 – 55 ohm-m) zone. This map shows that the pavement may extend towards the northwest (beyond the exposed section) under thin soil cover. It is also pertinent to note that locations of other outcropping potsherd pavements, by extension, fall within or are in the proximity of the resistivity range for the pavement above. It appears that the influence of the rain saturated topsoil/near-surface soils is maximum at this depth level.

At depth level of 0.39 m, the apparent resistivity map (with a recorded resistivity range of 45 – 226 ohm-m, Fig. 10b) shows a sharper and more clearly defined resistivity image of the exposed potsherd pavement. The potsherd, as mapped, falls significantly within a resistivity range of 115-226 ohm-m (note micro VES gave a range of 91-244 ohm-m) with perfect boundary fit at the southwestern/eastern and northwestern edge. The northern edge falls within resistivity range of 100-115 ohm-m. This map also indicates possible extension of the pavement towards the northwestern part under soil cover. Exposed potsherd pavements outside the investigated one are located within or are in proximity to the established resistivity range.

The apparent resistivity map for n=3 at depth level of 0.49 m (with range of resistivity values of 58 – 264 ohm-m, Fig. 10c) maintains a diagnostic resistivity range of 115 – 220 ohm-m with the

boundary fitting significantly well with that of the exposed pavement. The influence of the high resistivity basal lateritic layer has started manifesting at this depth level.

The resistivity maps for n=4 and 5 (Figs. 10d & e) are no longer diagnostic because of the increased influence of the relatively high resistivity basal lateritic layer which has subsumed the influence of the pavement. The above analysis shows that resistivity maps for expansion factors of n = 1-3 and up to depth level of 0.49 m are relevant in mapping the exposed potsherd pavements at the pilot site. This is in agreement with the estimated 0.5 m depth of archaeological relevance from the downward continued magnetic map.

(ii) 2D Resistivity Depth Slice Maps

The typical 2D resistivity images and correlated 1D micro VES interpretation models along traverses TR 23 and 23.5 are displayed in Figures 11a and b. The 1D VES models correlate significantly well with the 2D images. Figures 11c and d compare 2D resistivity images with dipole lengths of 0.5 and 1 m along traverse TR 23.5. The two 2D images correlate significantly well within the common upper 1.5 m. This shows that a dipole length of 1 m could have equally been significantly effective in this pilot study.

Resistivity depth slice maps were prepared from 2D resistivity images along main and orthogonal traverses at depth ranges of 0 - 0.25 m (Fig. 12a); 0.25 – 0.50 m (Fig. 12b); 0.50 – 1.0 m (Fig 12c) and 1.0 – 1.5 m (Fig. 12d). These maps are essentially weighted average resistivity maps within these depth ranges. The 0 - 0.25 m resistivity depth slice map (Fig. 12a) with a resistivity range of 25 – 191 ohm – m shows that the exposed potsherd pavement falls within a relatively low resistivity range of between 55 and 115 ohm-m with about half of the pavement (around the micro VES points) delineated as a relatively high resistivity (80 – 115 ohm – m) zone. This map poorly resolved the investigated pavement and other pavements outside the enclosure which fall within low resistivity zone. The 0.25 – 50 m resistivity depth slice map (Fig. 12b) resolves the potsherd pavement better, mapping significantly the established pavement boundaries in the southwestern, southeastern northeastern and northern flanks as relatively high resistivity (100 – 220 ohm-m) zone. This range correlates with the micro VES established potsherd pavement resistivity of 91 – 244 ohm – m. The map also indicates that the pavement may extend towards the northwestern flank. Potsherd pavement outcrops outside the investigated enclosure fall within the established pavement resistivity. This map is about the only diagnostic map of the

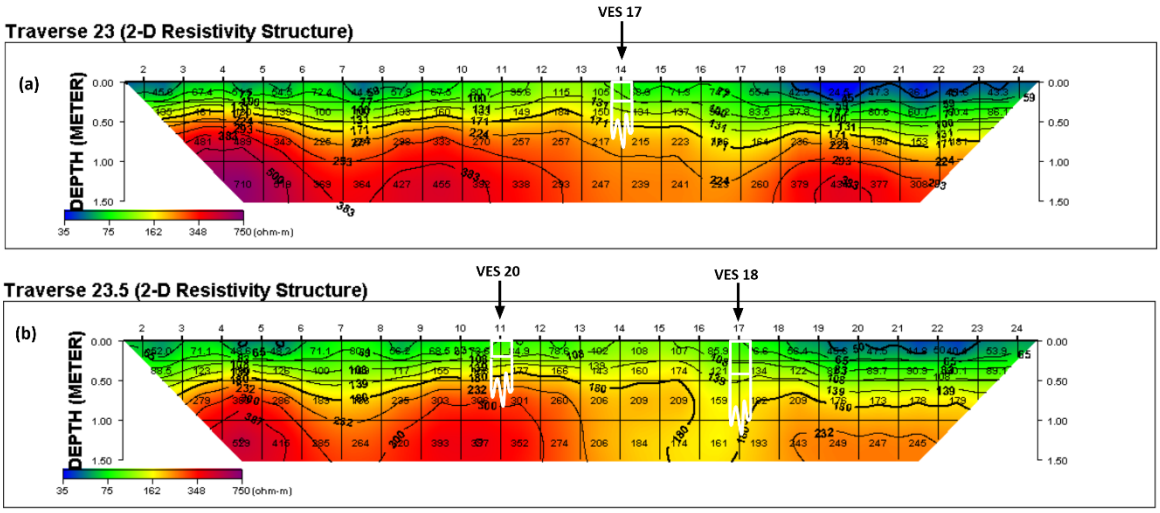

Figs. 11a&b: Typical 2D resistivity images with correlated 1D micro VES interpretation models along traverses TR 23 and 23.5 at the pilot study site

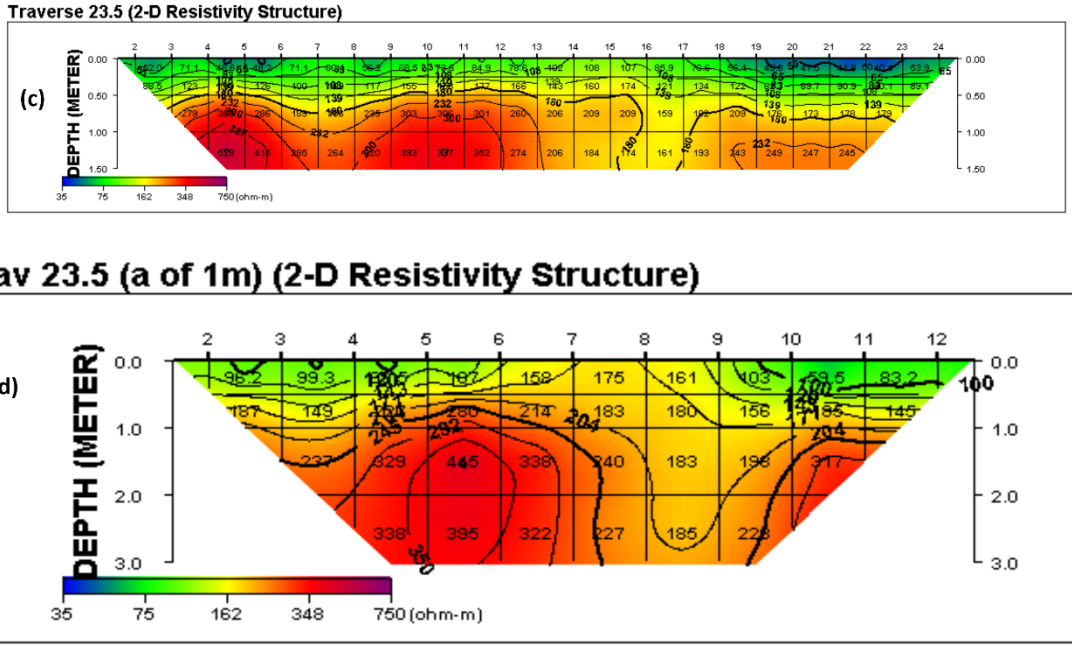

Figs. 11c&d: Comparison of 2D resistivity images derived from 0.5 m and 1 m dipole lengths along traverses TR 23.5 at the pilot study area

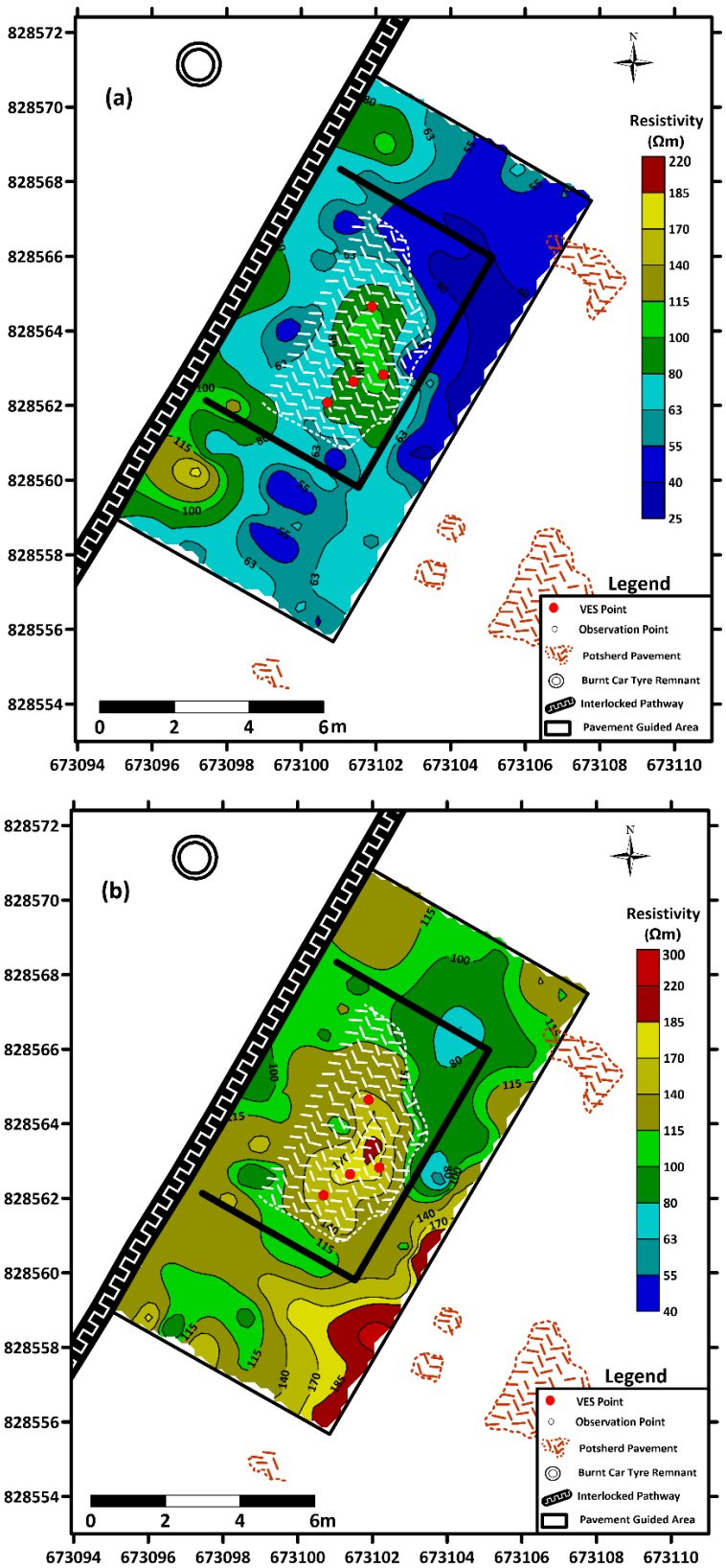

Fig. 12: Resistivity depth slice maps at (a) 0 - 0.25 m and (b) 0.25 - 0.5 m

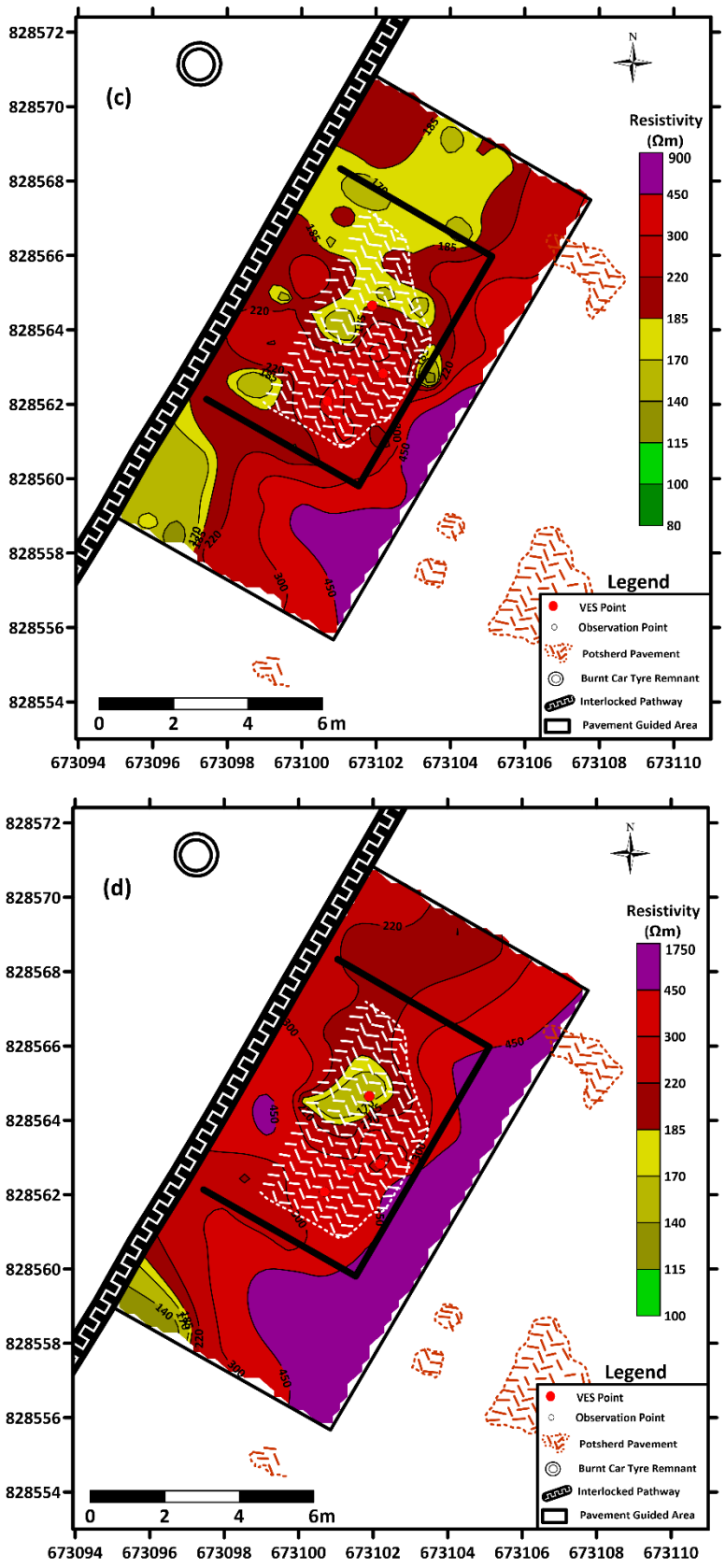

Fig. 12: Resistivity depth slice maps at (c) 0.5 - 1.0 m and (d) 1.0 - 1.5 m

series as the other two maps, 0.5 – 1.0 m (Fig. 12c) and 1.0 – 1.5m (Fig. 12d) are more reflective of the high resistivity basal lateritic layer and very poorly diagnostic of the exposed potsherd pavement geometry. Figure 12d however delineates an isolated oval-shaped relatively high resistivity zone (140 -185 ohm-m) typical of potsherd pavement at depth range of 1.0 – 1.5 m. This could be a suspected second unit of potsherd pavement or a different archaeological feature at deeper depth.

For the resistivity depth slice maps, only the 0 – 0.25 m and 0.25 – 0.5 m resistivity maps seem to be partially/significantly diagnostic of the exposed potsherd pavement and its geometry.

The results above show that apparent resistivity maps generated for different expansion factors (n) and specific depth levels are more diagnostic of the potsherd pavements and geometry than the weighted average depth slice resistivity maps generated for ranges of depths. The resolution could have been enhanced with more traverses and reduced traverse-traverse interval. For meaningful interpretation of the resistivity maps for pavement delineation, information on the geoelectric characteristics (layer resistivities and thicknesses) and depths of occurrence of the pavement are useful and derivable from vertical electrical soundings and direct pitting.

The 2D vertical images did not resolve the pavements possibly due to the scale of presentation of the images (the potsherd pavement is 0.03 – 0.04 m thick) but mapped the subsurface stratigraphy with the exception of the topsoil which merges with the underlying layer, except when significantly thick.

3.1.3. Geophysical Characteristics from the Pilot Study

Table 2 presents geophysical attributes, diagnostic characteristics and potency assessment of the magnetic and electrical resistivity methods deployed in the pilot study for the mapping of the exposed potsherd pavement.

The planar nature of the pavement demands for depth specific (not depth range) geophysical attributes for its delineation. The limited resolution of the magnetic attributes and depth range slice maps could be ascribed to this fact.

The results of this pilot study show that for potsherd pavement to be effectively mapped, some background information on its characteristics such as thicknesses and resistivity range, depth of occurrence and the environment's subsurface stratigraphy are useful to enable appropriate field

design (measurement station intervals, depth of probe and data display techniques etc.). While this pilot study rates the resistivity method over and above the magnetic method in potency in potsherd pavement mapping, there is still the need for integrated geophysical investigation that would resolve ambiguities associated with individual geophysical method.

Apparent resistivity maps at specific depth levels and at shallow depth seem to better resolve the potsherd pavement. As earlier stated, we did not have access to a ground penetrating radar equipment when this pilot study was carried out. We however suspect that its depth specific data presentation may also make it a potent tool in potsherd pavement mapping. We deployed the GPR equipment at the main study area and have used the results of its 3D configured data (in advance) to assess its potency in Table 2.

Table 2: Geophysical attributes, diagnostic characteristics and assessment of potency

Geophysical Method	Geophysical Attribute	Diagnostics Characteristics	Assessment of Potency
Magnetic	RTE Magnetic Gradient Map	Relatively weak magnetic response. Most pavements (enclosed and outside) were located within 0 to 15 nT/m anomaly range but some others were located within the range of 0 to -10 nT/m and >15 nT/m	The potency is limited. Pavements are located within a wide spectrum of magnetic anomalies which sometimes overlap with that of the barren host. The geophysical method is best adopted as a reconnaissance tool.
Electrical Resistivity	(a) Micro VES curves and Geoelectric Section	Characteristic Type Curve is the H type. Relatively high resistivity (91 – 244 ohm-m) unit overlying a relatively low resistivity (51 – 122 ohm-m) fill? with basal high resistivity (235 – 312 ohm-m) lateritic layer	Identifies exposed potsherd pavement distinctively and estimates both thickness and layer resistivity values to appreciable level of accuracy. It is not clear from this study if the very thin pavement will be resolved at deep depth due to suppression.

	(b) Apparent resistivity maps for different expansion factor, n, and at specific theoretical depth levels of 0.29, 0.39, 0.49, 0.59 and 0.68 m	Relatively high resistivity values (80 – 185; 115 – 226 and 115 – 220 ohm-m)	Very diagnostic for expansion factors n = 1, 2, and 3 at depth levels of 0.29, 0.39 and 0.49 m and maps the exposed potsherd pavement with appreciable boundary delimitation and established prospects for concealed unidentified pavements.
	(c) Resistivity depth slice maps for different depth intervals of 0 – 0.25; 0.5 – 1.0 and 1.0 – 1.5 m	Relatively high resistivity values (80 – 115; 60 – 220 and 140 – 185 ohm-m) in the range estimated from micro VES.	Only the 0 – 0.25 m and 0.25 – 0.5 m resistivity depth slice maps partially/significantly map the exposed pavement. At shallow depth the estimated pavement resistivities are relatively low possibly due to the fact that the values used are essentially weighted averages for the depth intervals. This may have impaired the resolution of this resistivity attribute.

Ground Penetrating Radar (GPR)	GPR Radargram	High amplitude bright coloured (yellow/red) significantly continuous and traceable radar reflections	This attribute is very effective in mapping potsherd/stone pavement and in estimating the depth of occurrence and lateral extent
	GPR (depth specific) Depth Slice Maps	High amplitude bright coloured (yellow/red) radar reflections	This attribute is very effective in mapping potsherd/stone pavement and in estimating its depth ranges and spatial distribution. When several of these depth slices are combined, a 3D volume is developed.

3.2 The Main Study Area

The main study area is located at the premises of Yemoo Grove (Fig. 1) – a shed constructed to protect an earlier excavated potsherd pavement by Willet and Adesina between 1959 and 2008. Recent (2022) excavation by the Choiun and Ogunfolakan group also identified juxtapositioned stone and potsherd pavement within Pit 1 and small potsherd pavement within Pit 3 while Pit 2 is barren (Fig. 1). The pavement within Pit 1 virtually outcrops (near-surface) at the southwestern edge and occurs at depths of 0.4 – 1 m north-northeast wards (NNE). These are the limited background information at our disposal. The primary objective of this main study therefore, is to establish the spatial distribution of the pavements so as to guide future excavation and minimize invasiveness. In this process, other existing features of archaeological interest could also be identified.

3.2.1 Magnetic Survey

Figures 13a&b show the magnetic anomaly map for low (1.42 m) and high (2.32 m) sensor heights with intensities of -948 to 1153 nT and -1072 to 1753 nT respectively. The high sensor configuration placed the magnetometer sensor close to the metal/aluminum roofing sheets of the adjoining Yemoo Grove, Toilet and Bar House buildings thereby increasing the cultural noise. This may have been responsible for the anomalously high amplitude magnetic intensities at high sensor height relative to the low sensor height. Both magnetic maps are however similar in anomaly pattern.

The magnetic gradient map (Fig. 13c) developed from the low and high sensor heights magnetic maps (Figs. 13a&b) attenuates the cultural noise and accentuates (sharpens) the magnetic effects of near-surface archaeological features. The magnetic gradient map was reduced to the magnetic equator (RTE) to centralise magnetic anomalies over causative targets. The RTE magnetic gradient map (Fig. 13d) will therefore be the subject of discussion.

The intensities of the RTE magnetic gradient map (Fig. 13d) vary from -317.8 to 327.1 nT/m and can broadly be classified into three zones – A, low (majorly negative) intensities from + 5 to – 318 nT/m in blue/green colour band; B, intermediate from +5 to 40 nT/m and in brown/yellow colour band and C, high intensities from 40 to 327nT/m in purple/red colour band. The excavated stone/potsherd pavement in Pit 1 and the small excavated potsherd at the northwestern edge in Pit 3 fall within the intermediate magnetic intensity (5 to 40 nT/m) zone B. The barren Pit 2 falls

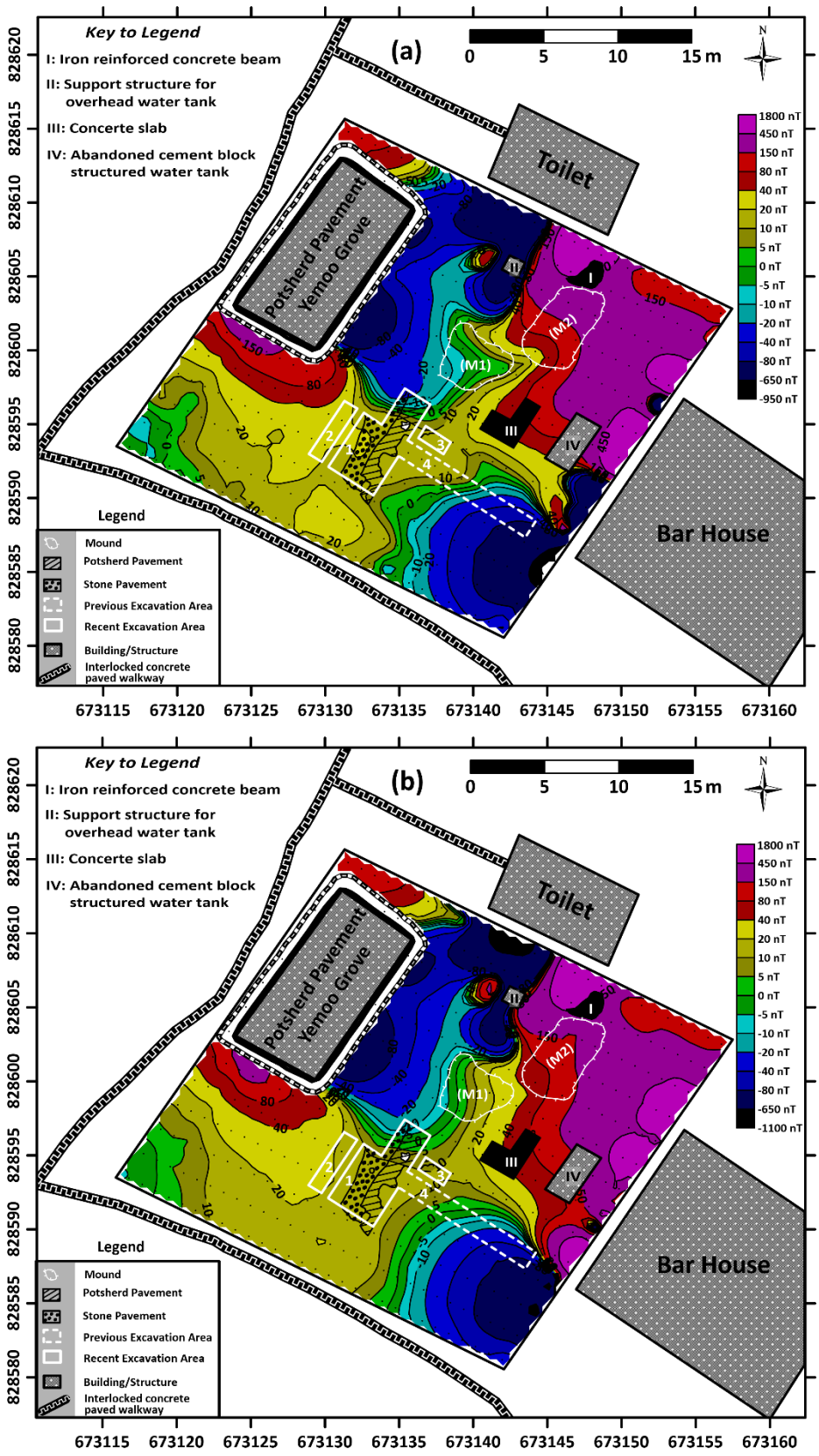

Fig. 13: Magnetic anomaly maps at (a) low (1.42 m) and (b) high (2.32 m) sensor heights

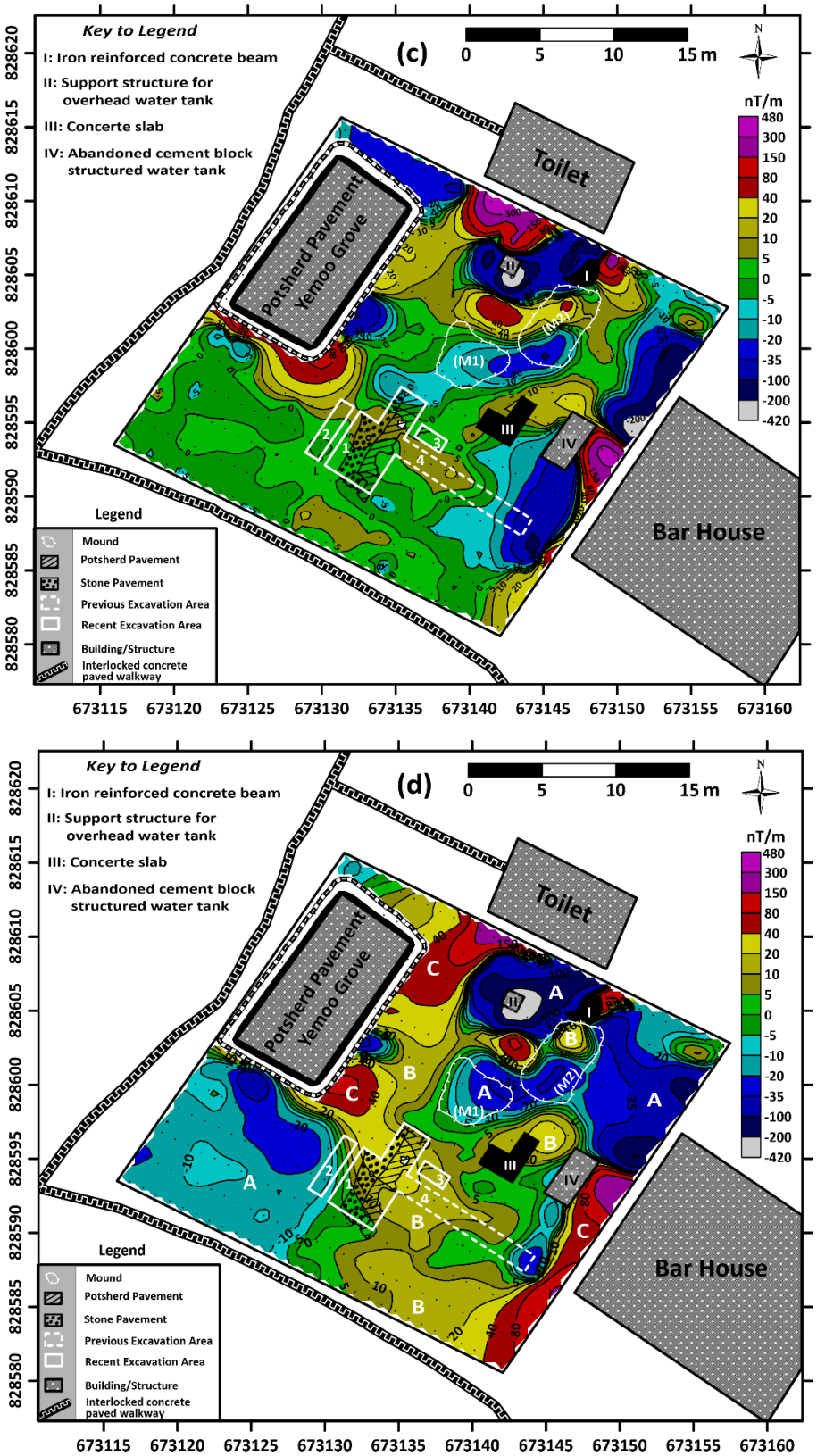

Fig. 13(c) Magnetic gradient anomaly map and (d) Reduced to the Equator (RTE) magnetic gradient map

within Zone A (5 to -318nT/m). A segment of the previously excavated and barren NW-SE trending Pit 4 and Pit 3 may host pavement at deeper depth. The prospective zone B extends to southwest of the Yemoo Grove and south/southwestern corner of the survey area. Zone B also extends to beneath the cement concrete slab and is isolated over mound M2 and northwest of the same mound. Outcrop of potsherd pavement was located within zone C (40 to 327nT/m) and at the southeastern corner of the survey area. In essence, there are field indications of prospective potsherd pavement within zones B and C. At the pilot study site, observed RTE magnetic gradient intensities vary from -28 to 27 nT/m - a range and amplitudes that are much smaller than the observed (-317.8 to 327.1 nT/m) at this main site. This is probably due to lower level of cultural noise at the former. At the pilot site, the major exposed potsherd pavement falls within an intermediate range of 0 to 15 nT/m and up to 27 nT/m which significantly overlap with the range of 5 to 40 nT/m at this main site.

Magnetic lows (negative polarity) can however be reflective of archaeological features most especially when such lows coincide with high resistivities (Olorunfemi *et al*., 2019; Oni *et al*., 2022 and Olorunfemi *et al*., 2022). In essence, the magnetic lows over mounds M1 and M2, southeast of mound M2 and in the premises of Yemoo Grove could be of archaeological interest. We however suspect that the high amplitude (negative/positive) magnetic responses at the periphery of the adjoining buildings (Yemoo Grove, Toilet/Water tank support structure, Bar House) and iron reinforced concrete beam could have been cultural noise created.

3.2.1.1 Estimation of Depth of Archaeological Relevance

The RTE magnetic gradient map was downward continued at 0.25 m interval to depth of 1.25m (Figs. 14a-e). This was to determine the relevant depth of archaeological interest from the magnetic map. The magnetic anomaly patterns were significantly retained up to 0.75 m and to some extent at 1.0 m (Figs. I4a-d) after which they were completely distorted. This implies that the maximum depth of significance of archaeological features at this site is slightly less than 1 m.

3.2.2 Resistivity Survey.

3.2.2.1 Micro Vertical Electrical Sounding (Micro VES)

Sixteen (16) Micro VES were carried out at the main survey area (Fig. 6a) to image the subsurface stratigraphy at shallow depth relevant to archaeological prospection. Although the analysis of the downward continued RTE magnetic gradient map shows that the effective depth

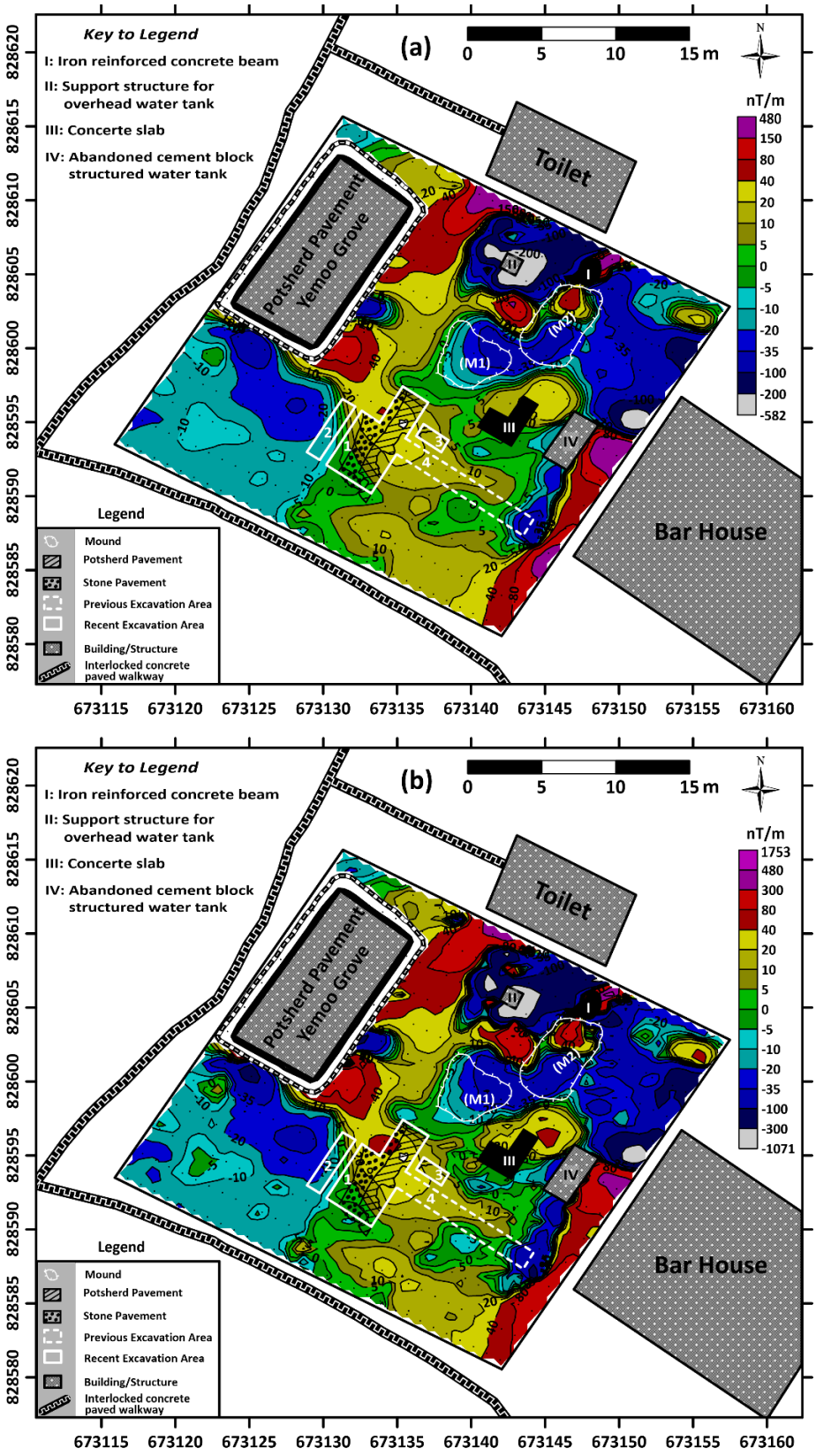

Fig. 14: Downward continued magnetic maps at (a) 0.25 m and (b) 0.5 m

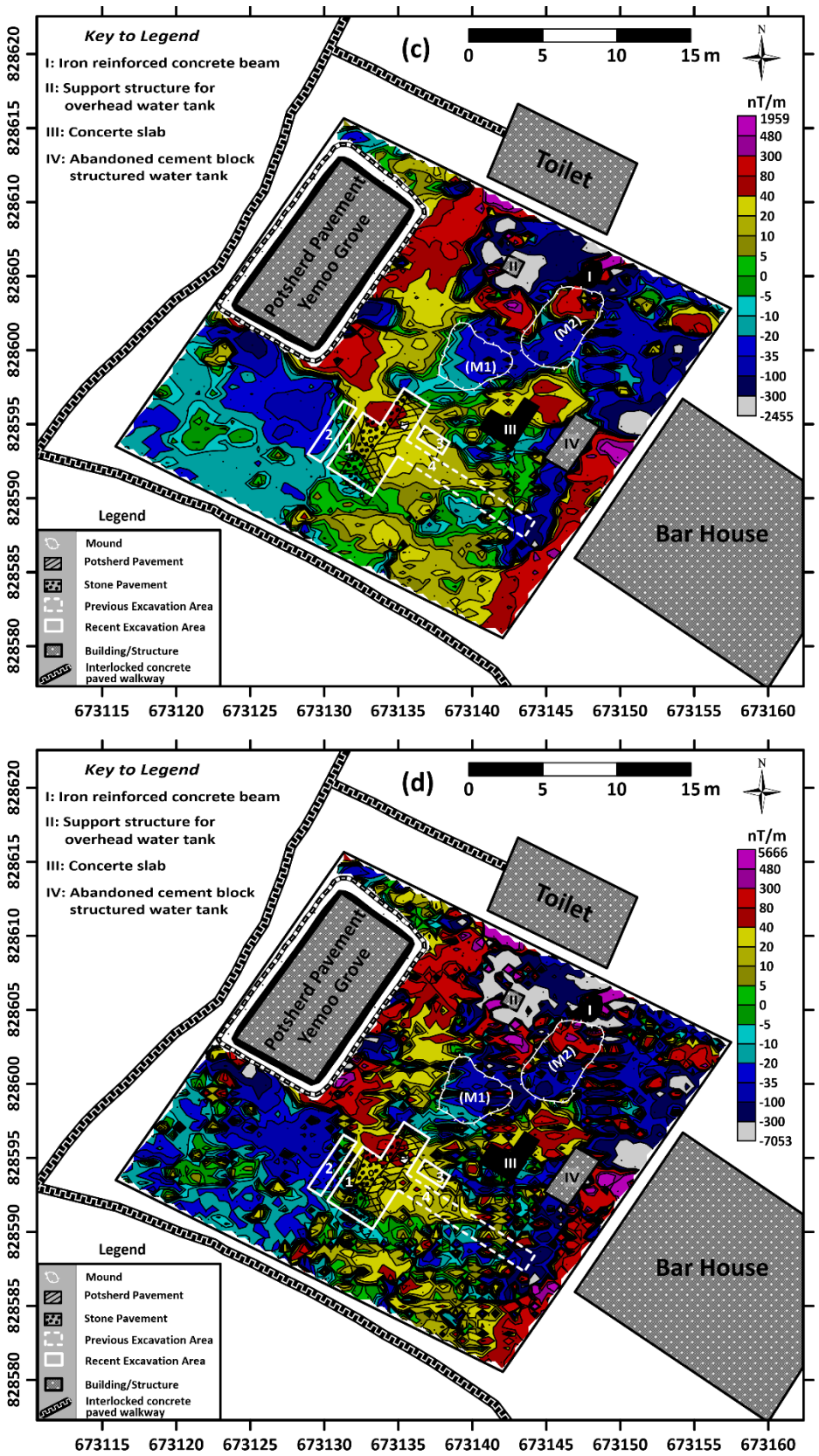

Fig. 14: Downward continued magnetic maps at (c) 0.75 m and (d) 1 m

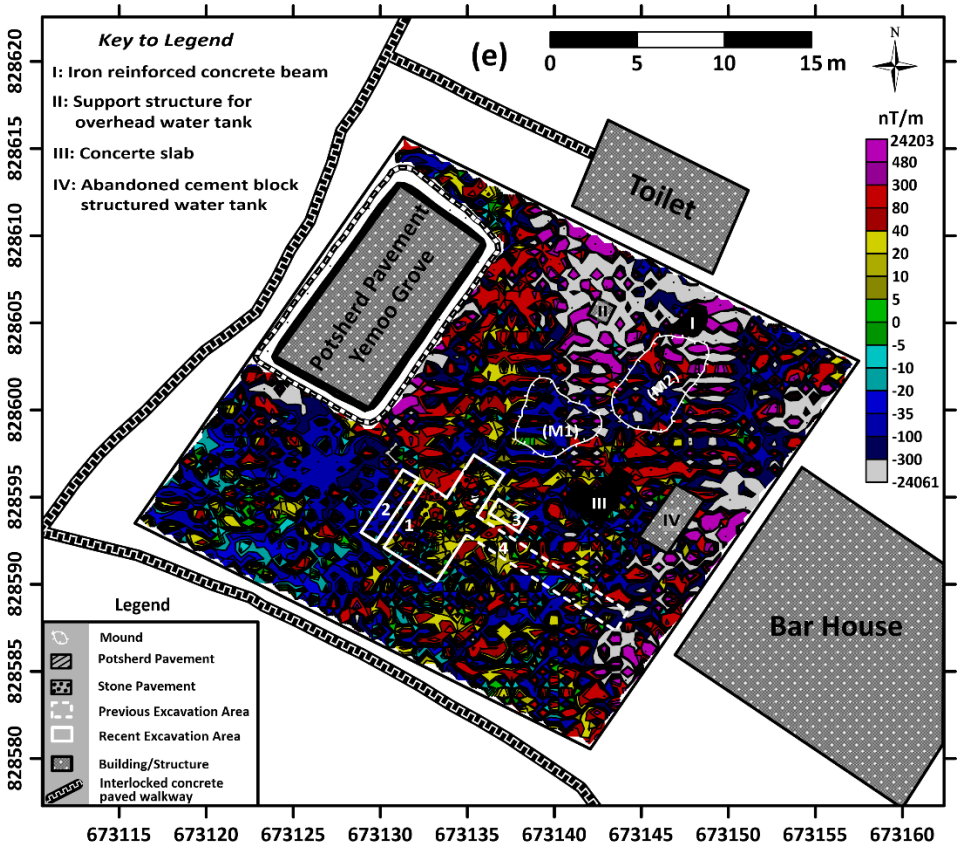

Fig. 14e: Downward continued magnetic map at 1.25 m

of relevance is less than 1 m, depth probing was extended to 2.5 m in order to assist the stratigraphic interpretation of the 2D images and the derivable resistivity depth slice maps. The VES points located within the excavated pits were to map the potsherd/stone pavement (as a stratigraphic unit) and determine the geoelectric characteristics (resistivity and thickness). These information could assist the interpretation of the 2D images for the identification of the horizon. Such information can also be used to constrain the interpretation of geoelectric sections beneath other micro VES locations, for possible existence of the pavement. The spatial distribution of the VES points are shown in Figure 6a. Within the limits of the current electrode spread (AB = 6 m), the observed VES curves vary from 2 – layer to A, K and KH type with the KH type predominating (75% of the total) (Fig. 15a and Table 3). The micro VES interpretation results are contained in Table 3 from which geoelectric sections were generated.

Table 3: Micro VES interpretation results at the main survey area.

VES NO.	DEPTH (m) $d_1/d_2/d_3/\ldots\ldots d_{n-1}$	RESISTIVITY (ohm-m) $\rho_1/\rho_2/\rho_3\ldots..\rho_n$	RESISTIVITY TYPE CURVE
1	0.07/0.18/0.87	47/240/95/239	KH
2	0.07/0.39	71/819/193	K
3	0.12/0.24	57/427/∞	A
4	0.07/0.33/1.5	66/375/68/∞	KH
5	0.03/0.16/0.34	6/41/25/245	KH
6	0.08/0.38/2.4	81/224/105/∞	KH
7	0.06/0.1/1.3	34/20,029/120/∞	KH
8	0.06/0.13/0.4	69/151/89/168	KH
9	0.08/0.4/2.0	46/244/58/∞	KH
10	0.05/0.09/0.44	36/311/80/∞	KH
11	0.06/0.14/0.8	70/171/97/∞	KH
12	0.06	50/179	2 – Layer
13	0.05/0.17/0.79	32/267/135/424	KH
14	0.19/1.1	47/83/416	A
15	0.08/0.53/2.5	48/191/88/∞	KH
16	0.09/0.43/2.0	74/316/107/∞	KH

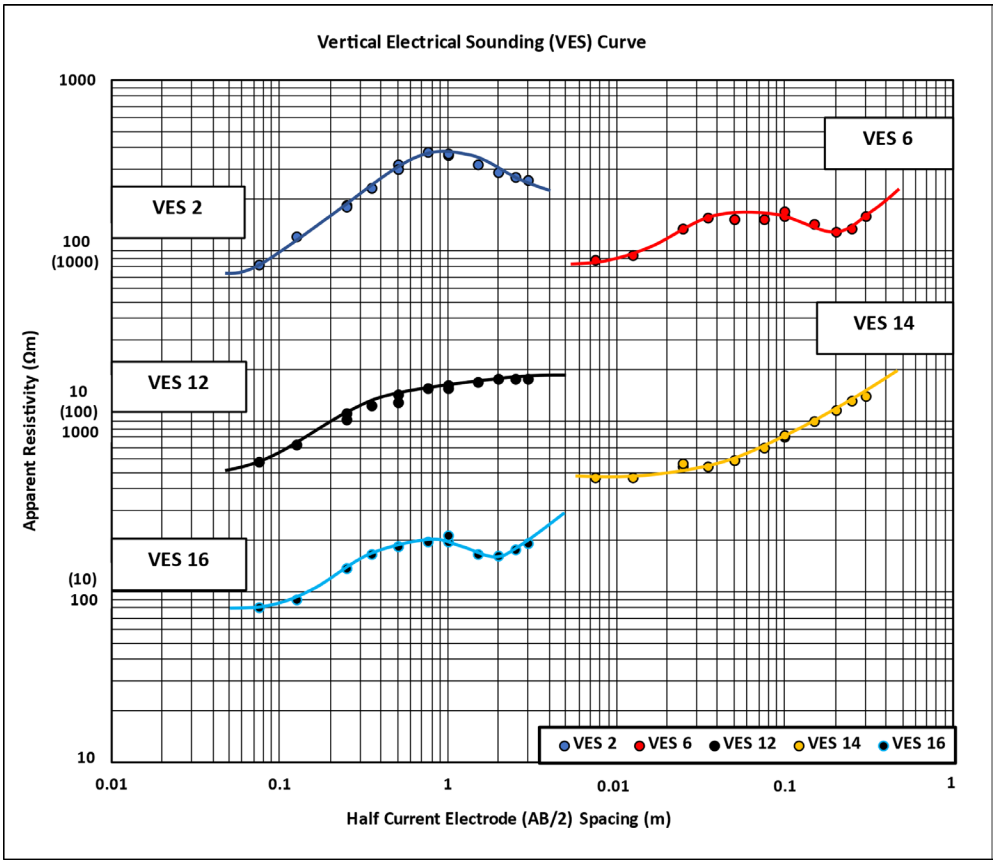

Fig. 15a: Typical VES type curves at the main survey area

Three geoelectric sections (Figs. 15b-d) were generated along two orthogonal sections (approximately SW-NE; SE-NW) and one through the excavated Pit 1 (approximately SSW-NNE) (see Fig. 6a). The geoelectric sections delineate maximum of four layers outside the excavated area, as detailed below

1st Layer: Topsoil
Resistivity: 36 -179 ohm -m; Thickness: 0.03 – 0.19 m
(60 ohm-m at water logged VES 5)

2nd Layer: Lateritic Clay (I)
Resistivity: 151 -819 ohm-m; Thickness: 0.04 – 0.45 m
(41 ohm-m at waterlogged VES 5)

3rd Layer Weathered Layer or Fill? (composed of clay/sandy clay)
Resistivity: 25 – 193 ohm – m; Thickness; 0.18 – 1.97 m

4th Layer: Lateritic Clay (II)
Resistivity: 168 – ∞ ohm-m; Rockhead at: 0.33 – 2.5 m

Within the excavated area and beneath VES 7 and 3 (Fig. 15d) containing a fill, the stratigraphy has been altered to three geoelectric layers, as detailed below.

1st layer: Topsoil (upper fill of excavated soils)
Resistivity: 34 – 57 ohm - m; Thickness: 0.1 – 0.12 m

2nd Layer: Fill (excavated soils/coarse grained pegmatite gangue)
Resistivity: 120 – 427 ohm; Thickness: 0.12 -1.2 m
(spurious high resistivity of 20,029 ohm-m beneath VES 7)

3rd Layer: Potsherd Pavement/Lateritic Clay (II)
Resistivity: ∞ ohm-m; Rockhead at: 0.24 -1.2 m

Comment: The potsherd interface is lined with an impermeable poorly conductive polyethylene nylon. This may have been responsible for the anomalous infinitely resistive potsherd/lateritic clay layer resistivity. The overlapping resistivity of the pavement with that of the underlying layer and the very small thickness may have caused the pavement to be suppressed and its identification as a stratigraphic unit virtually impossible. Also, because the excavated pits were not backfilled to the ground level and fill settlement had taken place consequent of heavy rainfall, depths to top of pavements from VES could have been under estimated.

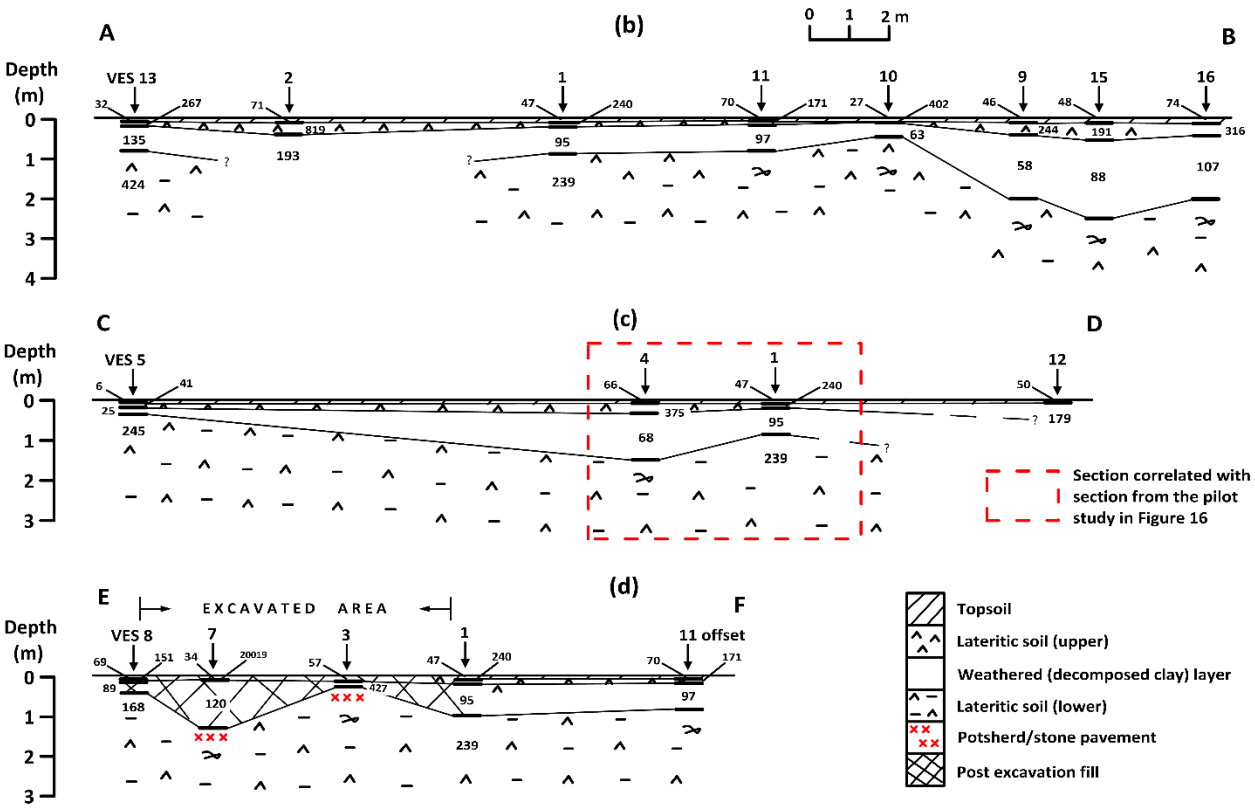

Fig. 15: Geoelectric sections beneath traverses (b) A – B (c) C – D and (d) E - F

Deductions

(i) The geoelectric sections identify maximum of four geoelectric layers in the upper 2.5 m two of which are relatively high resistivity lateritic clay (I & II). Figure 15d indicates that the excavated stone/potsherd pavement may have been founded on the upper and deeper lateritic clay with pavements encountered at varying depths of between 0.10 and 1.2 m and 0.24 m beneath VES 7 and 3 respectively. The exposed potsherd pavements at the pilot study site may have been founded on the upper lateritic clay (I) (Fig 16). Figure 16 compares a section of geoelectric section C - D (Fig. 15c) with the geoelectric section developed at the pilot study site.

(ii) If as speculated, the potsherd pavement identified within the recently excavated site at the main study area is founded directly on the lateritic clays with overlapping resistivity values, this very thin (0.03 – 0.04 m) pavement, at deep depth, may be difficult to delineate as a separate stratigraphic unit due to suppression. The use of micro VES to identify such unit will therefore be limited to the near-surface.

(iii) The upper lateritic clay (I) occurs generally in the upper 0.5 m with its interface at less than 0.1 m below the ground level in most places. Resistivity maps generated at very shallow depth will be influenced by its resistivities and that of the overlying equally high resistivity upper pavements, as experienced at the pilot study site.

3.2.2.2 2D Dipole-Dipole Imaging

As in the pilot study, the 2D dipole-dipole data were presented as apparent resistivity maps for different expansion factors (n = 1-5) using the observed field data and as resistivity depth slice maps generated from extracted inverted true resistivity values from 2D images between some depth intervals. Resistivity data for these maps were generated from fourteen (14) main and seven (7) orthogonal traverses.

(i) Apparent Resistivity Maps

The apparent resistivity maps (Figs. 17a-e) were developed for expansion factors n = 1 – 5 and specific theoretical depths of 0.59, 0.78, 0.98, 1.17 and 1.37 m. The stone/potsherd pavement encountered within Pit 1 occurs at near-surface (almost outcropping at the SSW edge of the pit) and with other depths ranging from 0.4 to 1.0 m below the ground level. The chosen depths of investigation cover the depths of occurrence of the pavements. A small outcrop of a potsherd pavement is located at the SSE edge of the survey area.

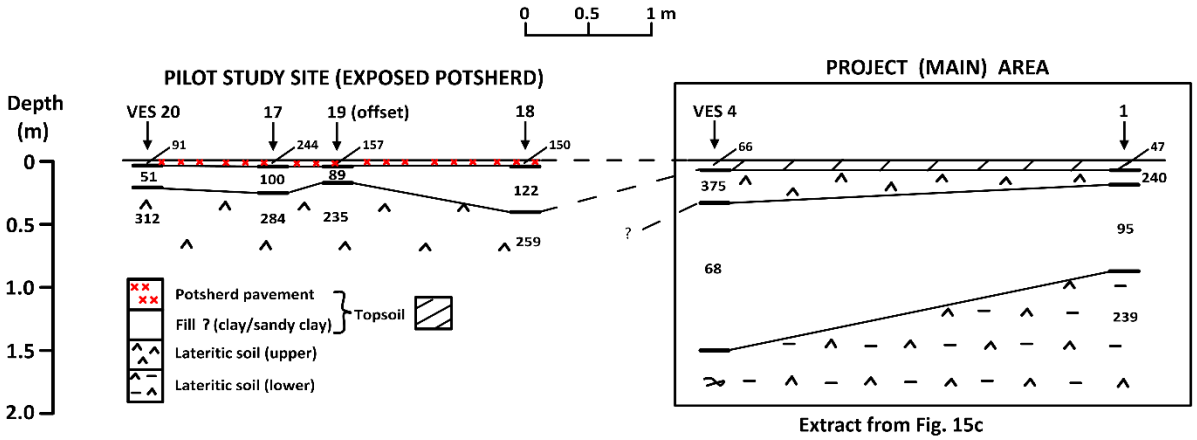

Fig. 16: Stratigraphic correlation between (a) pilot study area and (b) the main survey area

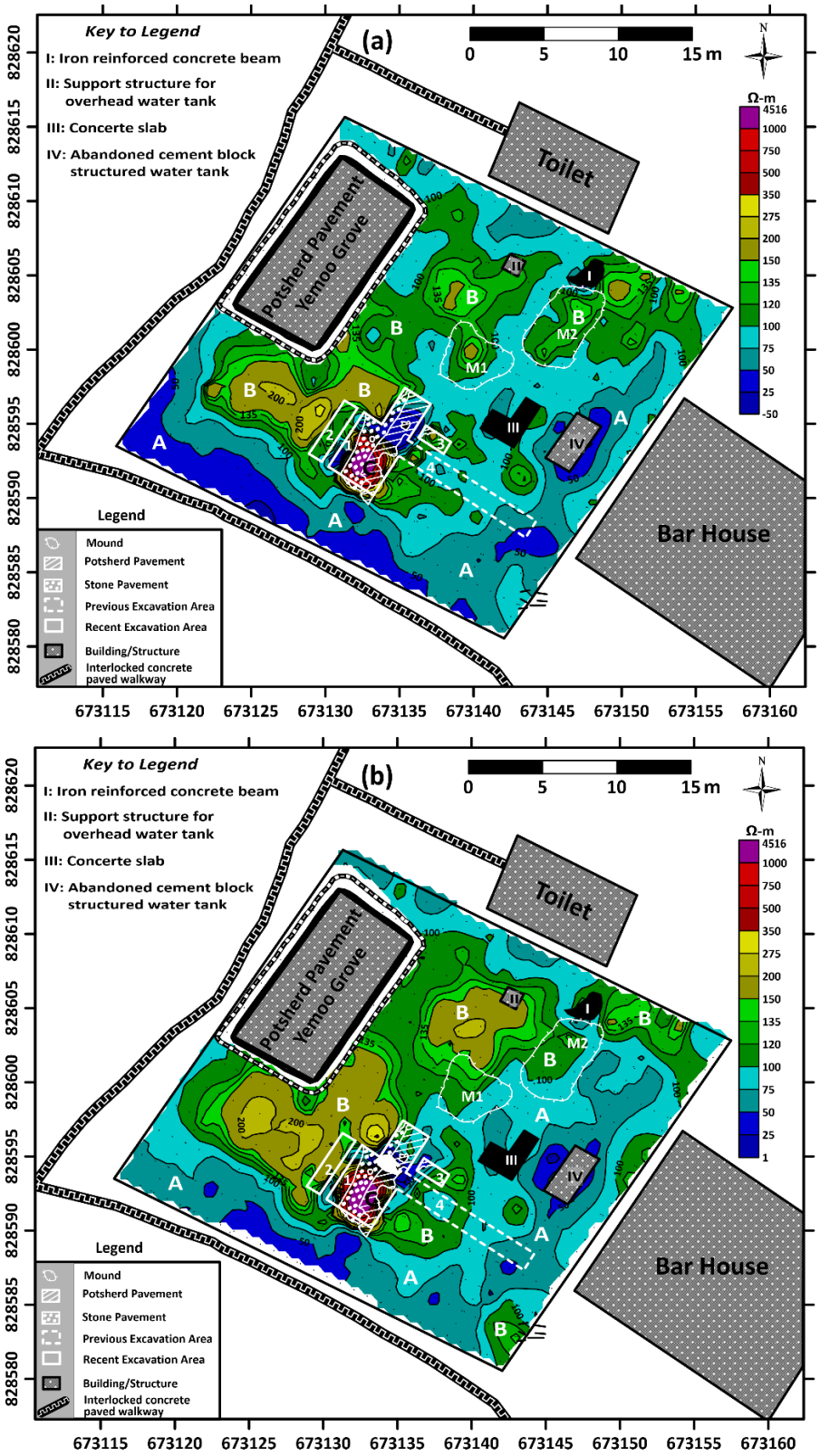

Fig. 17: Apparent resistivity maps at (a) expansion factor (n) of 1 and theoretical depth of 0.59 m and (b) expansion factor (n) of 2 and theoretical depth of 0.78 m

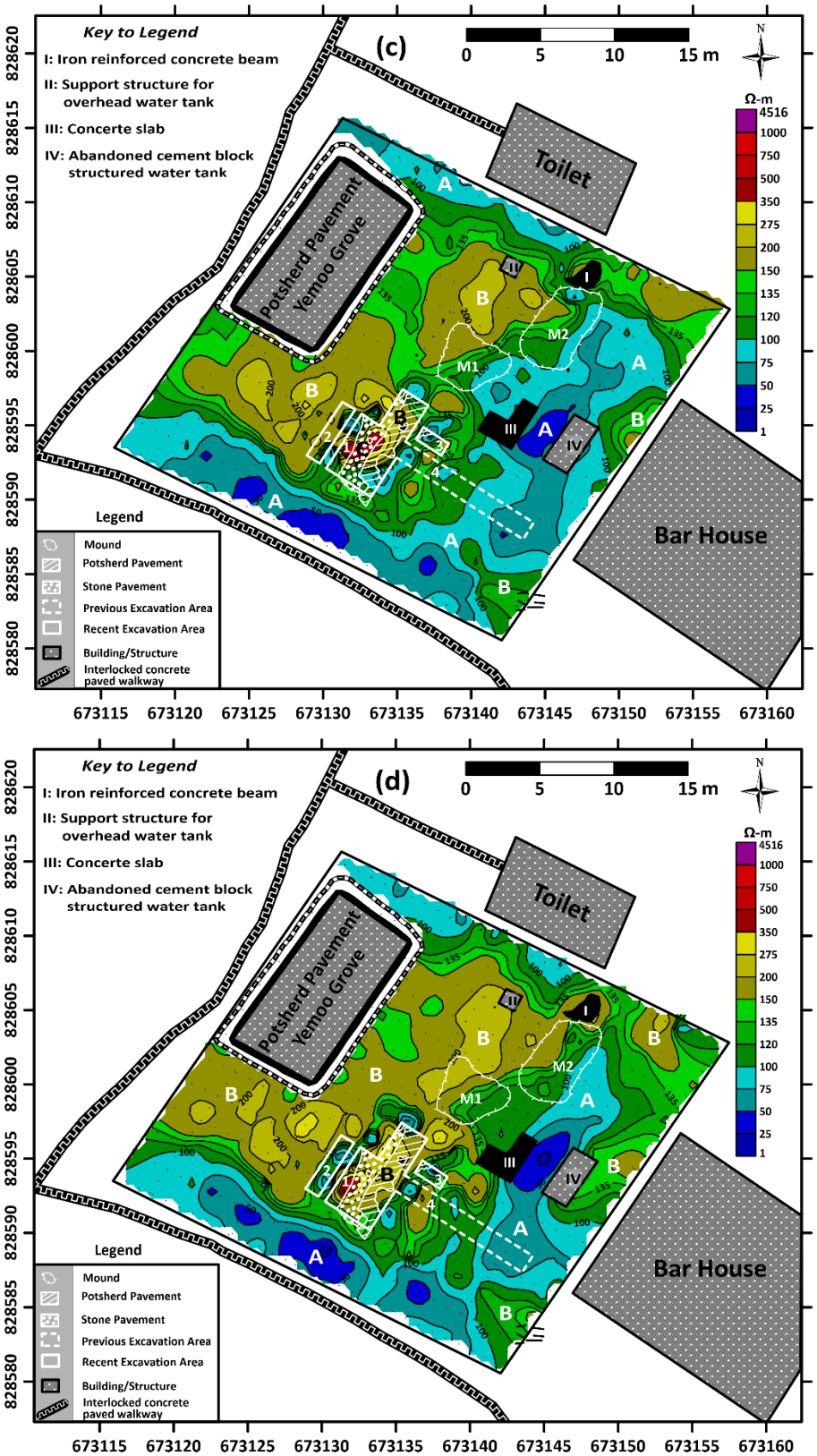

Fig. 17: Apparent resistivity maps at (c) expansion factor (n) of 3 and theoretical depth of 0.98 m and (d) expansion factor (n) of 4 and theoretical depth of 1.17 m

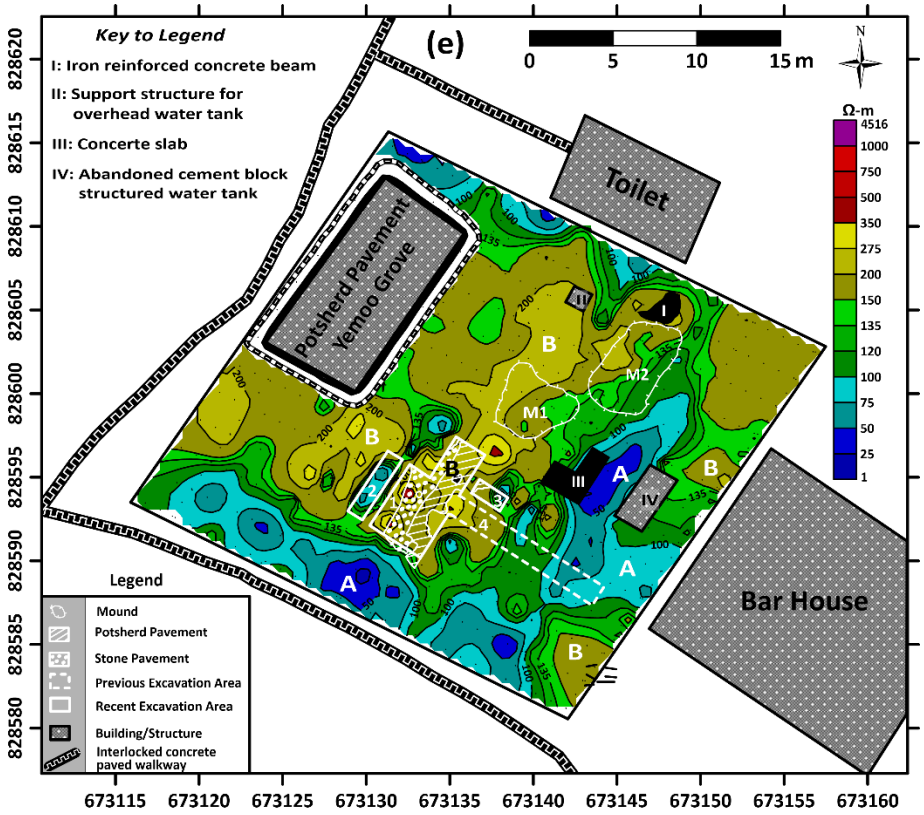

Fig. 17e: Apparent resistivity maps at expansion factor (n) of 5 and theoretical depth of 1.37 m

Figure 17a shows the apparent resistivity map at 0.59 m depth level. The resistivity values range from 1 to 2837 ohm-m. Based on color range/contour lines, the survey area can be classified into three zones – A, with resistivity values of 1 – 100 ohm-m and colour range of light to deep blue; B, with resistivity values of 100 – 350 ohm-m and colour range of deep green to light brown and yellow and C (in purple colour), with resistivity values in the range of 350 - 2837 ohm-m. Zone C falls on the near-surface segment of the stone/potsherd pavement with overlying coarse grained pegmatite gangue in Pit 1. The second half of the pavement displays spurious low resistivity anomaly (typical of zone A) created by a water logged fill. The impermeable polyethylene nylon lining inhibit infiltration of rain water into the subsurface thereby precipitating fill water-log. The barren section of this pit displays zone A with characteristic low resistivity values. The barren Pit 2 and Pit 3 with small find of potsherd fall on the low spectrum end of the resistivity range of zone B. The map indicates that the stone/potsherd pavement likely extends westwards and is characterized by resistivity values in the range of 150 – 350 ohm-m in zone B. The low resistivity (1 - 100 ohm-m) zone A constitutes the background resistivity range covering the rain water runoff-fed (from interlock walkway pavement) southern/southwestern edge, the southeastern/eastern flank and parts of the central and northern flanks. The weathered and water-logged relics of potsherd pavement identified within this zone may have displayed false low resistivity anomaly due to its saturated state. Zone B resistivity (100 – 350 ohm-m) closures (including the mounds), as identified, is the major archaeologically prospective zone. It will be recalled that the micro VES at the pilot study site puts potsherd pavement resistivity at 90 - 244 ohm-m range.

The very low resistivity (typical of zone A) and the extremely high resistivity (typical of zone C) observed over the stone/potsherd pavement bearing Pit 1 are consequence of the state and nature of the fill and may not be reflective of the true resistivity values of the pavement.

At 0.78 m depth level (Fig. 17b), the resistivity map retains significantly the anomaly patterns at 0.59 m depth level. The low resistivity (1 - 100 ohm-m) zone A remains the background resistivity range while the intermediate resistivity (100 – 350 ohm-m) zone B also retains its geometry significantly with the inner 150 - 350 ohm-m region expanding at the western and north central flanks. The low resistivity (zone A) at the NNE end and the high resistivity (zone C) at the SSW segment of stone/potsherd pavement laden Pit 1 are considered artificial, as earlier explained. The exposed potsherd pavement at the southeastern corner of the survey area displays appropriately

high resistivity values (100 - 135 ohm-m) at this depth level. This map also reinforces the inference that the stone pavement likely extends beyond Pit 1 westwards and that a pavement may exist beneath the presently barren Pit 2 at deep depth. It also shows, like the resistivity map at 0.59 m depth level, that no pavement exists beyond the present southern-southwestern edge of Pit 1. A significant segment of the SE trending Pit 4 could be barren.

At the depth level of 0.98 m (recall the magnetic derived depth of significance of archaeological features of about 1.0 m), the apparent resistivity map (Fig 17c) retains significantly the zonal geometries of Figure 17b (0.78 m depth) with slightly enlarged upper spectrum (150 – 275 ohm-m) of the intermediate resistivity zone B. It displays relatively high resistivity on the stone/potsherd pavement and indicates possible presence of pavement within a segment of the currently barren Pit 2 at this depth level while creating for the first time, a small high resistivity closure at the northeastern edge of Pit 1. It confirms that Pit 4 could still be barren at this depth while reinforcing the intermediate resistivity over the exposed potsherd pavement at the SE edge of the survey area and a new zone B northeast of the abandoned cement block structured water tank. At 1.17 m and 1.37 m depth levels (which are below the magnetic derived archaeological depth of significance of 1.0 m) the apparent resistivity maps (Figs. 17d&e) are in most cases reflective of the high resistivity lateritic clay (II). The anomaly patterns are not significantly different from that of 0.98 m depth level except that the central high resistivity (150 – 350 ohm-m) segment of zone B are now fragmented. The stone/potsherd laden Pit 1 displays intermediate resistivity while Pits 2, 3 and 4 are barren at these depth levels. At these depth levels, it is difficult to differentiate anomalies due to pavement from that of lateritic clay because of overlapping resistivity values (91 – 244 ohm–m from pilot study for potsherd pavement; 100 – 350 ohm-m intermediate resistivity range for stone/potsherd pavements from the main site and 168 - ∞ ohm–m for lateritic clay II from the geoelectric sections).

Apart from the spurious anomalously low/high resistivity values over the excavated stone/potsherd pavement arising from water-logged excavated soil/fill and coarse grained pegmatite gangue respectively, the apparent resistivity maps for depth levels of up to 0.98 m (within the magnetic derived optimum 1 m depth of significance of archaeological features) are diagnostic of excavated pavements and exposed pavement within the investigated survey area. These archaeological features are characterized by intermediate resistivity values in the range of 150 – 350 ohm–m. This

range of value overlaps with the range of 91 – 244 ohm-m established through micro sounding for an exposed potsherd pavement at a pilot study site within Ita Yemoo. The maps also accounted for the barrenness of Pits 2 and 4 but indicate the possibility of encountering pavements at depths of 0.78 – 0.98 m beneath Pit 2. The maps also establish possible extension of stone/potsherd pavement beyond the excavated Pit 1 westwards and into around the northcentral region. The coincidence of intermediately high resistivity closures over mounds M1 and M2 and at the southern edge of Yemoo Groove with magnetic low (negative polarity) anomalies could indicate existence of archaeological features (Olorunfemi *et al.,* 2019, Oni *et al*., 2022 and Olorunfemi *et al*. 2022).

(ii) 2D Resistivity Depth Slice Maps

Figures 18(a–e) display typical 2D resistivity images with correlated 1D micro VES interpretation models which show good correlation between the 2D and 1D models. The 2D resistivity images along traverses TR4 – 6 identify the spurious anomalously low resistivity values within the recently excavated pits and depth variations from the ground level to the top of the pavement which range from almost (zero) 0 m to about 1.2 m. The poorly conductive polyethylene nylon lining above the stone/potsherd pavement must have created the image of the very resistive layer (in purple colour) beneath the pavement. Figure 19 compares 2D resistivity models generated along traverse TR 10 with dipole lengths of 1.0 m (a) and 0.5 m (b). At the maximum depth (1.5 m) of imaging of the 0.5 m dipole length, the 2D resistivity image compares perfectly well with the 1.0 m dipole length 2D resistivity image, indicating that either of the dipole lengths is adoptable.

Resistivity depth slice maps were generated for 0 – 0.5 m; 0.5 – 1.0 m, 1 - 2 m and 2 - 3 m depth ranges (Figs. 20a-d). Going by the magnetic derived depth of archaeological significance of slightly less than 1.0 m, only the 0 – 0.5 m and 0.5 – 1.0 m depth slice maps are expected to be relevant.

Figure 20a displays the resistivity depth slice map for the depth range of 0-0.5 m. The true resistivity values range from 2.1 to 1232 ohm-m which can also be classified into three resistivity zones – low resistivity zone A (2.1 – 100 ohm-m), intermediate resistivity zone B (100 – 350 ohm-m) and high resistivity zone C (350 – 1232 ohm-m). This map compares significantly well

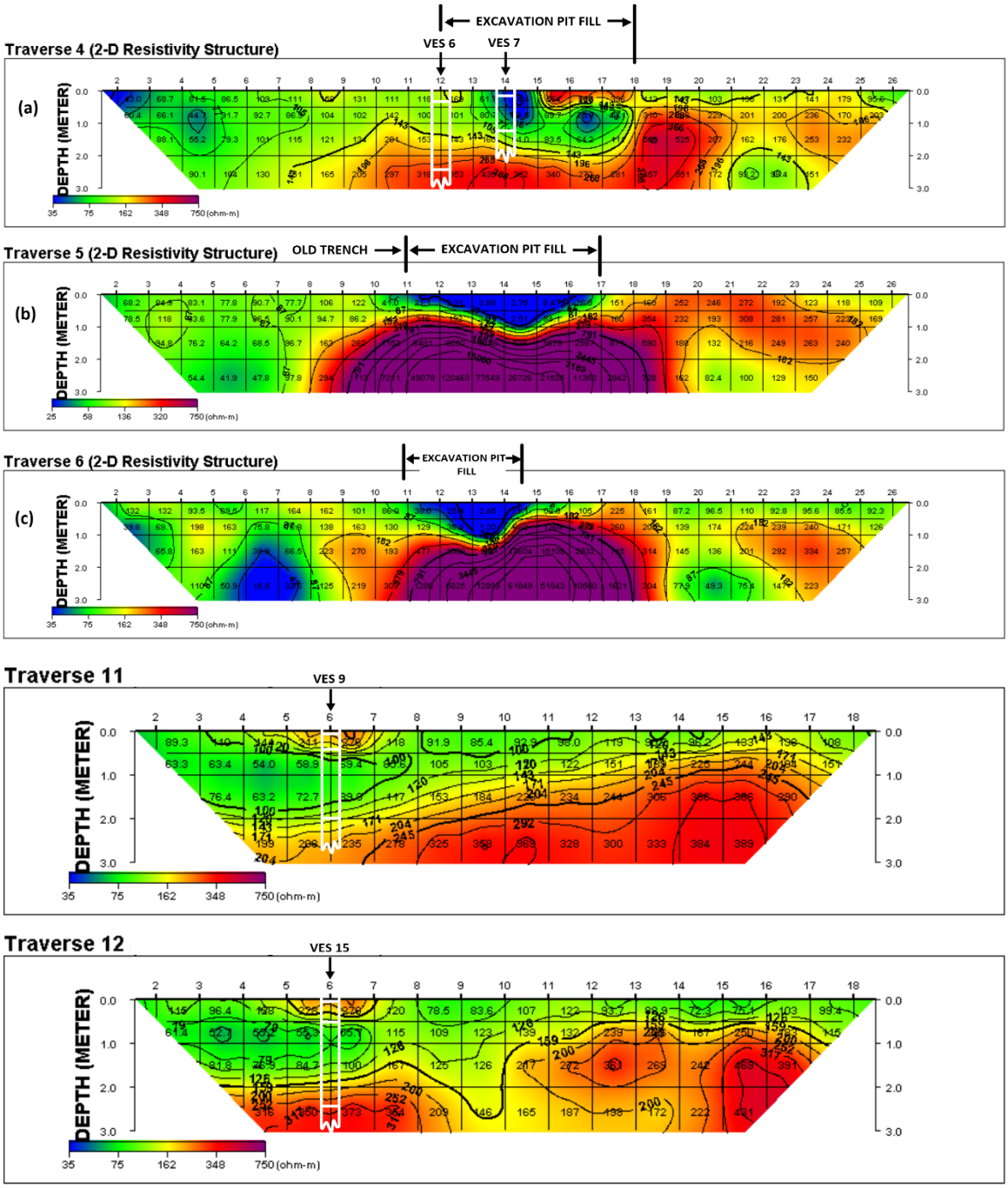

Figs. 18a-e: Typical 2D resistivity images with correlated 1D micro VES interpretation models at the main survey area

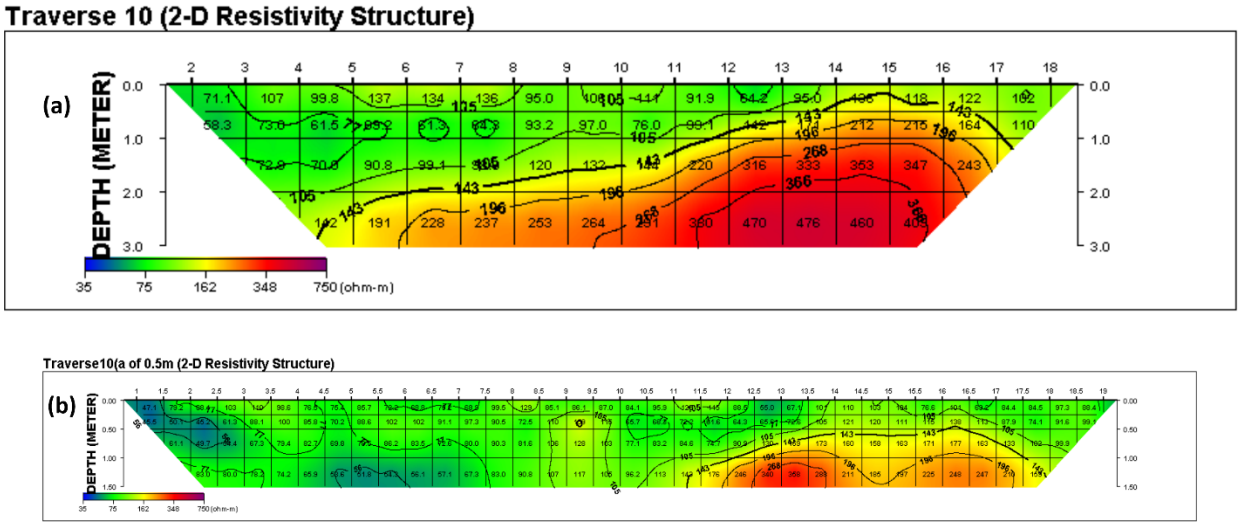

Fig. 19: Comparison of 2D resistivity images generated along traverse TR10 with dipole length of (a) 1.0 m and (b) 0.5 m at the main survey area

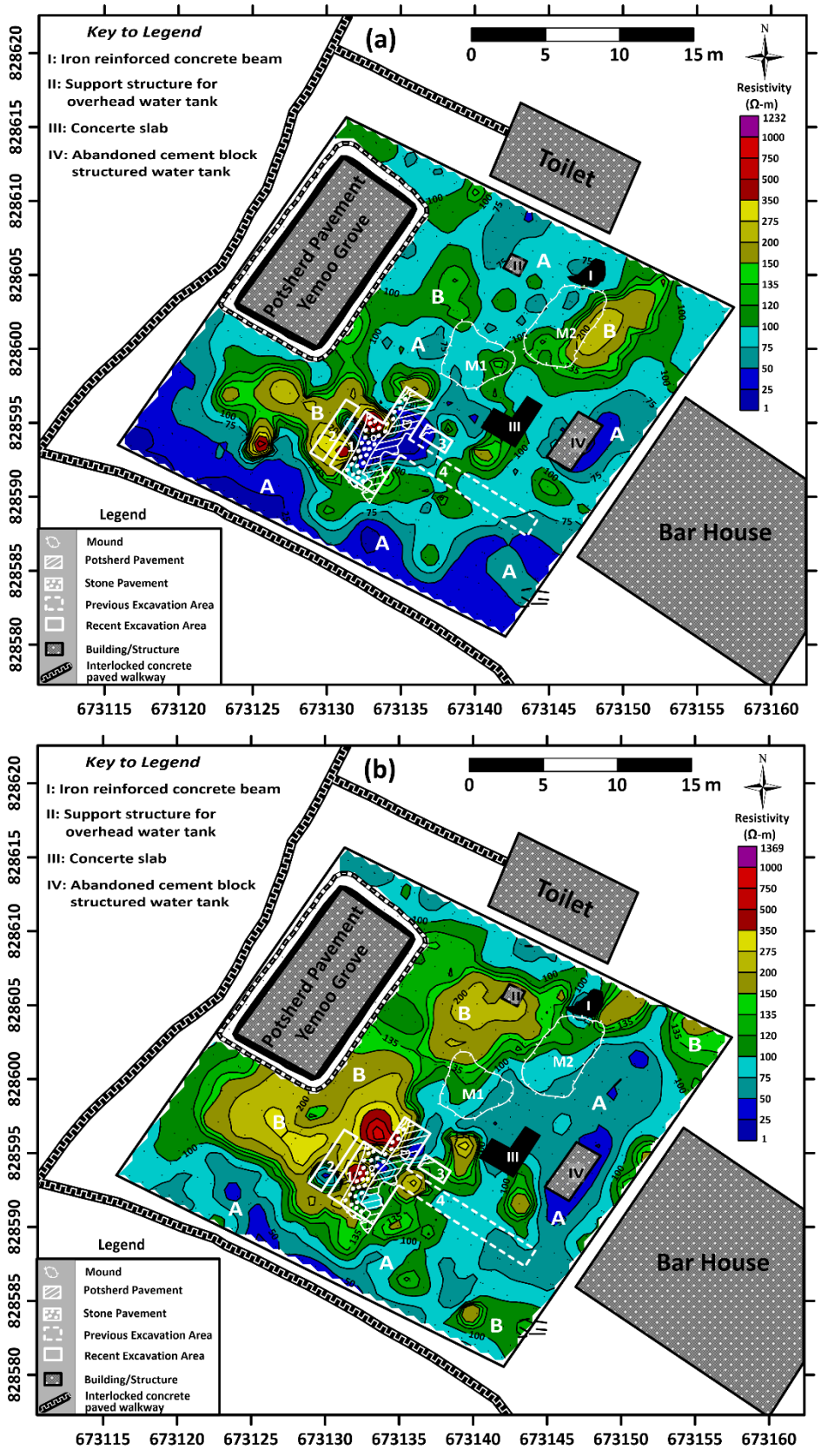

Fig. 20: Resistivity depth slice maps at (a) 0 – 0.5 m and (b) 0.5 – 1.0 m

with the apparent resistivity map at 0.59 m (Fig.17a). The low resistivity displayed within Pit 1 over the stone/potsherd pavement is anomalous, as displayed on the 2D resistivity images along traverses TR4 - 6 (Figs. 18a-c). This is due to water logged fill above the impermeable polyethylene nylon lining. The low resistivity zone A constitutes the background resistivity with no prospect for archaeological feature. The exposed potsherd pavement at the southeastern edge is weathered and waterlogged with consequently low resistivity value. Zone B and C are the prospective zones within this map which indicates the extension of pavement occurrence westward from the current excavated Pit 1. There are prospects beneath mounds M1 and M2 and in the area east of mound M2. The map indicates low prospect, if any, beneath Pit 4 and Pit 3 within these depth level.

The 0.5 – 1.0 m resistivity depth slice map (Fig. 20b) compares significantly well with the apparent resistivity map at 0.98 m depth level (Fig. 17c) in anomaly patterns. The map reinforces the possible extension westward of the excavated pavement within Pit 1 with characteristic intermediate resistivity range of 100 – 350 ohm-m (zone B) and > 350 ohm-m (zone C) and the possibility of encountering pavement beneath the currently barren Pit 2 at deep depth of between 0.5 and 1m. It shows that the possibility of encountering pavement beneath Pit 3 at this depth is remote. The map also forestalls the extension of the currently excavated pavement within Pit 1 south-southwestward. It creates an isolated intermediate anomaly closure south of mound M1. Both 1 - 2 m and 2 - 3 m resistivity depth slice maps (Fig. 20c&d) are beyond the depth of archaeological relevance and are more reflective of the high resistivity lateritic clay (II) (see Fig. 15).

It seems that only 0 - 0.5 m and 0.5 – 1.0 m depth slice maps are diagnostic of possible existence of stone/potsherd pavement. The maps are however not as distinctive as the equivalent apparent resistivity maps at comparable but depth specific levels of 0.59, 0.78 and 0.98 m.

3.2.3 Ground Penetrating Radar Survey

As at the time we carried out the pilot study on the outcropping potsherd pavement in front of the Heritage Multipurpose Hall, we did not have access to a Ground Penetrating Radar (GPR) equipment. It was therefore not possible for us to develop a template or GPR characteristics for the identification of potsherd pavement at the main study area. The GPR field design (Fig. 6b) involved 2D coverage at 1 x 2 m grid network (for a 28 x 26 m block) spanning the entire study

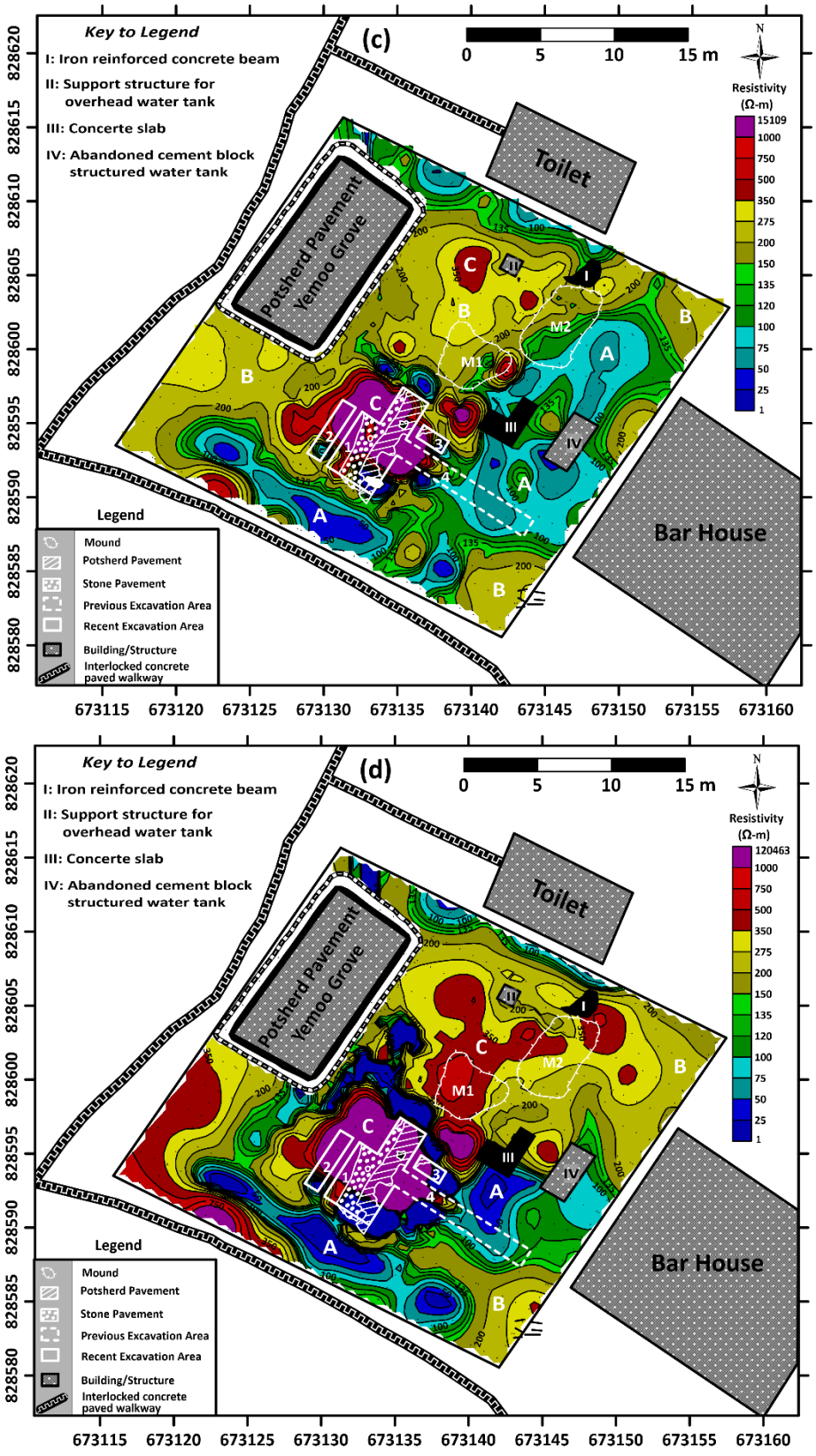

Fig. 20: Resistivity depth slice maps at (c) 1.0 – 2.0 m and (b) 2.0 – 3.0 m

area and 3D denser coverage with 1 x 1 m grid network (for a 14 x 18 m block) covering the recently/previously excavated Pits 1 – 4 and two suspected mounds.

We intend to use the 3D dense coverage to do both pilot and detailed study over the excavated area with finds within the pits as control. This was to enable us to assess the potency of the geophysical method in pavement mapping. The field layout, as configured by the GPR recorder with superimposed features, is displayed in Figure 21. The prospecting frequency in this study was 450 MHz with estimated 5.0 m depth of investigation. This investigation involved nineteen (19) in-line (main) traverses and fifteen (15) cross-line (orthogonal) traverses (Fig. 21).

3.2.3.1 GPR Radargrams (3D Data Coverage)

Representative depth-amplitude vertical sections (radargrams) are shown in Figs. 22(a-h). The amplitudes of the radar reflections are displayed in colour menu with strongest reflections in brightest (yellow/red) colour. High amplitude, significantly continuous, and traceable reflection signals characteristic of high dielectric contrasting features (including stone/potsherd pavement) are limited to virtually the upper 1 m of the radargrams. Below this depth level, the resolution of the radargrams decreased substantially.

Figure 22a shows the radargram along in-line 6 (TR 4, Fig. 6b) that traversed the potsherd/stone pavement between stations 6 and 9 (Fig. 21). Beneath VES 7, the potsherd pavement occurs at depth of 0.1 m while the suspected pavement high amplitude reflection occurs at depth of about 0.25 m. The pavement did not extend to the southeastern edge of Pit 1 as corroborated by the referenced traced reflections (see Fig. 22a). The radar reflections can be traced within the excavated area with possibility of extending northwestward (Fig. 22a) through stations 9 to 11, at deeper depths of 0.4 – 0.5 m. This implies that there is the possibility of pavement occurring within the presently barren portion of Pit 1 and extending to the presently barren Pit 2, at deep depth. Also apparent from this radargram are diffractions at the edges of the pits and the likely existence of high amplitude reflections at shallow depth (0. 25 m) between stations 0 -2.

Figure 22b displays the radargram beneath in-line 8 (TR 5, Fig. 6b) where potsherd/stone pavement was excavated between stations 7 and 9.5. Beneath VES 3, the pavement interface was delineated at a depth of 0.24 m while a high amplitude reflection characteristic of the pavement occurs at depth of about 0.5 m. The GPR section shows that the pavement interface drops to about 0.75 m beneath station 8.5 with the likelihood of its extension northwestward through the

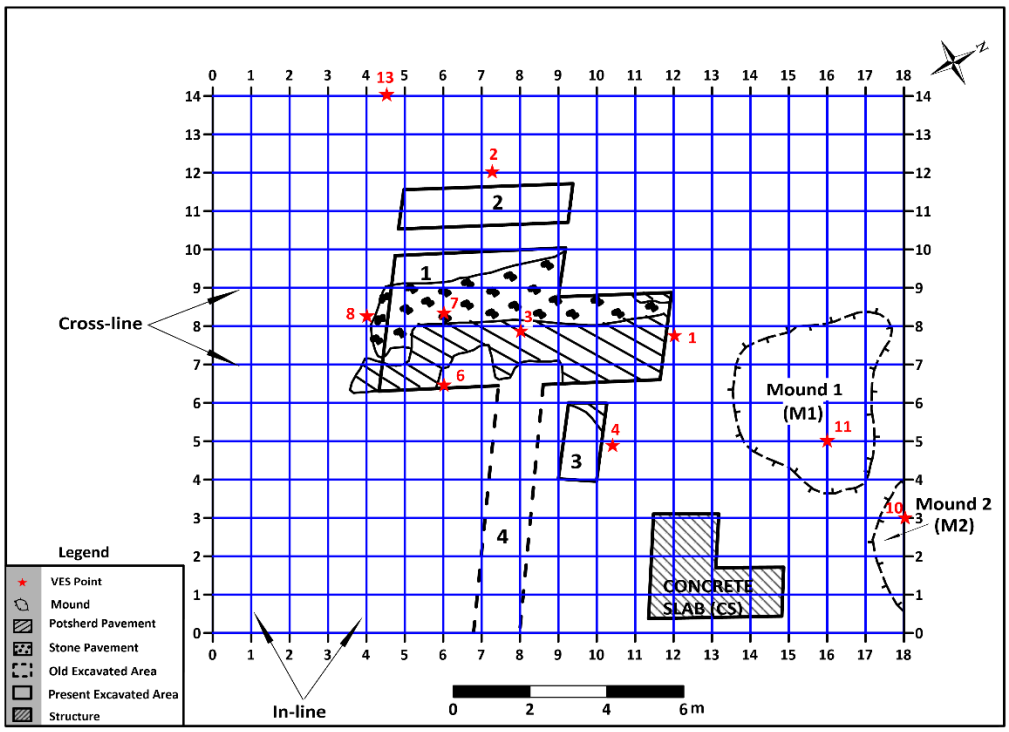

Fig. 21: GPR 3D (1×1 m) grid network

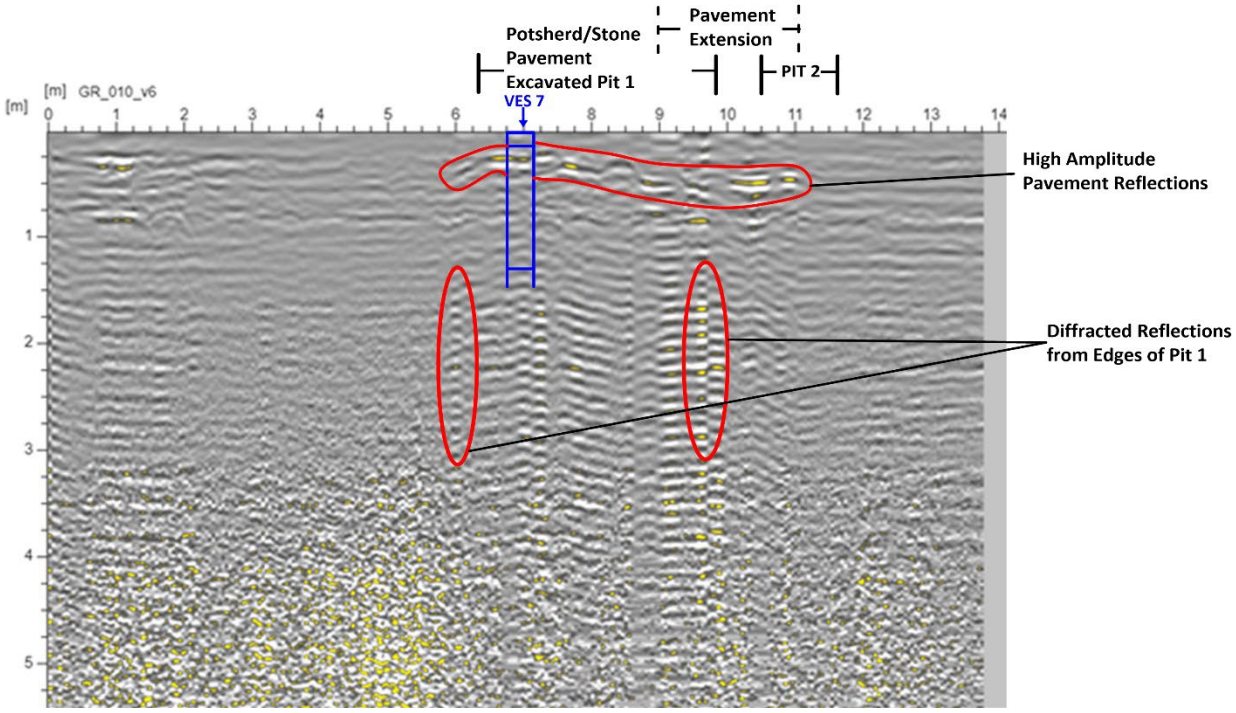

Fig. 22a: Vertical section radargram along In-line 6 (TR 4)

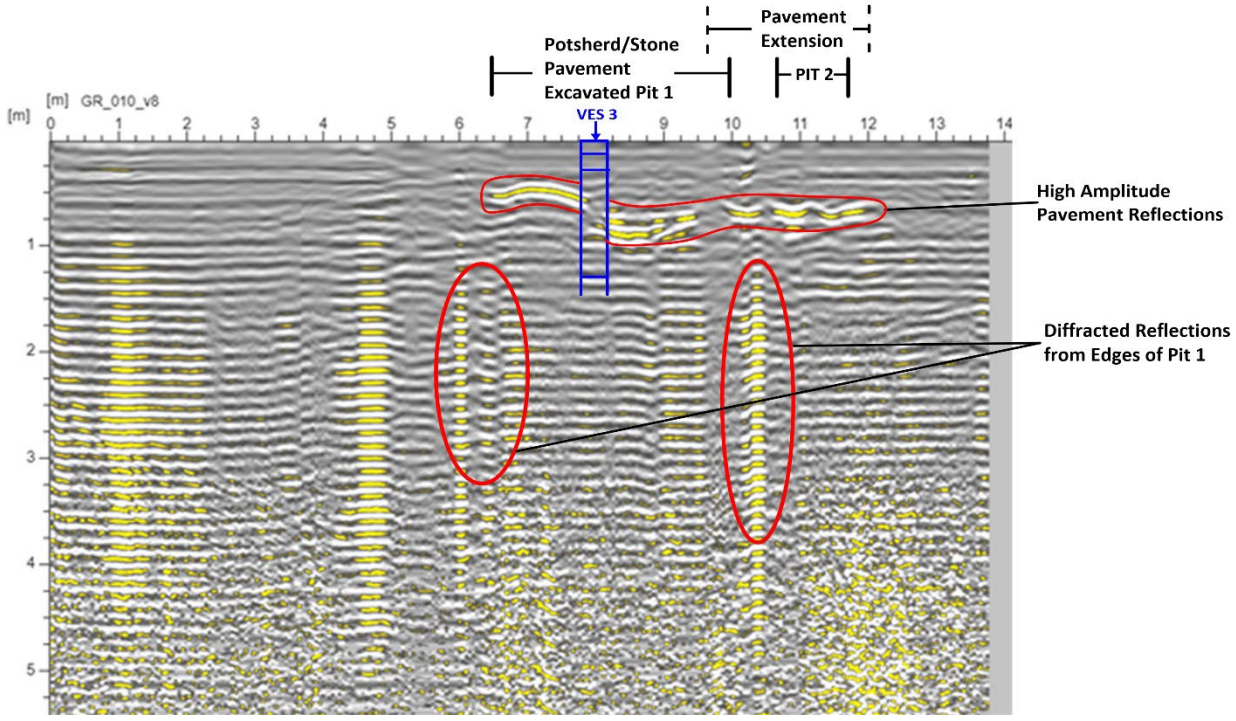

Fig. 22b: Vertical section radargram along In-line 8 (TR 5)

barren Pit 2 to station 12. There are also evidences of pit edge radar diffractions on the radargram. The under estimation of depths to the pavement at shallow depth beneath VES stations 7 and 3 within Pit 1 (Figs. 22a&b), as explained in section 3.2.2, is attributable to the fact that the recently excavated Pits 1-3 were not backfilled to ground level and had experienced settlement due to heavy rainfall.

Figure 22c presents the radargram generated beneath in-line 10 (TR 6, Fig. 6b). Continuous high amplitude reflections occur between stations 6.5 and 13. Potsherd/stone pavement was encountered between stations 6.5 and 9 at depths ranging from 0.5 – 0.8 m with the likelihood of its extension northwestward to station 13.

The radargram beneath in-line 12 (TR 7, Fig. 6b) is presented in Figure 22d. High amplitude reflections typical of pavement are delineated between stations 1-3 beneath the cement concrete slab and between stations 8 and 9 (northeastern edge of the stone pavement in Pit 1). The stone pavement is at depth of about 0.6 m - 0.7 m. The suspected stone pavement beneath the cement concrete slab occurs at depths of 0 – 0.25 m.

Four typical cross-lines (orthogonal traverses) radargrams (Figs. 22e–h) will also be presented and discussed.

Figure 22e displays the radargram along cross-line 7 (TR 17e, Fig. 6b) which traversed the excavated potsherd between stations 4 and 12. High amplitude radar reflections characteristic of potsherd pavement exists between the referenced stations and at depth varying from zero at the southwestern edge of Pit 1 to 0.5 – 0.6 m towards station 11 at the northeastern end. Between stations 11 and 12 the pavement seems to occur at shallow depth of about 0.25 m with no evidence of extension. The anomalous radar diffractions at around station 16 occur beneath mound M1.

Figure 22f presents a radargram that traversed the stone pavement along cross-line 9 (TR 18, Fig. 6b) between stations 4.5 and 9. The traced high amplitude reflections characterized the stone pavement at depths varying from near zero to about 0.8 – 0.9 m beneath station 8/9 where excavation was terminated. This section however shows that the stone pavement likely extends to station 12, northeastwards.

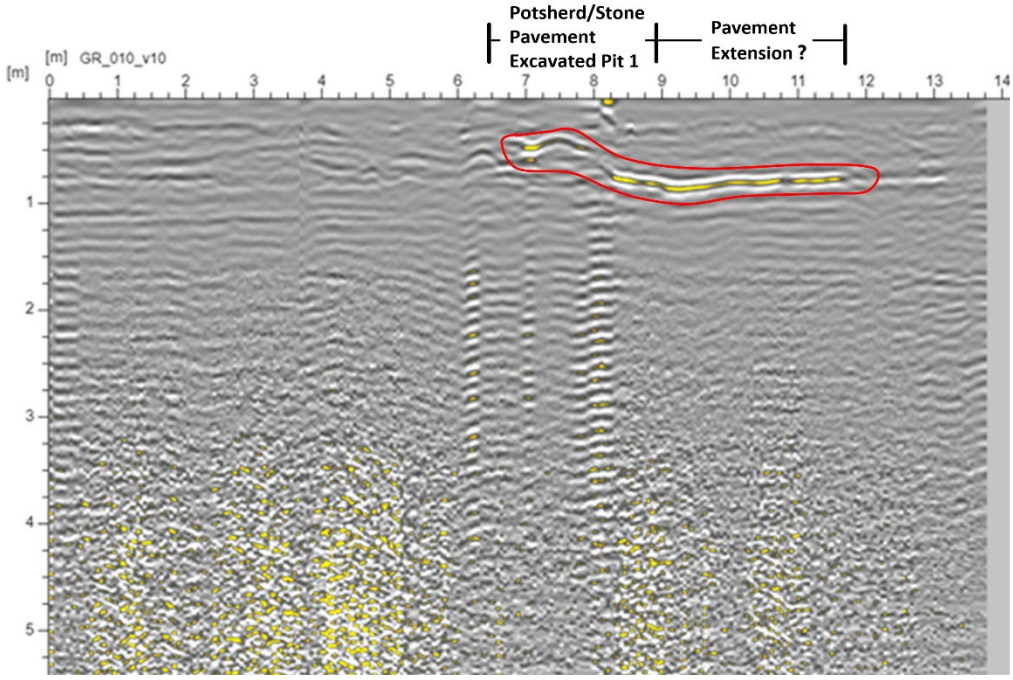

Fig. 22c: Vertical section radargram along In-line 10 (TR6)

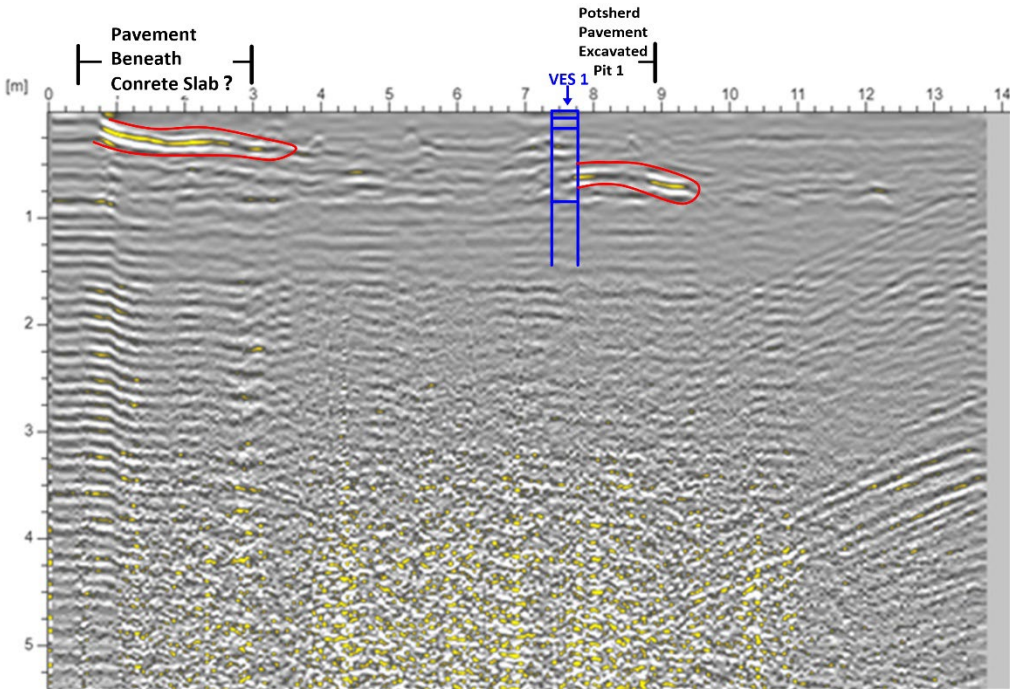

Fig. 22d: Vertical section radargram along In-line 12 (TR 7)

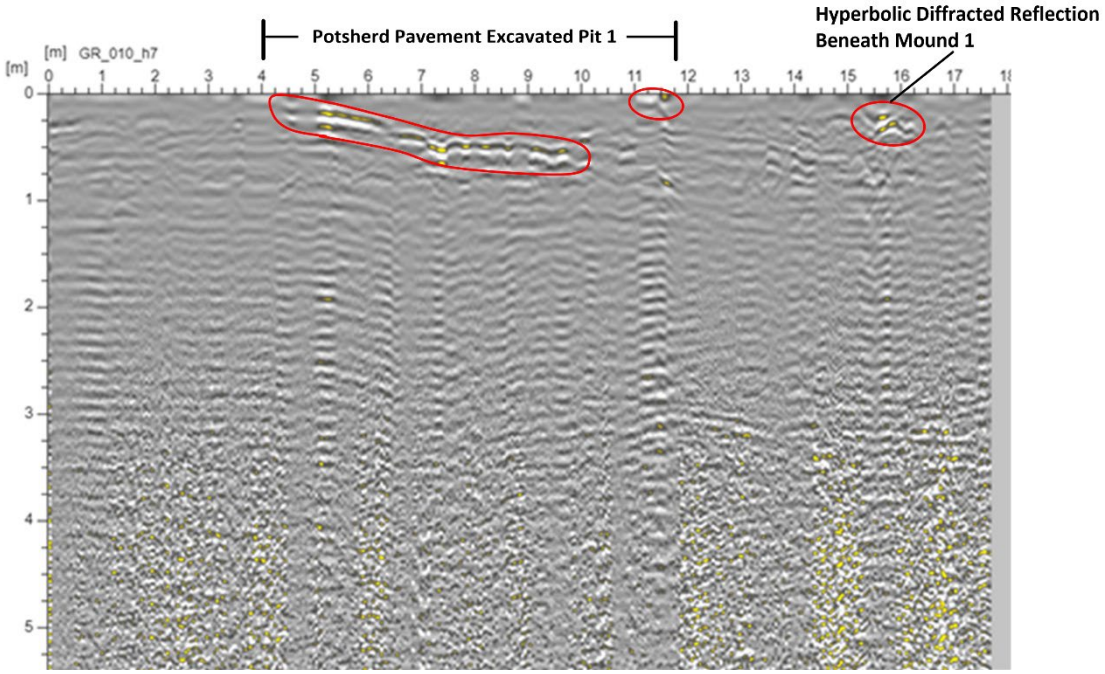

Fig. 22e: Vertical section radargram along cross-line 7

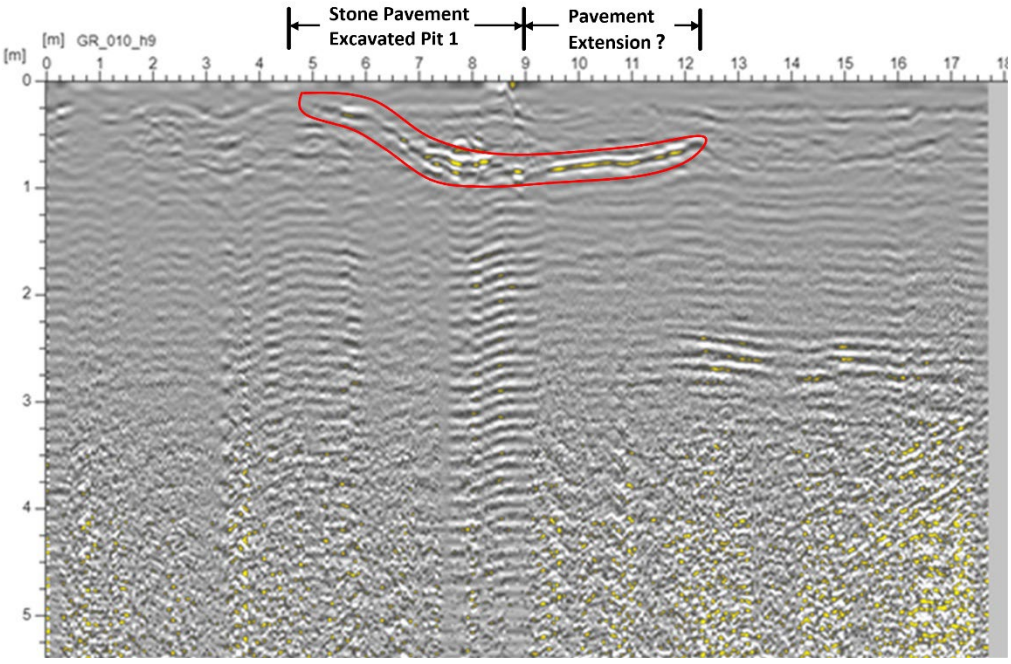

Fig. 22f: Vertical section radargram along cross-line 9 (TR 18)

The radargram along cross-line 11 (TR 18c, Fig. 6b) is displayed in Figure 22g. High amplitude reflections were identified between stations 5 and 11 at depths ranging from 0.25 – 0.75 m in the northeastern direction. This is an indication that pavements likely exist beneath the current barren Pit 2 and slightly beyond.

Figure 22h presents the radargram along cross-line 12 (TR 18d, Fig. 6b). High amplitude reflections were identified between stations 6 and 11 at depths varying from about 0.5 – 0.75 m in the direction of the northeast. This is an indication of a westward extension of the pavement from Pit 2.

The above demonstrates the effectiveness of radargram in identifying potsherd/stone pavement, estimating their depths of occurrence and determining their lateral extent on a vertical section. Both 2D geoelectric section and 2D resistivity structure could not map the pavements on such vertical sections because of suppression. Pavements are too thin to be clearly delineated by these vertical resistivity images and at the scale at which they were presented.

It is also pertinent to indicate that radargrams also could display spurious anomalies due to diffracted radar signals from discreet subsurface objects (Al-Khalidy and Kadhum, 2018) including edges of pits as shown in Figures 23 a & b.

3.2.3.2 GPR Depth Slice Maps (3D Data Coverage)

Several main and orthogonal GPR radargrams can be processed in 2D plan at different levels, as a means of providing information on location and spatial distribution of the pavements. Although in this study, depth slice maps were generated at intervals of 0.0625 m and from depths 0 – 5.0 m, selected depth slice maps, majorly at depth range of 0 – 1.0 m (depth of significance of archaeological features at the present study area), will be presented and discussed.

As indicated in section 2.3 (c), the current GPR depth slice maps will be qualitatively interpreted based on the fact that relatively high resistivity potsherd and stone pavement materials are characterized by high amplitude radar reflections with yellowish /reddish colour contrast against a presumably barren host in background light to deep green colour.

At ground level (0.0 m depth level), Figure 24a identifies four major anomalous zones (A-D). High impedance anomalous zone A is located at the southwestern edge of Pit 1, an area where excavated potsherd/stone pavement virtually outcrops and is also characterised by very high

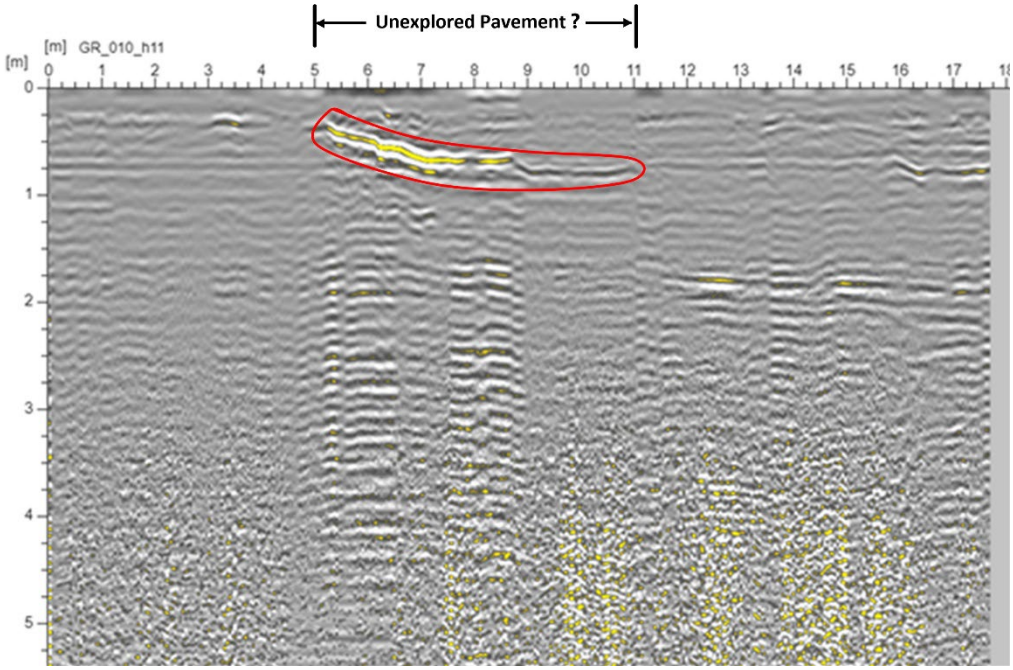

Fig. 22g: Vertical section radargram along cross-line 11

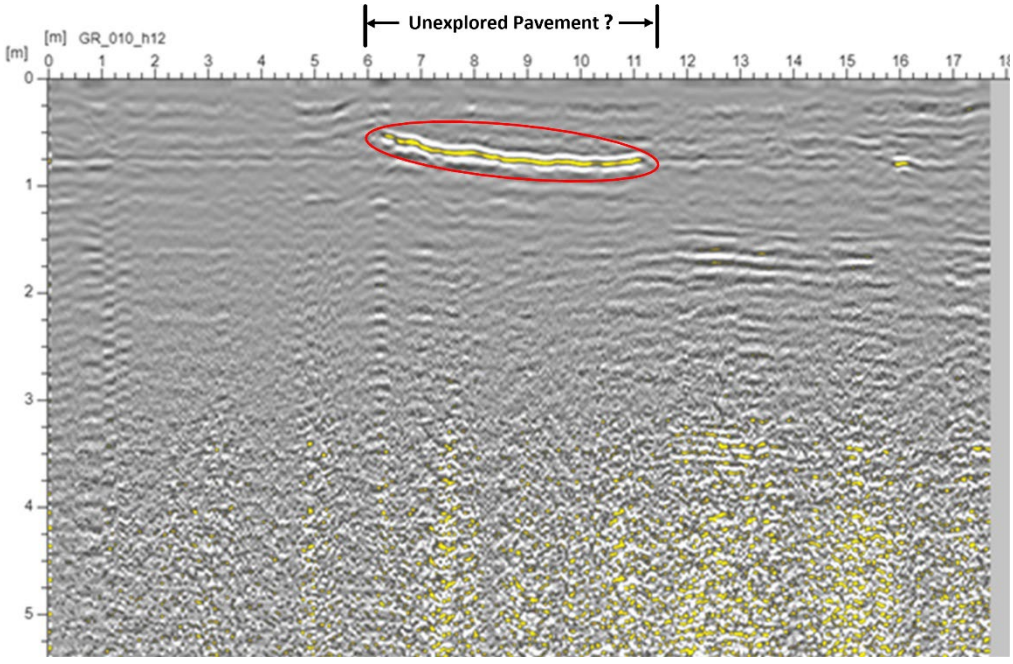

Fig. 22h: Vertical section radargram along cross-line 12 (TR 18c)

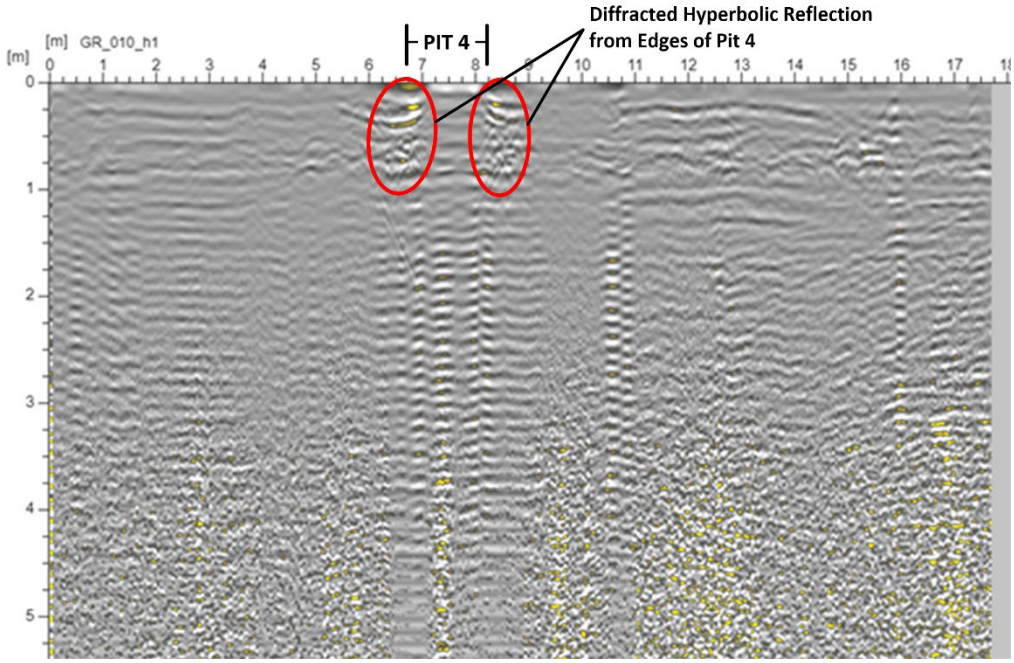

Fig. 23a: Vertical section radargram along cross-line 1 (TR 16c)

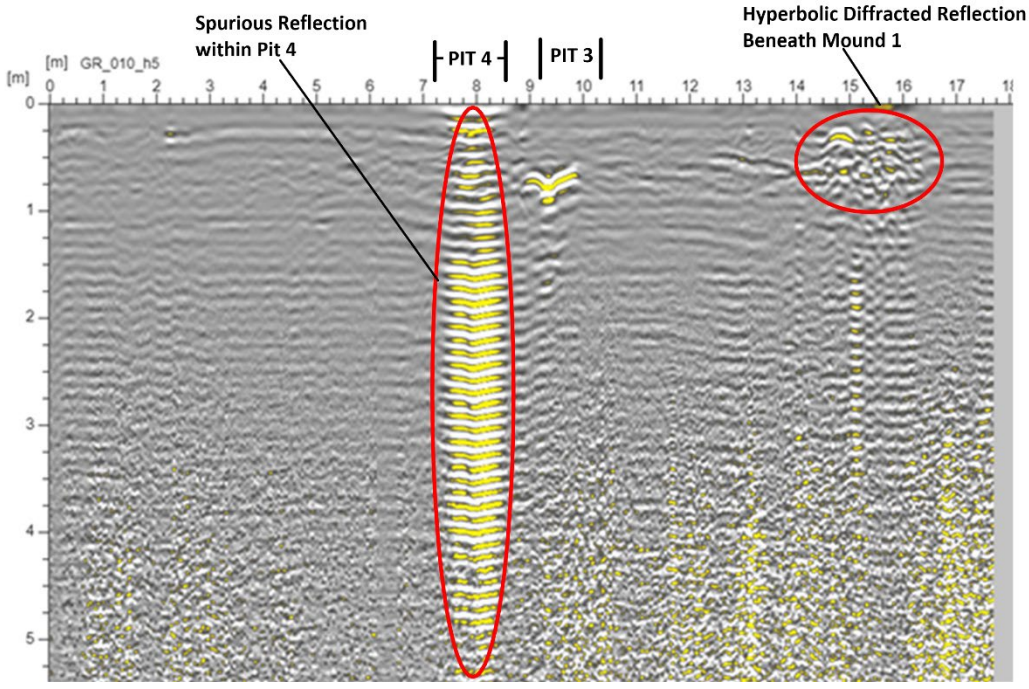

Fig. 23b: Vertical section radargram along cross-line 5 (TR 17c)

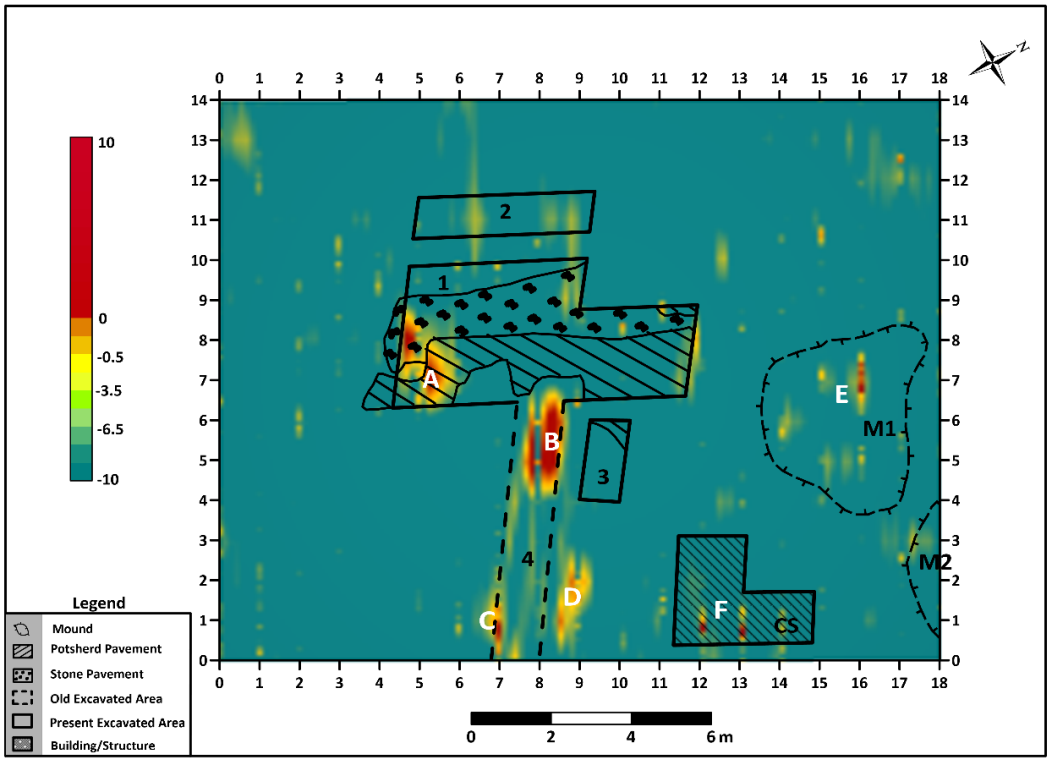

Fig. 24a: GPR depth slice map at 0.0 m

resistivity values on the apparent resistivity maps (Figs. 17a&b). Anomalous zone B is delineated at the NW end of the southeastern trending previously excavated Pit 4 while C and D are located at the edges of Pit 4 towards the southeastern end. Anomalous zone A coincides with excavated potsherd/stone pavement in Pit 1. Pits 2 and 3 show no characteristic feature typical of pavement at this depth level and are indeed barren. Not so prominent anomalous zones E and F are respectively observed over mound M1 and a cement concrete slab. These anomalies are suspected to be pavements or other archaeological features. Anomalies B, C and D may have resulted from diffracted GPR signals at both edges of the SE trending Pit 4 as evident from some cross-line radargrams (Figs. 23a&b). The GPR depth slice maps at 0.0625 and 0.125 m have the same characteristics as the 0.0 m depth slice map.

At 0.1875 m depth level (Fig. 24b), the amplitudes of anomalous zones A-D have attenuated. The attenuation of the reflection intensities of anomalous zone A may indicate GPR signals coming from beneath the pavement (pavement thicknesses are estimated to range from 0.03 – 0.04 m). Anomalous zones E (within mound M1) and F beneath the concrete slab have been enhanced in intensities and increased in spatial distribution. At depth level 0.25 m (Fig. 24c) a new anomalous zone G has emerged within Pit 2 which indicates the probability of the existence of a pavement at this depth level and at the southwestern edge of the pit.

Figure 24d displays the GPR depth slice map at 0.3125 m depth level. While anomalous zone A is gradually disappearing at the southwestern edge of Pit 1, it is emerging on the northeastern half where the potsherd/stone pavement is encountered at deeper depths (> 0.3 m). The amplitudes of anomalous zone G are enhanced while anomalous zone E has extended to the southwestern flank of mound M2. Depth slice maps at 0.375 m and 0.4375 m depth levels are not significantly different in anomaly patterns but have enhanced intensities and enlarged anomalous zone G and the emergence of anomalous zone H within Pit 3.

At 0.5 m depth level (Fig. 24e), the enlarged anomalous zone G has significantly extended beyond Pit 2 westwards with an enhanced anomalous zone H within Pit 3. The GPR image at this depth level correlates significantly with both the apparent resistivity map at 0.49 m depth level (Fig. 17a) and resistivity depth slice map at 0-0.5 m depth level (Fig. 20a). At 0.560 m and 0.625 m depth levels, the anomaly patterns are similar to that at 0.5 m depth level with both anomalous zones G and A becoming enlarged and merging west of Pits 1 and 2.

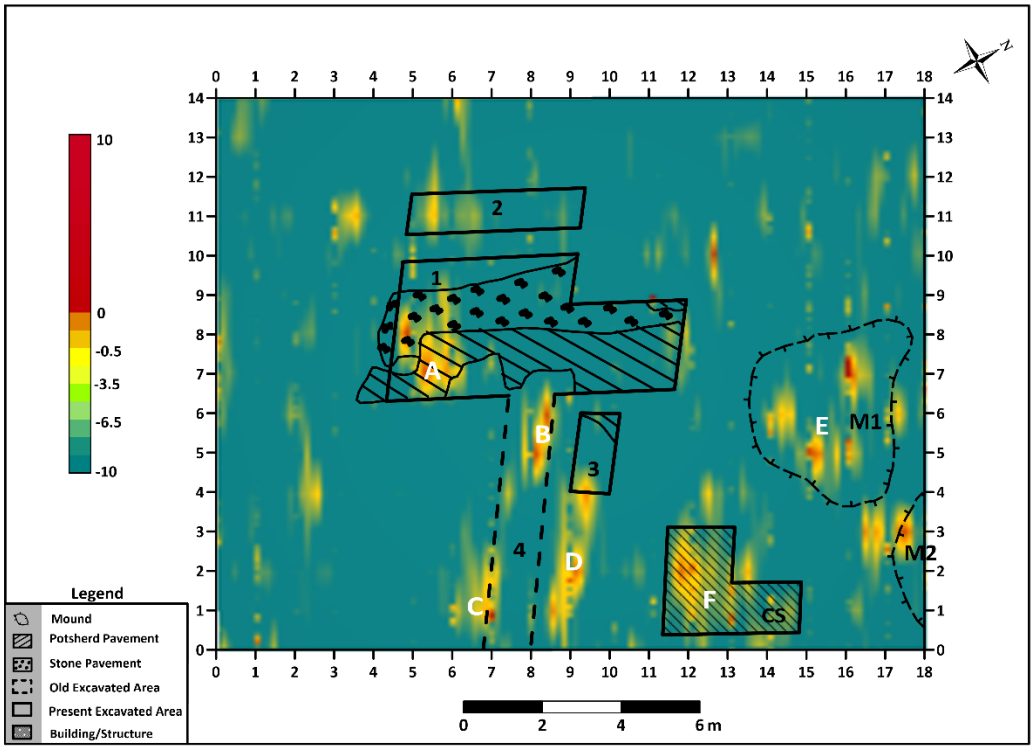

Fig. 24b: GPR depth slice map at 0.1875 m

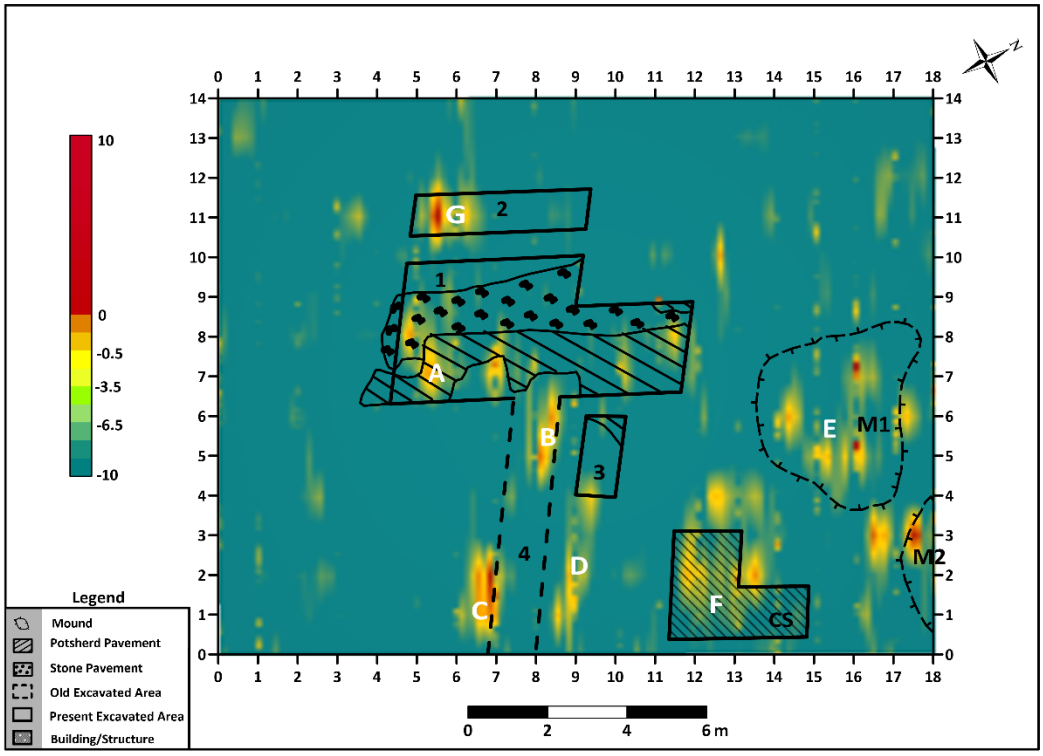

Fig. 24c: GPR depth slice map at 0.25 m

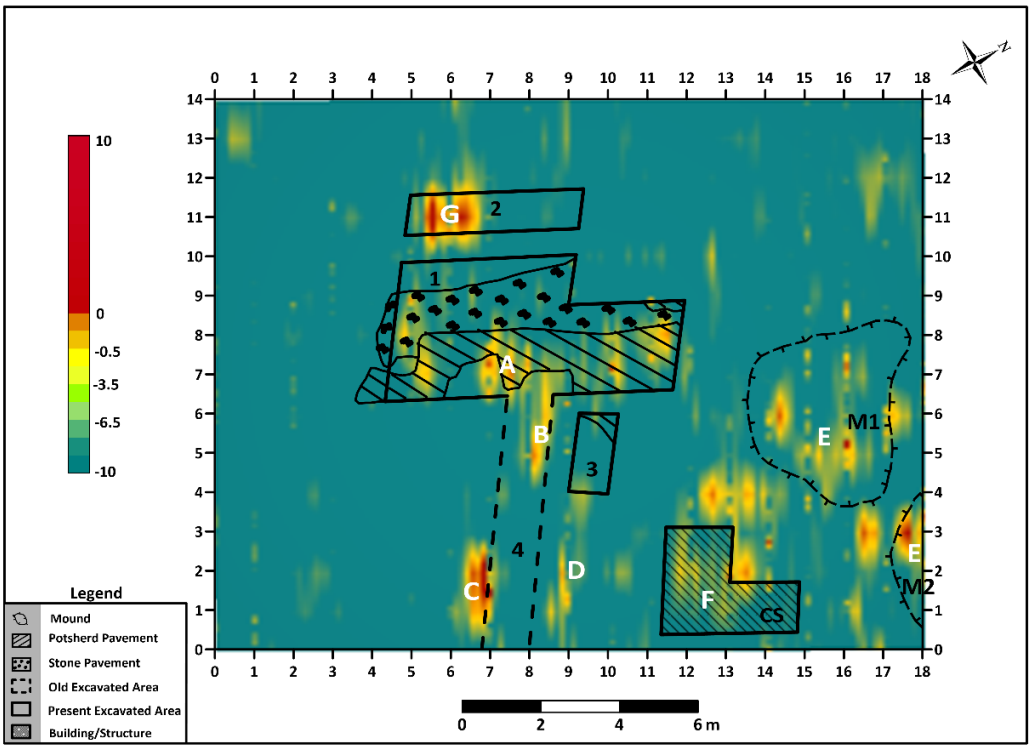

Fig. 24d: GPR depth slice map at 0.3125 m

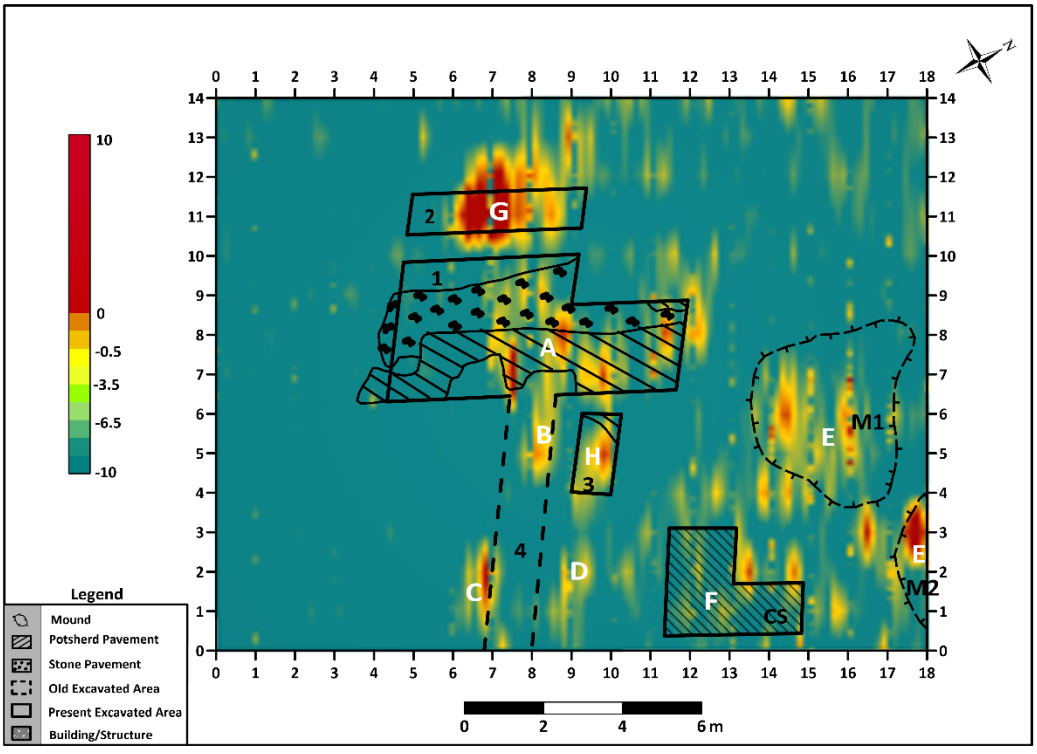

Fig. 24e: GPR depth slice map at 0.50 m

At 0.6875 m depth level (Fig. 24f), the GPR signals seem to be coming from below a significant segment of the potsherd/stone pavement with attenuated radar reflection amplitudes. Anomalous zone G is also attenuating within Pit 2. The merger of anomalous zones G and A indicates a westward extension of the stone pavement as indicated in the apparent resistivity map at around this depth level (Fig. 17b). Anomalous zones E and F have significantly attenuated at this depth level.

The GPR depth slice map at 0.75 m is displayed in Figure 24g. Except for the spatially limited anomalous zone H within Pit 3, the amplitudes of all the anomalous zones have attenuated significantly indicating that the GPR signals are either coming from beneath the archaeological features of interest or that the GPR signals have attenuated significantly at this depth level. At this depth level, both the apparent resistivity map at 0.78 m (Fig. 17b) and the resistivity depth slice map at 0.5 -1.0 m (Fig. 20b) are still diagnostic.

At 0.8125 m depth level (Fig. 24h), the amplitudes of all the near-surface archaeological features have attenuated significantly with only the spurious anomalous zone B remaining. By the depth of 0.875 m (Fig. 24i) only anomalous zone B can be effectively said to subsist. The spurious anomalous zone B remains prominent up to depth of 4.5 m. At depth levels greater than 1.375 m, there is increasing influence of the layer high resistivity lateritic clay (see Fig. 15) which becomes very prominent from depth level of 3.375 m (Fig. 24j).

Deductions

The following deductions can be made from the foregoing discussion that:

(i) The potsherd/stone pavement in Pit 1 occurs at varying depths from the ground surface and so is delineated at different depth levels – in the present case, at two depth levels: - at shallow (near zero) depth at the southwestern flank of Pit 1 and relatively deep depth from about two third the entire length moving northeastward.

(ii) There is virtually no indication that the pavement extends beyond the present southwestern and northeastern end of Pit 1. The apparent resistivity maps (Figs. 17a-c) and resistivity depth slice maps (Figs. 20a & b) also gave this indication.

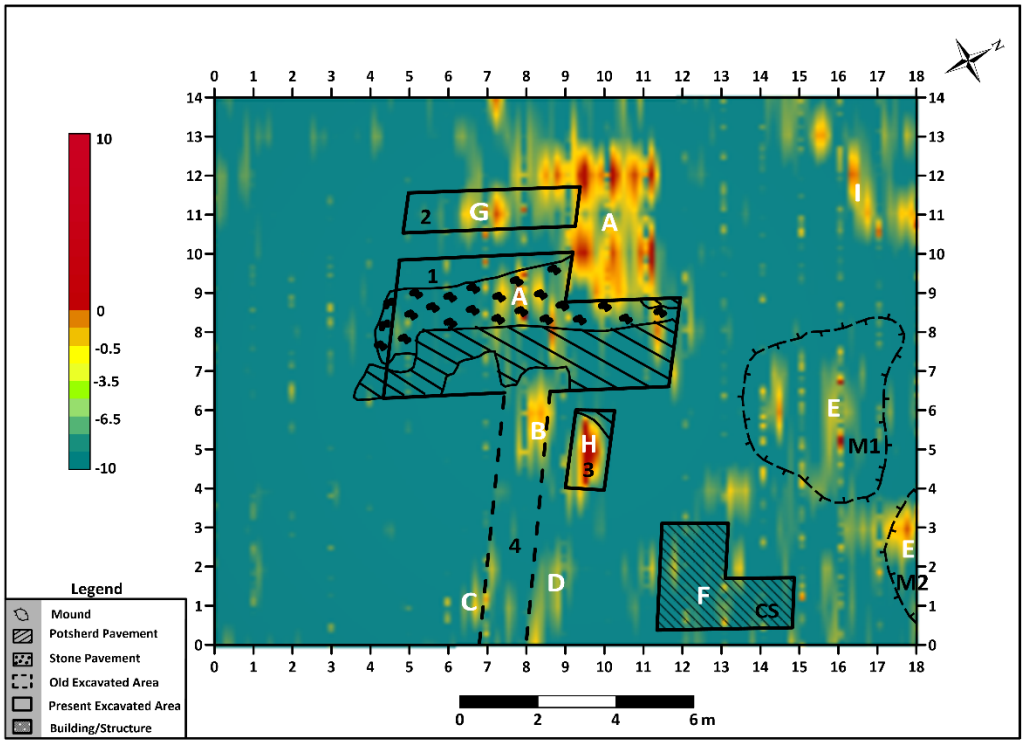

Fig. 24f: GPR depth slice map at 0.6875 m

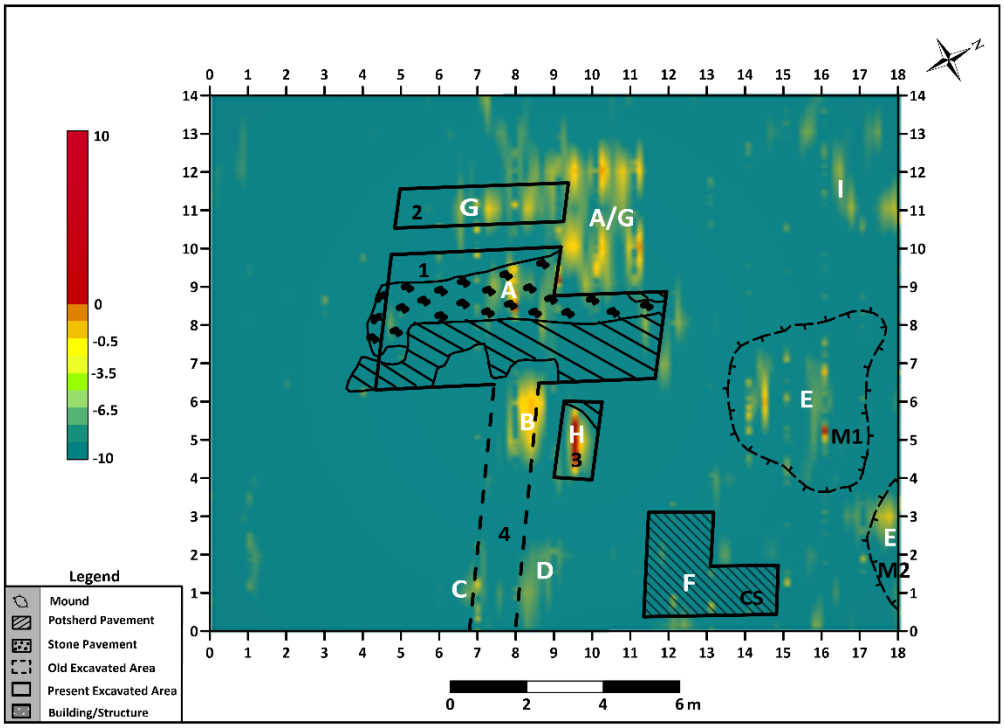

Fig. 24g: GPR depth slice map at 0.75 m

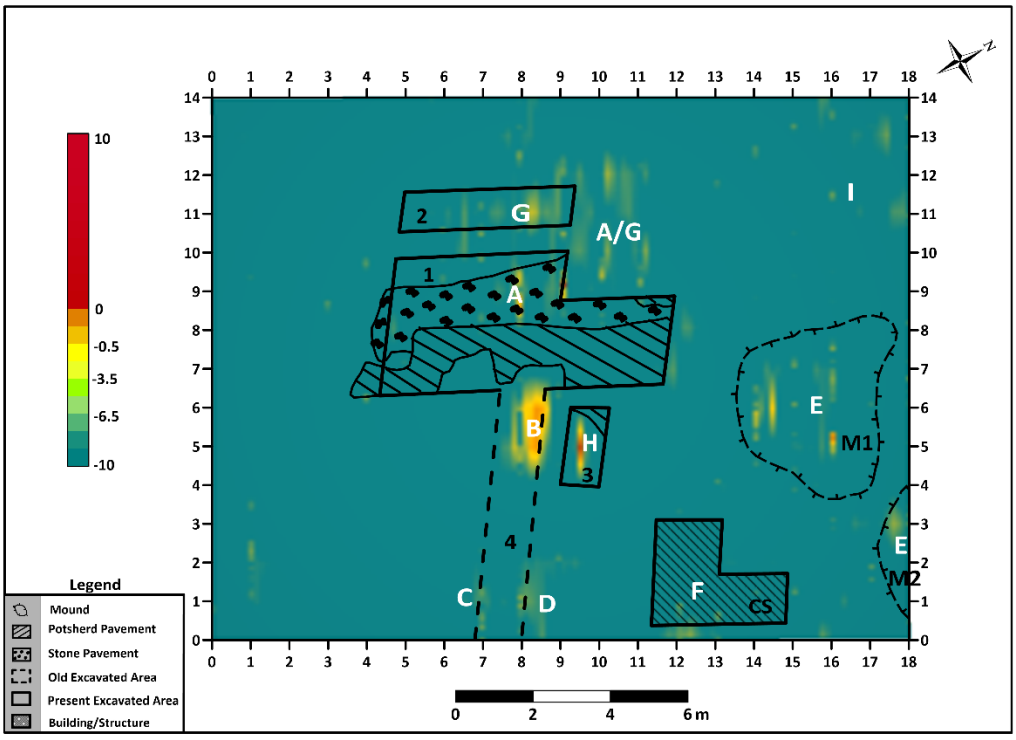

Fig. 24h: GPR depth slice map at 0.8125 m

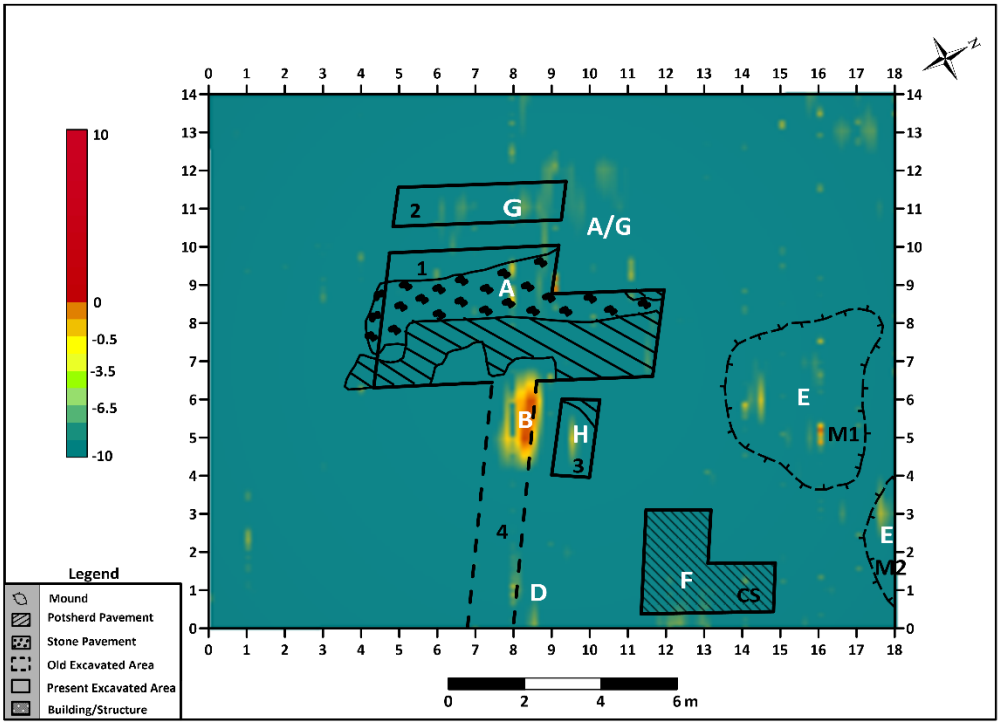

Fig. 24i: GPR depth slice map at 0.875 m

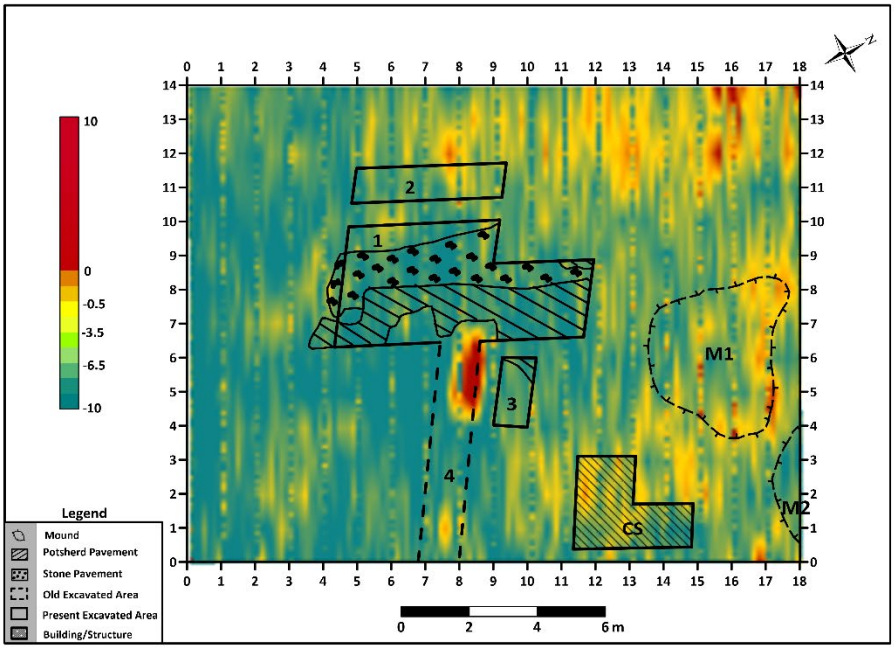

Fig. 24j: GPR depth slice map at 3.375 m

(iii) There is indication from the GPR map that the presently barren Pit 2 may contain pavement at depth levels of 0.25 m – 0.65 m. The resistivity maps also indicate such possibility between depth levels of 0.49 m – 0.78 m (Fig. 17 a & b) and resistivity depth slice maps (Figs. 20a & b).

(iv) There is also an indication that Pit 3 with minor trace of potsherd pavement could host the feature between depth levels of 0.50 – 0.75 m as corroborated by the apparent resistivity maps (Figs. 17 a & b) and resistivity depth slice map at 0.5 – 1.0 m (Fig 20b)

(v) There is an indication that the stone/potsherd pavement could extend westwards from the northeastern end between depth levels of 0.56 – 0.75 m as corroborated by the apparent resistivity maps at 0.49 – 0.98 m depth levels (Figs. 17a – c) and resistivity depth slice maps at 0 – 0.5 m and 0.5 - 1.0 m depth levels (Figs. 20a & b).

(vi) Archaeological features may exist beneath the mounds at depth levels of 0.125 m – 0.625 m and extending towards and beneath the cement concrete slab at depth levels of 0.125 – 0.45 m. The resistivity maps display relatively high resistivities over the mounds and over the cement pavement at depth level of 0.49 m (Fig. 17a) and 0 – 0.5 m depth level (Fig. 20a).

(vii) The GPR depth slice maps show indication that diagnostic high amplitude anomalies attenuate almost completely at depth level of 0.875 m which is the depth of significance of the archaeological features. This is in agreement with the less than 1 m depth of significance estimated from the magnetic method.

(viii) Apart from the very spurious but consistently high amplitude anomaly B (existing up to depth of 4.5 m) at the northwestern edge of the SE trending Pit 4, it seems the old pit is barren.

(ix)With a prior background knowledge of the depth of occurrence of stone/potsherd pavements and the fact that the pavements present significant contrasts in dielectric constant (or conductivity) particularly the stone pavement, 2D Vertical GPR sections (radargram) are very effective in directly mapping the pavements (Figs. 23a-h). The GPR method seems to be superior to the electrical resistivity method in this regard.

3.2.3.3 GPR Radargrams (2D Data Coverage)

The 3D configured data cover less than half (about 40%) of the main survey area. This necessitated a 2D configured data coverage for the entire area (which overlaps with the 3D data coverage) with

twenty-seven (27) main traverses at 1 m interval and seventeen (17) orthogonal traverses majorly at 2 m interval (see Fig. 6b). The 2D configured data were acquired with prospecting frequencies of 450 MHz and 750 MHz respectively. The idea was to see if the higher prospecting frequency would give higher radar resolution at shallow depth (up to 1 m) that is of interest in this study.

Figures 25-28 provide comparison of radar images along four selected traverses TR 4 (in-line 6), TR 5 (in-line 8), TR 10 (in-line 18) and TR 18 (cross-line 9) along which there are pit finds and mounds as control. The radar images correlated perfectly for both the 2D and 3D configured data at 450 MHz prospecting frequency while the 750 MHz radar images were not diagnostic particularly for pavement identification. We suspect the 750 MHz Transmitter Antenna may not have been properly calibrated by the operator.

In developing a composite image from the GPR for synthesis of geophysical results, radargrams and depth slice images from 450 MHz prospecting frequency will only be engaged.

3.2.3.4 GPR Depth Slice Maps (2D Data Coverage)

Depth slice maps generated from the 2D configured data cover the entire survey area. The maps are required to provide archaeological information both within the 3D data block (for correlation and quality check) and most especially outside the block for completeness of coverage.

For quality check, depth slice maps developed at selected depth levels of 0.25 m, 0.50 m, 0.75 m and 0.875 m (within the effective archaeologically relevant depth of 1.0 m) were compared with equivalent depth slice maps generated at same depth levels from the 3D configured data, as displayed in Figures 29-32.

The referenced depth slice maps correlated significantly well with the 3D configured data depth slice maps but with understandably slightly lower resolution due to lower data density (1x2 m (2D) grid as against 1x1 m (3D) grid).

At 0.25 m depth level, Figure 29a delineates all the prominent anomalous zones A, B, C, D, E and F and an imprint of G identified on Figure 29b. It additionally identifies an anomalous zone over Pit 3/southeast of the northwestern end of Pit 1. Another prominent anomalous zones are a southeastern extension of zone E from mound M1 and F southeast of the cement concrete slab.

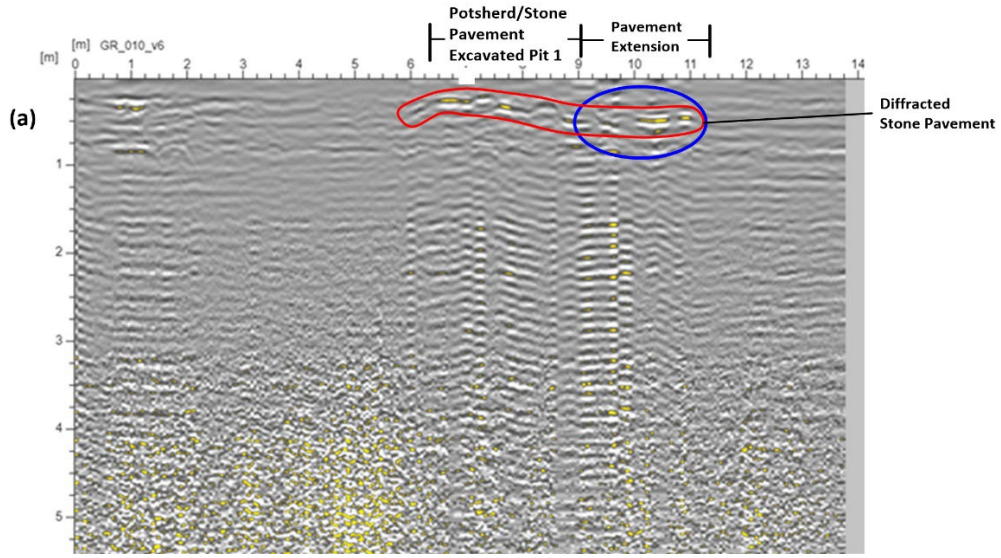

Fig. 25a: Vertical section radargram (450 MHz) along In-line 6 (segment of Traverse TR 4) [Note that station 0 corresponds to station 6 on Traverse TR4]

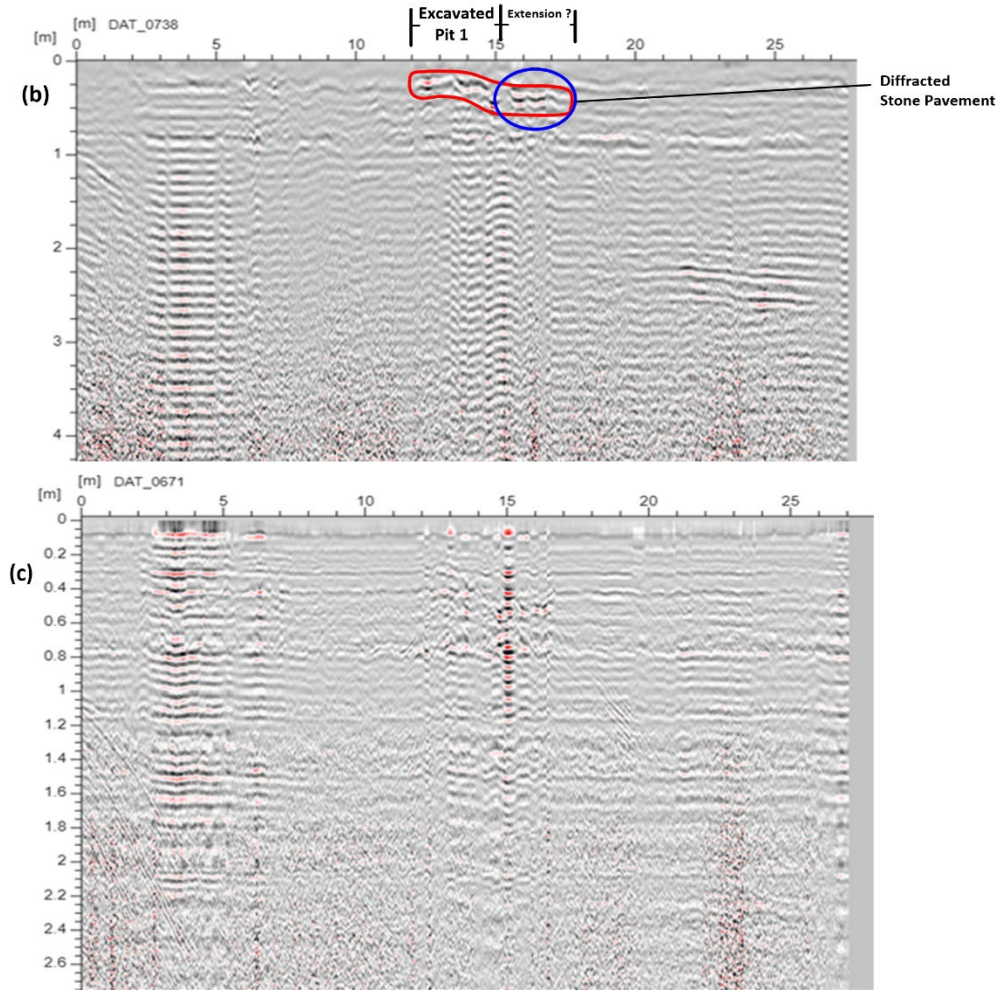

Fig. 25: (b) Vertical section radargram (450 MHz) along Traverse TR4 and (c) Vertical section radargram (750 MHz) along Traverse TR4

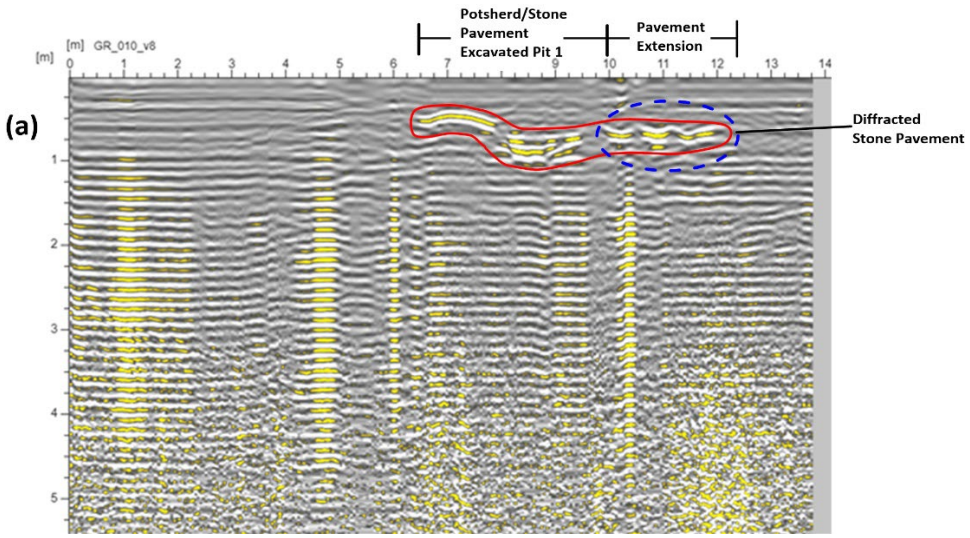

Fig. 26a: Vertical section radargram (450 MHz) along In-line 8 (segment of Traverse TR 5) [Note that station 0 corresponds to station 6 on Traverse TR 5]

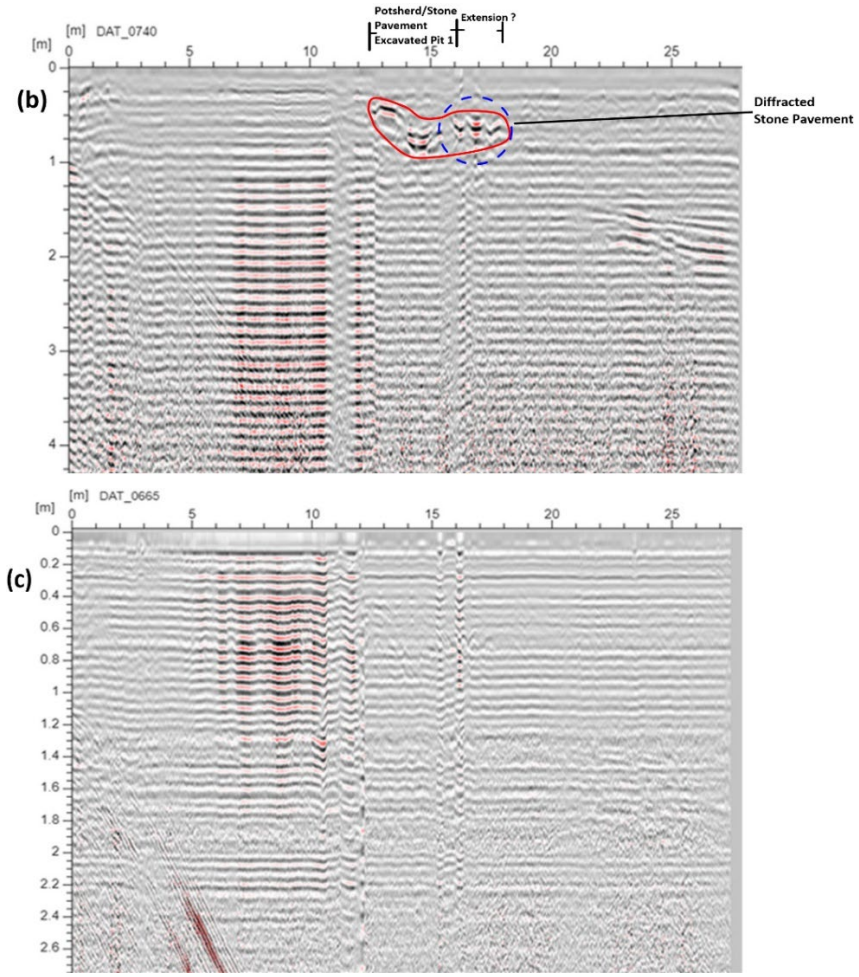

Fig. 26: (b) Vertical section radargram (450 MHz) along Traverse TR5 and (c) Vertical section radargram (750 MHz) along Traverse TR5

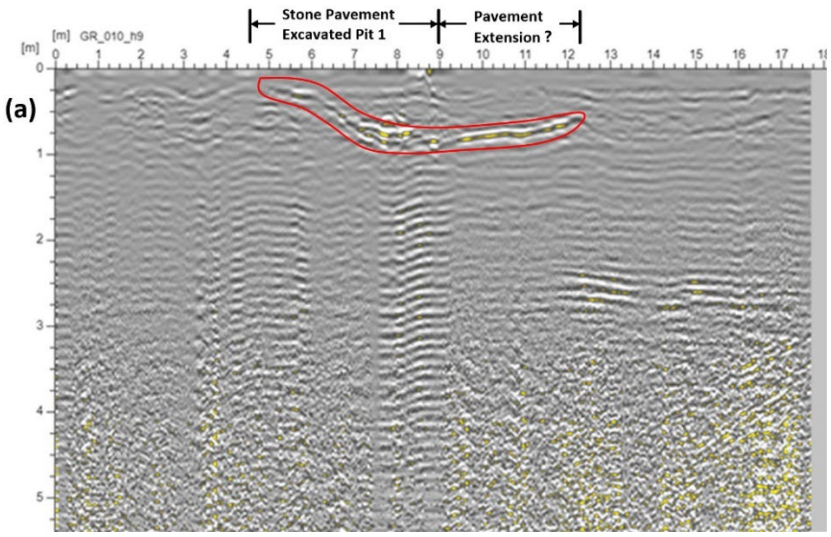

Fig. 27a: Vertical section radargram (450 MHz) along Cross-line 9 (segment of Traverse TR 18)

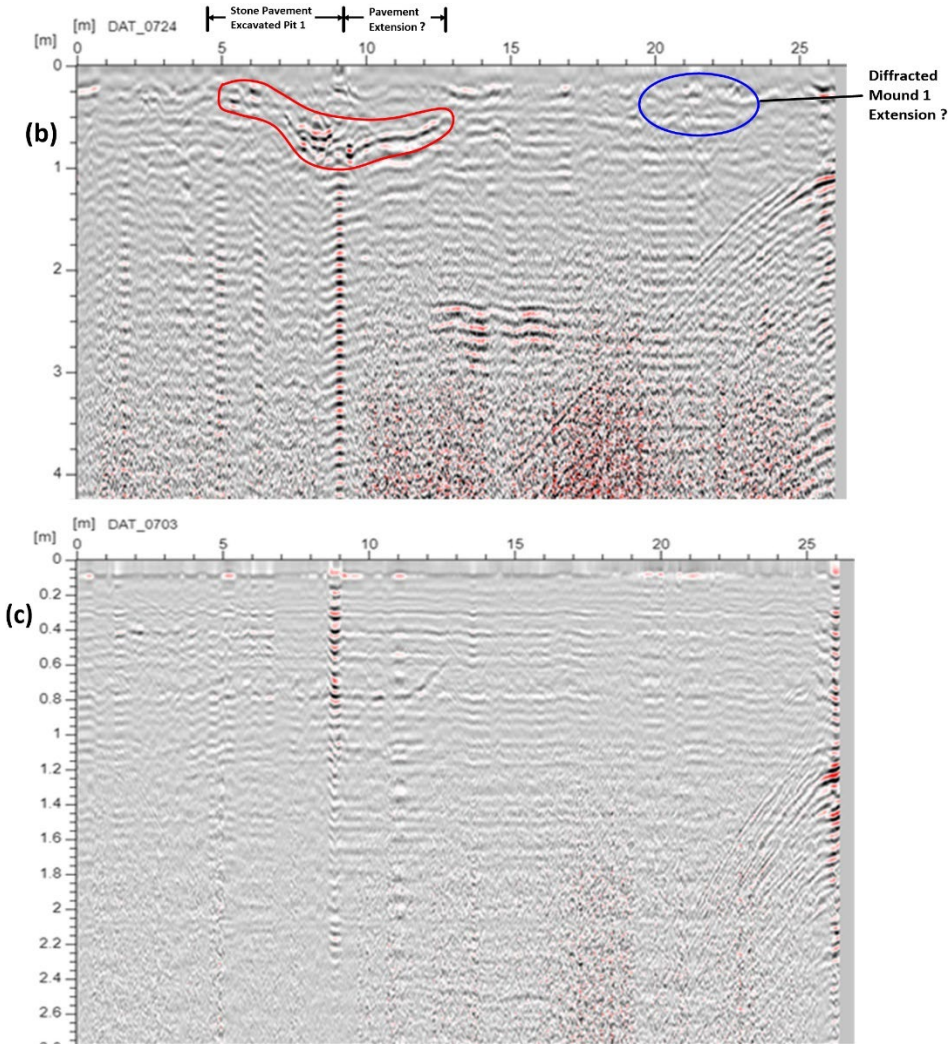

Fig. 27: (b) Vertical section radargram (450 MHz) along Traverse TR18 and (c) Vertical section radargram (750 MHz) along Traverse TR18

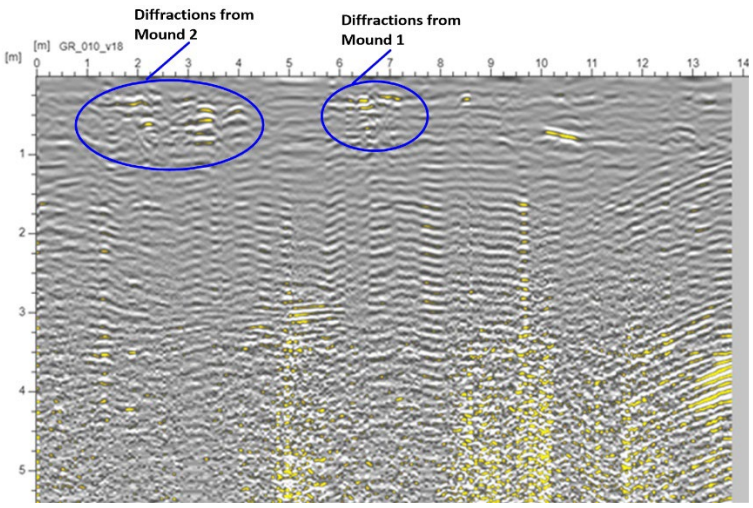

Fig. 28a: Vertical section radargram (450 MHz) along In-line 18 (segment of Traverse TR 10)[Note that station 0 corresponds to station 6 on Traverse TR 10]

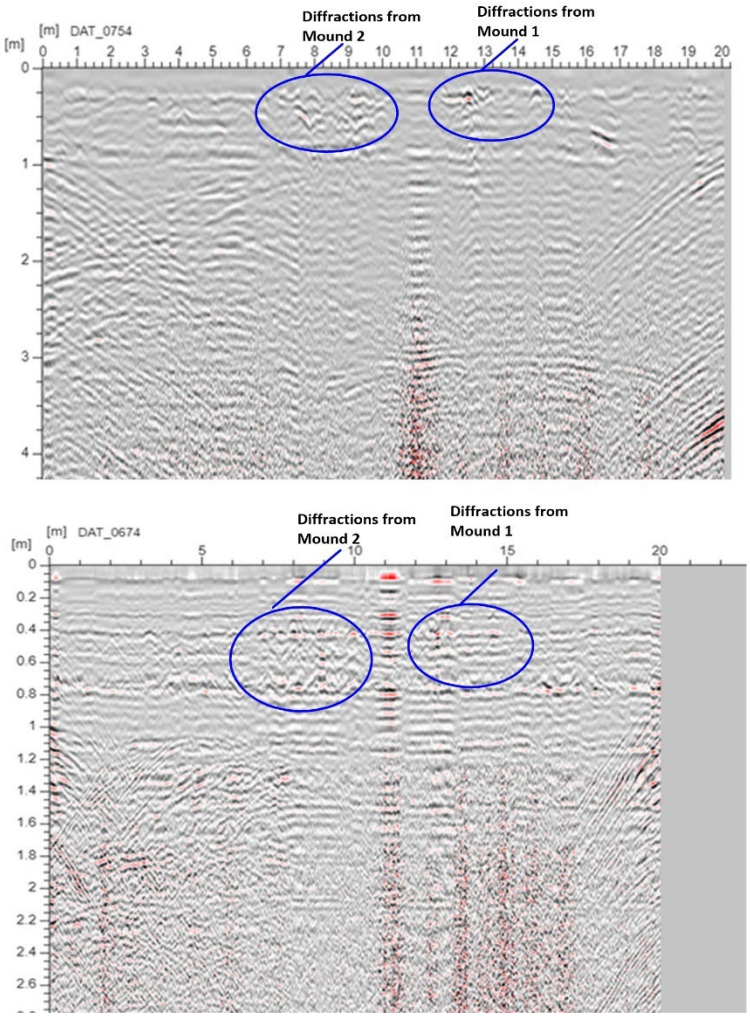

Fig. 28: (b) Vertical section radargram (450 MHz) along Traverse TR10 and (c) Vertical section radargram (750 MHz) along Traverse TR10

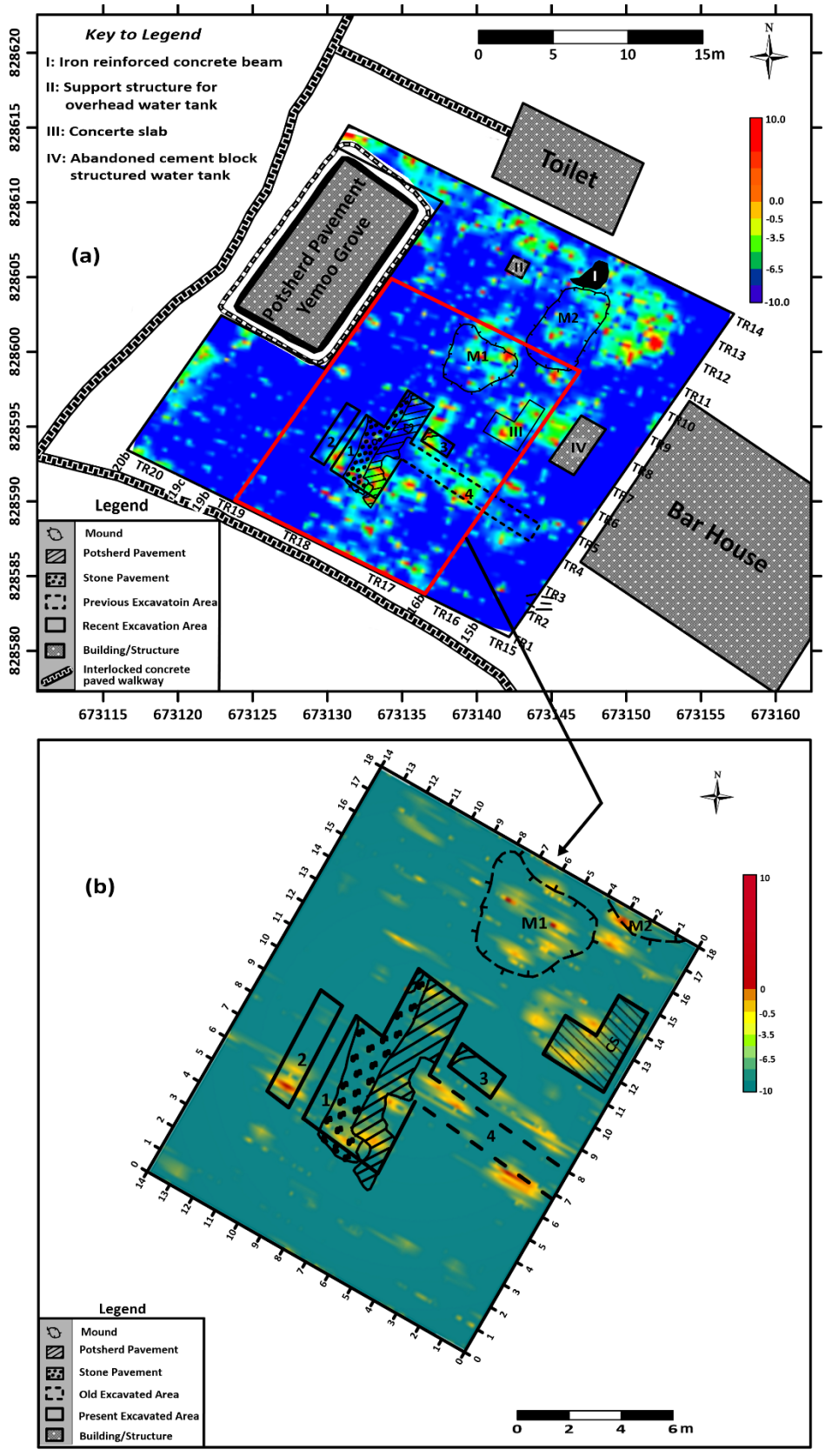

Fig. 29(a): 2D GPR depth slice map at 0.25 m and (b) 3D GPR depth slice map at 0.20 m

At 0.50 m depth level (Fig. 30a), anomalous zones A and G and its extension westward, H, E and F as identified in Figure 30b correlate significantly well. The extension of zones F and E with respect to mound M2 have slightly attenuated.

At 0.75 m depth level (Fig. 31a), the anomalous zones are as delineated in Figure 31b with prominent extension of the stone pavement westward and enhanced anomaly within mound M2.

At 0.875 m depth level (Fig. 32a), the anomalous zones have significantly attenuated as observed in Figure 32b. anomalous zone E remains significant over mound M2 while the anomalous zone at the northwestern end of Pit 3 which remains prominent up to deep depth of greater than 2 m could be a spurious anomaly.

The depth slice maps, generated from the 2D configured data, identify all the anomalous zones delineated by depth slice maps developed from 3D configured data and in addition reinforces the anomalous zones E over mounds M1 and M2 and identify a southeastern extension of anomalous zone F over the cement concrete slab. Depth slice maps generated from both the 3D and 2D configured data will be integrated at depth levels of 0.0 – 0.75 m to develop a composite GPR prospect map.

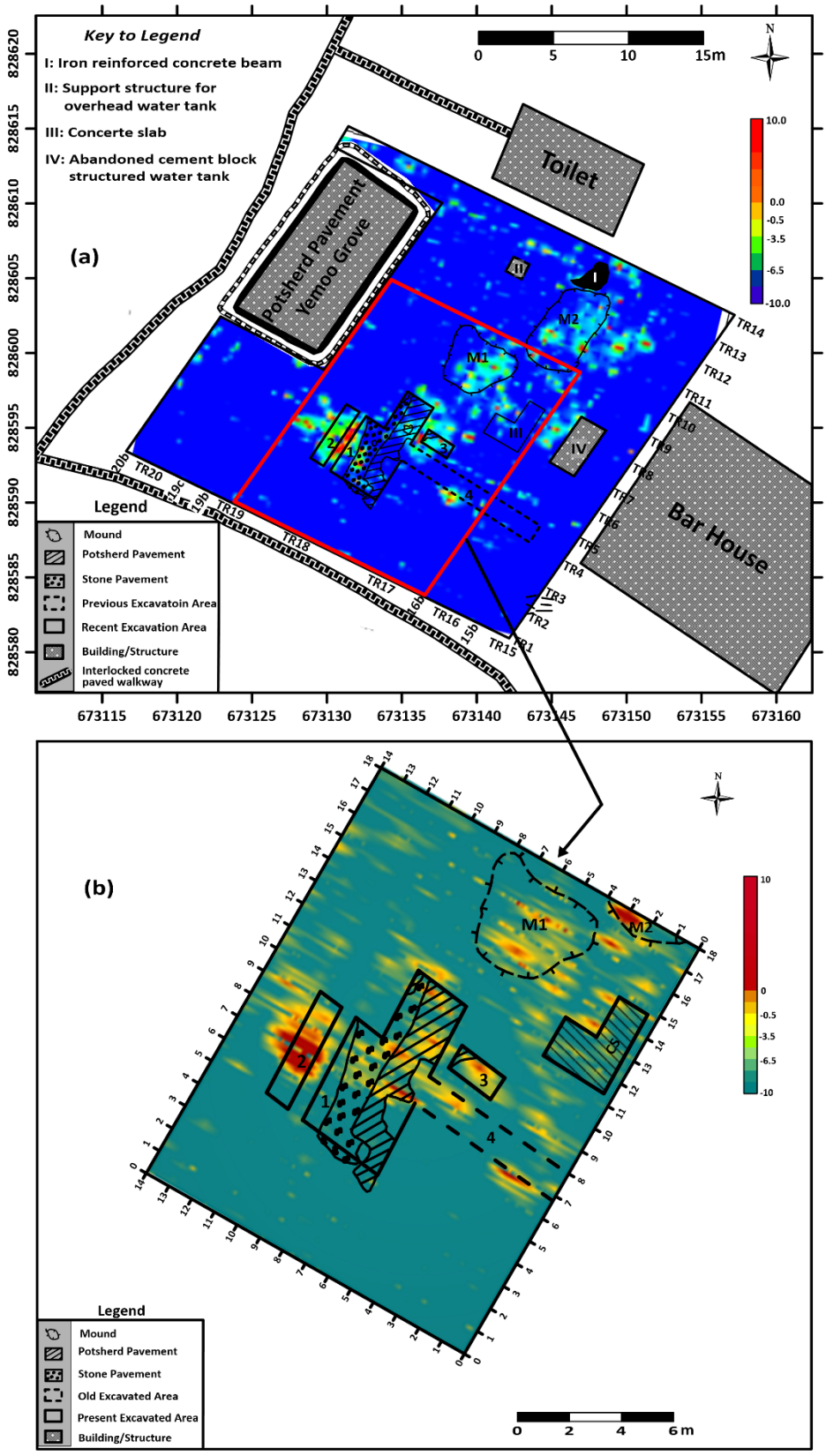

Fig. 30(a): 2D GPR depth slice map at 0.5 m and (b) 3D GPR depth slice map at 0.5 m

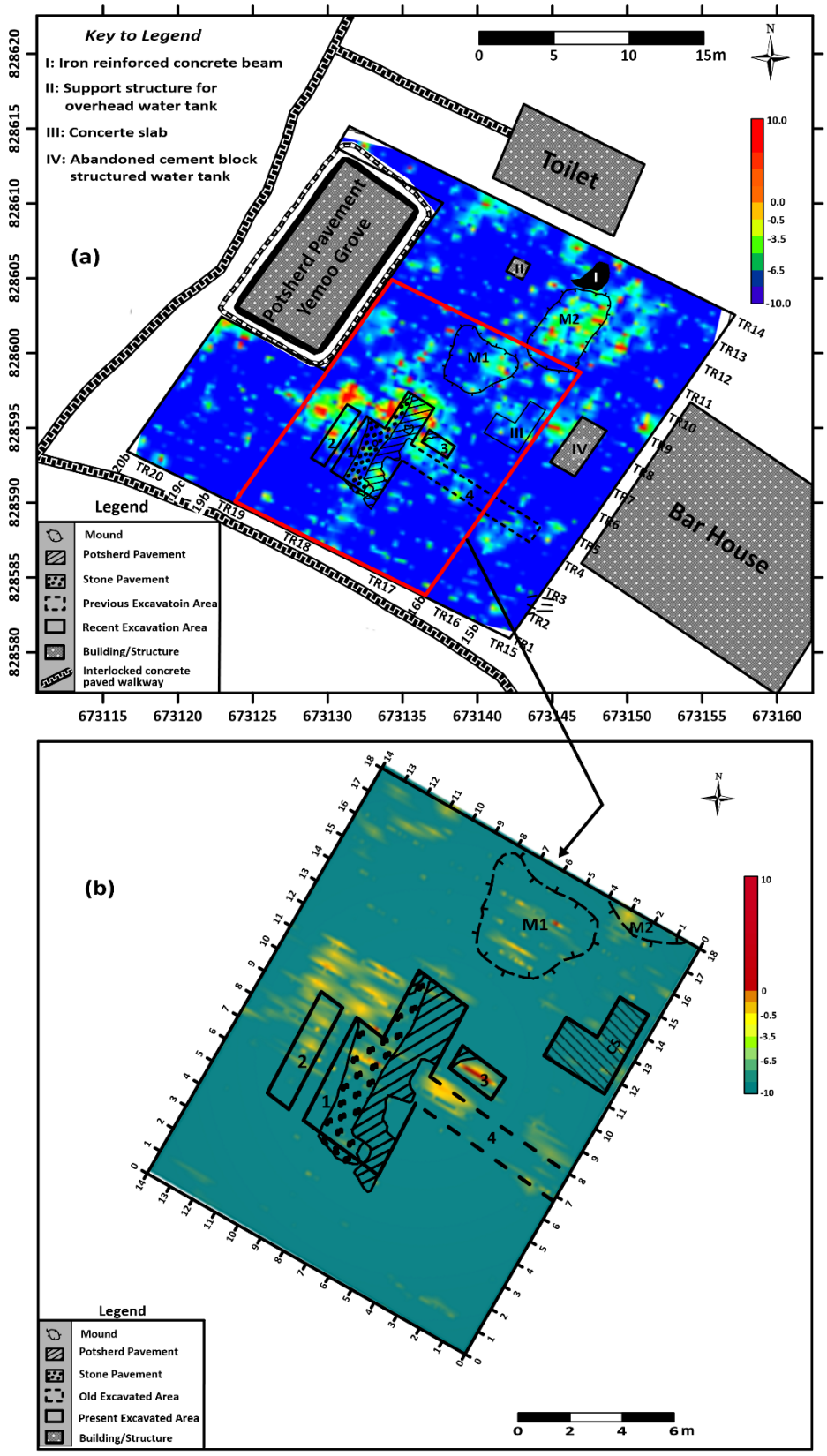

Fig. 31(a): 2D GPR depth slice map at 0.75 m and (b) 3D GPR depth slice map at 0.75 m

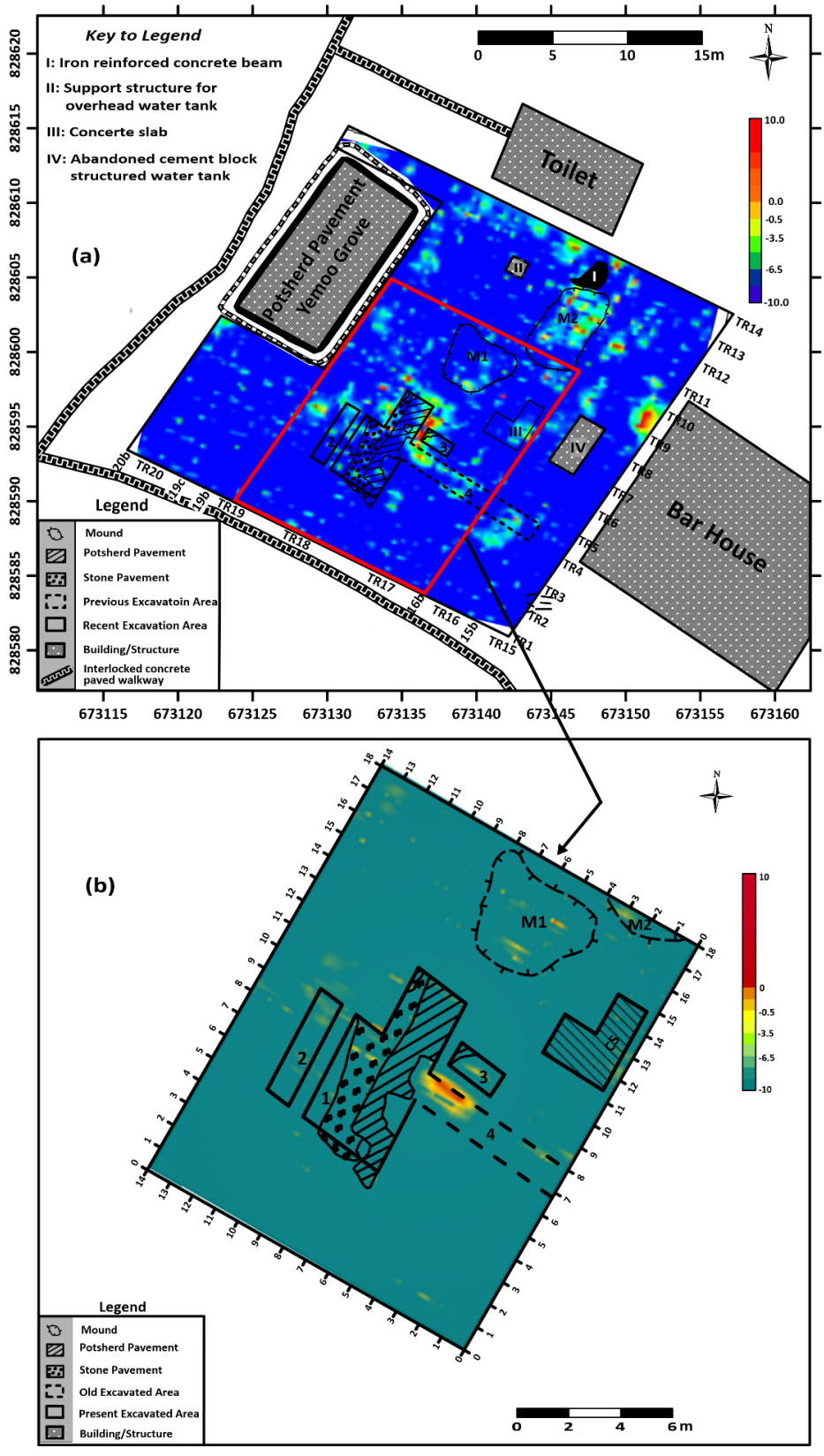

Fig. 32(a): 2D GPR depth slice map at 0.875 m and (b) 3D GPR depth slice map at 0.875 m

4.0 SYNTHESIS OF GEOPHYSICAL RESULTS

We have engaged three geophysical methods – magnetic, electrical resistivity and ground penetrating radar, in our quest to map potsherd/stone pavement and other archaeological features within a portion of the Ita Yemoo archaeological site. In the process, we have been able to assess the potency of each geophysical method.

The magnetic method revealed that potsherd/stone pavements are weakly magnetic with the magnetic responses overlapping significantly with that of the also weakly magnetic basement derived clayey weathered overburden host materials. Although it is established from the present study that pavements are majorly associated with intermediate (0-40 nT/m) magnetic effect, the archaeological feature was also identified within zones with classified low (0 to -318 nT/m) and high (40 – 327 nT/m) magnetic intensities. This implies that pavements are associated with virtually the entire magnetic spectrum. This limitation does not make the magnetic method an index method in pavement mapping. The method however, has its relevance established in the estimation of depth of archaeological significance required in field design. The geophysical method therefore, remains relevant as a reconnaissance method. The magnetic map which reflects the bulk overburden (inclusive of pavements) magnetic response may not be appropriate in the direct mapping of pavement (which is interface related) and the establishment of its spatial distribution and hence will not be adopted as such in the present study. The magnetic map will nevertheless be engaged in our interpretation of the investigated site for other possible archaeological features. For example, the coincidence of magnetic lows (negative polarity) with high resistivity has been established to be indicative of archaeological features (Olorunfemi *et al.*, 2019; Oni *et al.,* 2022 and Olorunfemi *et al.*, 2022).

This study established that the 1D Micro VES technique of the electrical resistivity method is effective for the mapping of potsherd pavement only at shallow depth/outcropping when both layer resistivities and thicknesses can be effectively estimated. We found such parameters useful in the interpretation of 2D resistivity maps. Due to the very thin (0.03 – 0.04 m) nature of the pavements, the delineation of the archaeological feature is virtually impossible at deep depth due to suppression. This technique has limited application, if any, in the mapping of spatial distribution of pavements.

The 2D resistivity maps were generated from raw field data (2D apparent resistivity maps) and from data extracted within specific depth ranges of the inverted 2D resistivity structures (images) (2D resistivity depth slice maps). The former are depth specific 2D apparent resistivity maps for different expansion factors while the latter are resistivity maps generated for different depth ranges of the inverted 2D resistivity structures.

Because pavements are interface related, the features are best imaged by depth specific (and not depth range or bulk) images. For this reason, the depth specific 2D apparent resistivity maps have been found to be more diagnostic of pavements with the images correlating more with pit finds and images from the depth specific 2D images from the ground penetrating radar. The planar nature of potsherd/stone pavements and the significant contrasts in the dielectric constant (or conductivity) relative to the host materials make the ground penetrating radar (GPR) radargrams (2D vertical sections) and the depth specific 2D depth slice maps very effective in directly mapping the pavements and establishing the spatial distribution. This study however, established that strong and continuous radar reflections were rarely observed at depths greater than 1.0 m. In fact, at depth level of 0.875 m, diagnostic high amplitude anomalies on the 2D map have attenuated completely. Resistivity maps are still diagnostic at this depth level.

Because both the magnetic and ground penetrating radar methods indicate an archaeologically relevant depth of less than 1 m for the study area, only depth slice maps of apparent resistivity and GPR at this depth range will be used for the mapping of the pavement spatial distribution either individually or in an integrated form.

Based on resistivity characteristics of 120-350 ohm-m and using the finds from the excavated pits and other field observation as constraints, prospective zones for pavements will be delineated at 0.59, 0.78 and 0.98 m depth levels. A composite pavement prospect map will be generated from the three maps. Similar prospect maps will be generated from the GPR 2D depth slice maps at depths of 0.50 and 0.85 m and compared with equivalent depth specific apparent resistivity maps. Composite GPR prospect map will be generated from the synthesis of depth slice maps from 0.0 – 0.85 m (for 3D and 2D data coverage) so as to incorporate pavements at all depth levels.

A final composite pavement prospect map will be generated from the synthesis of the composite apparent resistivity maps and ground penetrating radar maps. On this final map, prospect for other archaeological features will be indicated.

Figure 33a presents a resistivity derived archaeological prospect map at three depth levels of 0.59, 0.78 and 0.98 m based on a resistivity threshold range of 120-350 ohm-m. The 0.98 m depth level resistivity thematic map constitutes the background with the prospective zone in brownish colour and the presumably archaeologically barren zone in green colour. The shells (boundaries) of the prospective zones of the 0.59 m depth level resistivity thematic map (in dotted blue colour lines) and the 0.78 m thematic map (in dotted red colour lines) are superimposed on the 0.98 m thematic map. Zones of overlapping prospectivity were stacked to produce the composite resistivity derived archaeological prospective map (Fig. 33b). These zones are suspected to host potsherd/stone pavements and other buried archaeological artefacts. The zones include the premises of the recently excavated Pits 1-3, beneath and adjoining mounds M1 and M2 and around and over an outcropping potsherd pavement southwest of Pit 4. Archaeological finds from the recently excavated Pits 1 and 3 and field observation established the reliability of the composite resistivity thematic map.

Figure 34a displays shells (boundaries) of GPR anomalous zones generated at depth ranges of 0 – 0.25 m (continuous lines); 0.25 – 0.50 m (dotted lines) and 0.50 – 0.85 m (double lines) for the 2D configured data coverage (in blue colour) and 3D configured data coverage (in red colour). Where the 2D and 3D data coverage overlap (in the area around the recently excavated Pits 1-3 and mound M1 and the cement concrete slab (III) (blocked out in Fig. 34a)), the blue and red shell lines correlate significantly indicating consistency in field data and results. This map confirms the variable depth of occurrence of the potsherd/stone pavements and reinforces the earlier inference that there may be more than one level of pavement occurrence.

A composite GPR thematic map (Fig. 34b) was generated from stacked anomalous zones in areas with overlapping 2D and 3D data coverage and other 2D anomalous zones outside the block. The archaeological prospective zones are in the premises of the recently excavated Pits 1-3, in the area around mounds M1 and M2 and beneath the cement concrete slab (III). This map correlates to a significant extent with the composite resistivity derived composite map (Fig. 33b). The boundaries of the prospective archaeological zones derived from the composite resistivity thematic map was superimposed on the GPR composite thematic map (Fig. 35). There is significant correlation between the two maps with the exception of the area around the cement concrete slab (III). This

reinforces the effectiveness and the complimentary role of both electrical resistivity and GPR

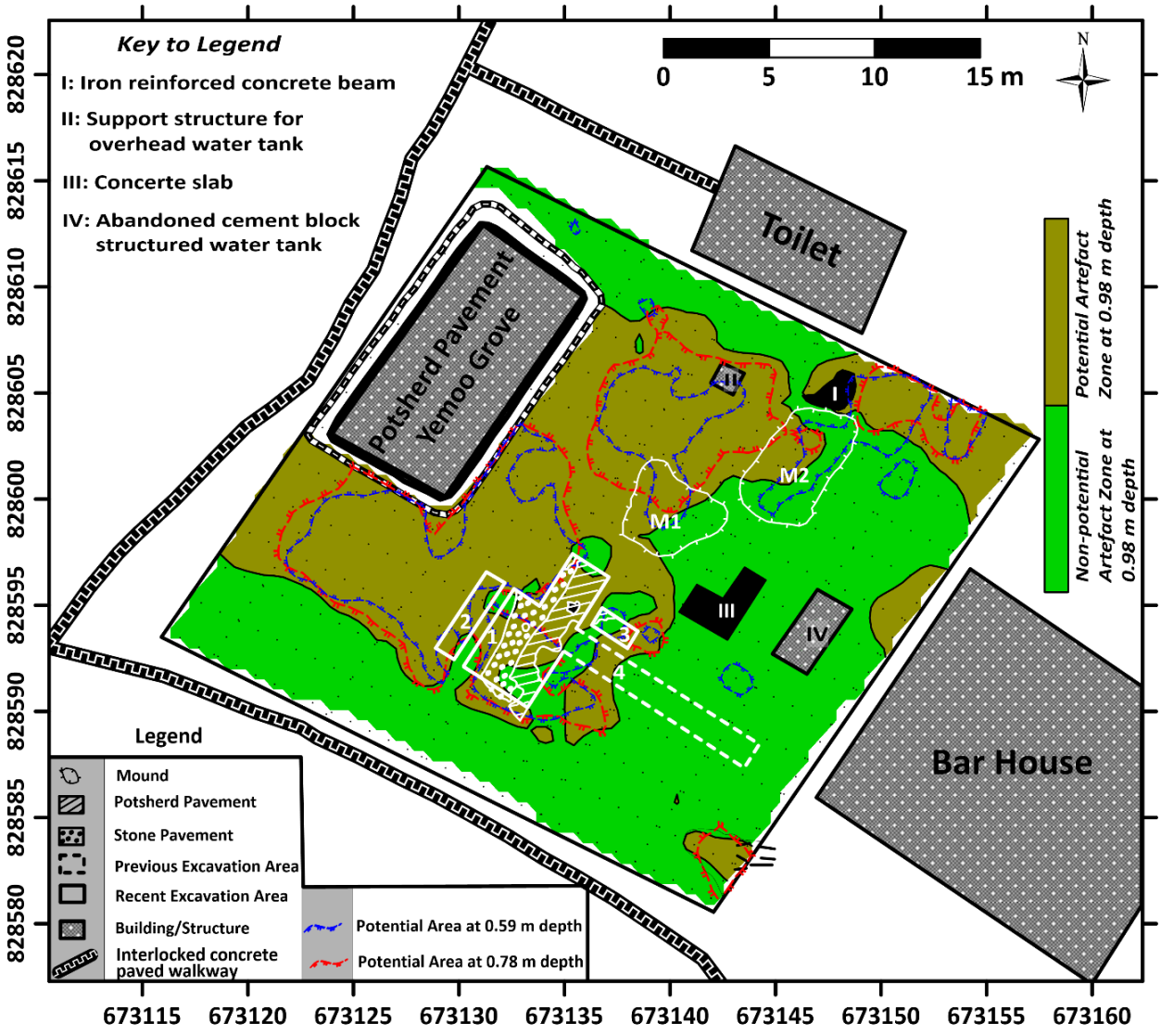

Fig. 33a: Apparent resistivity thematic map at 0.98 m depth level with superimposed shells of corresponding thematic maps at 0.59 m and 0.78 m depths showing archaeological prospective zones

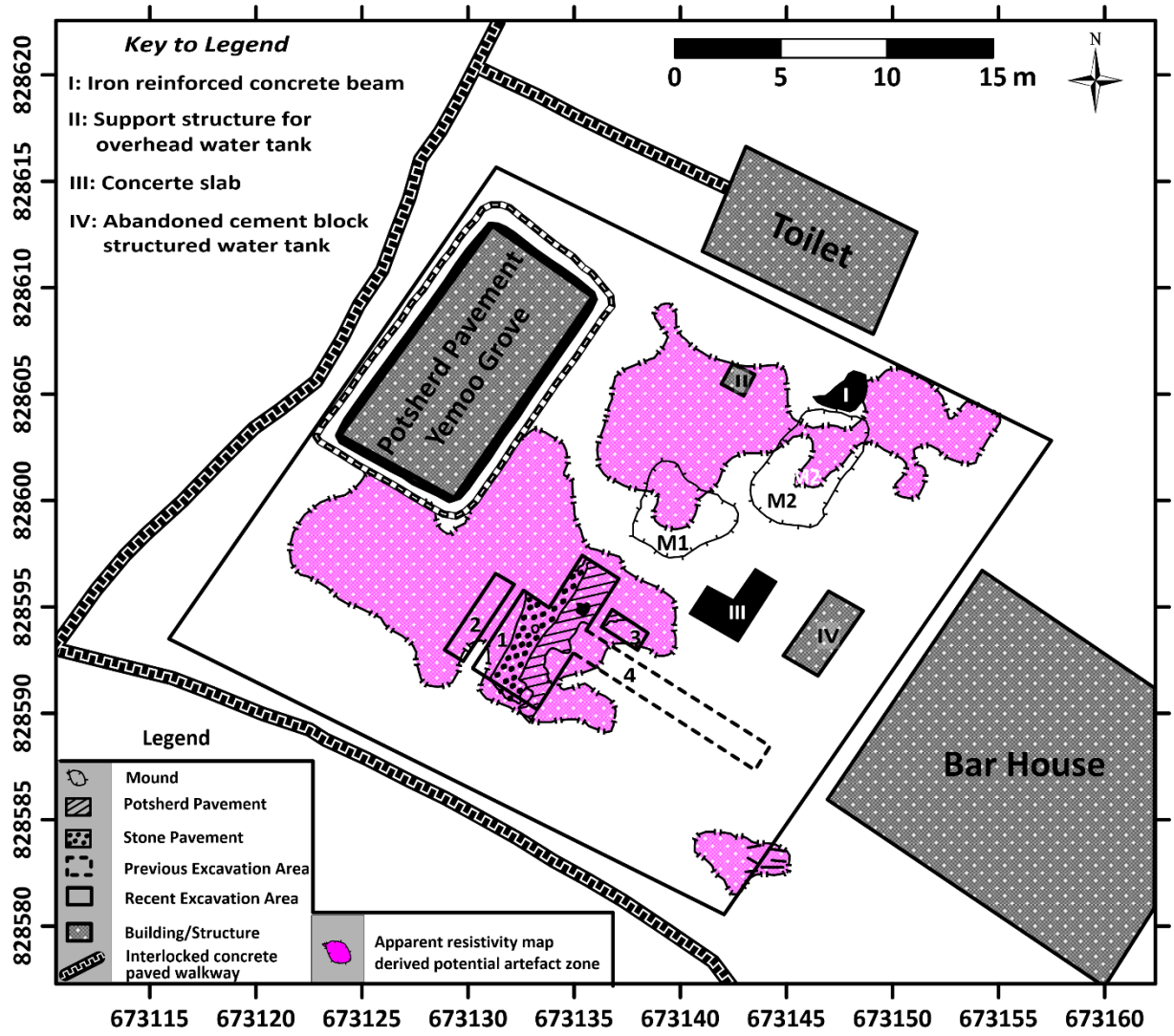

Fig. 33b: Composite apparent resistivity thematic map showing archaeological prospective zones within the study area

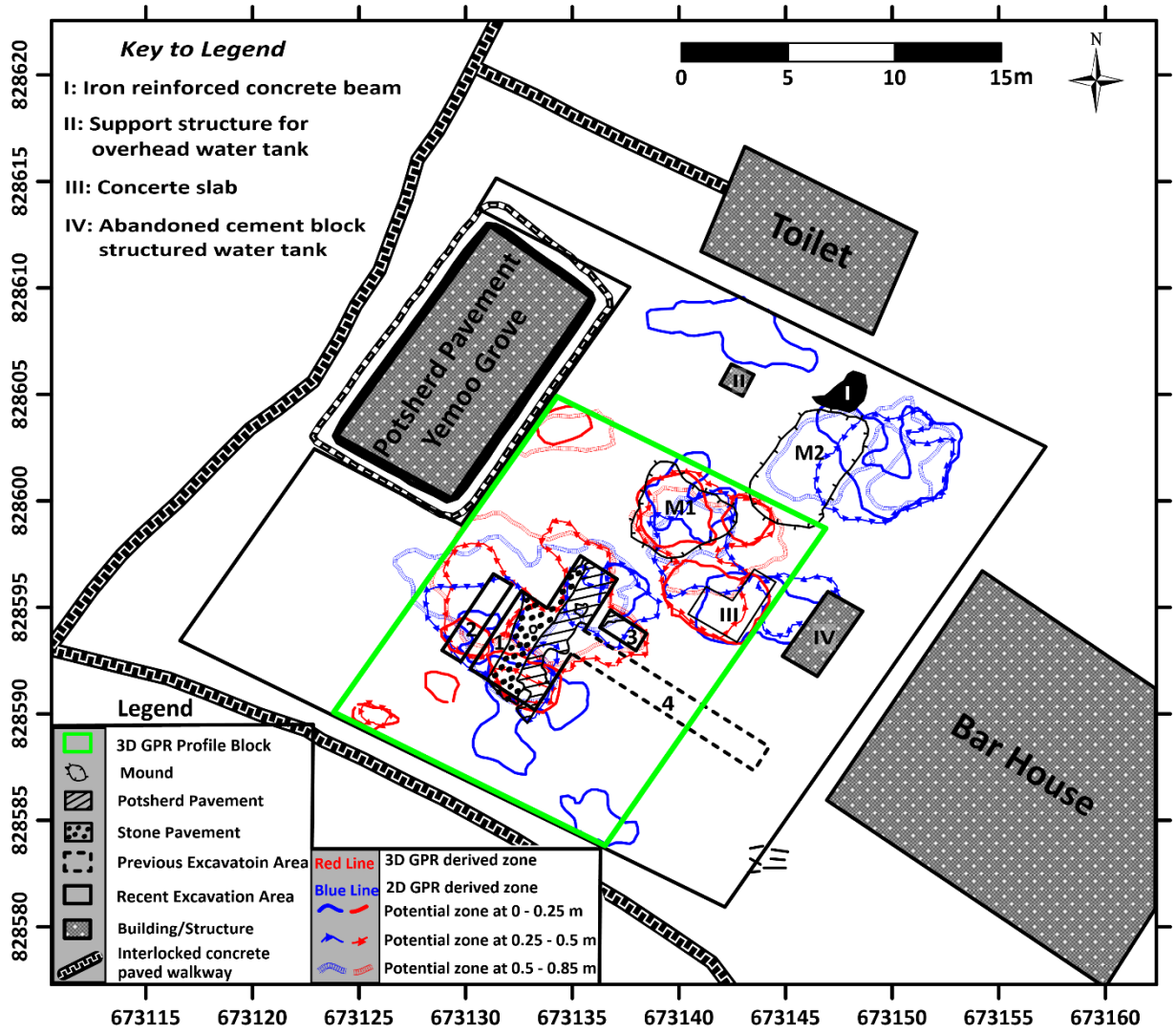

Fig. 34a: Superimposed shells of GPR derived prospective zones at different depth ranges of 0-0.25 m, 0.25-0.50 m and 0.50-0.85 m for 2D and 3D configured data

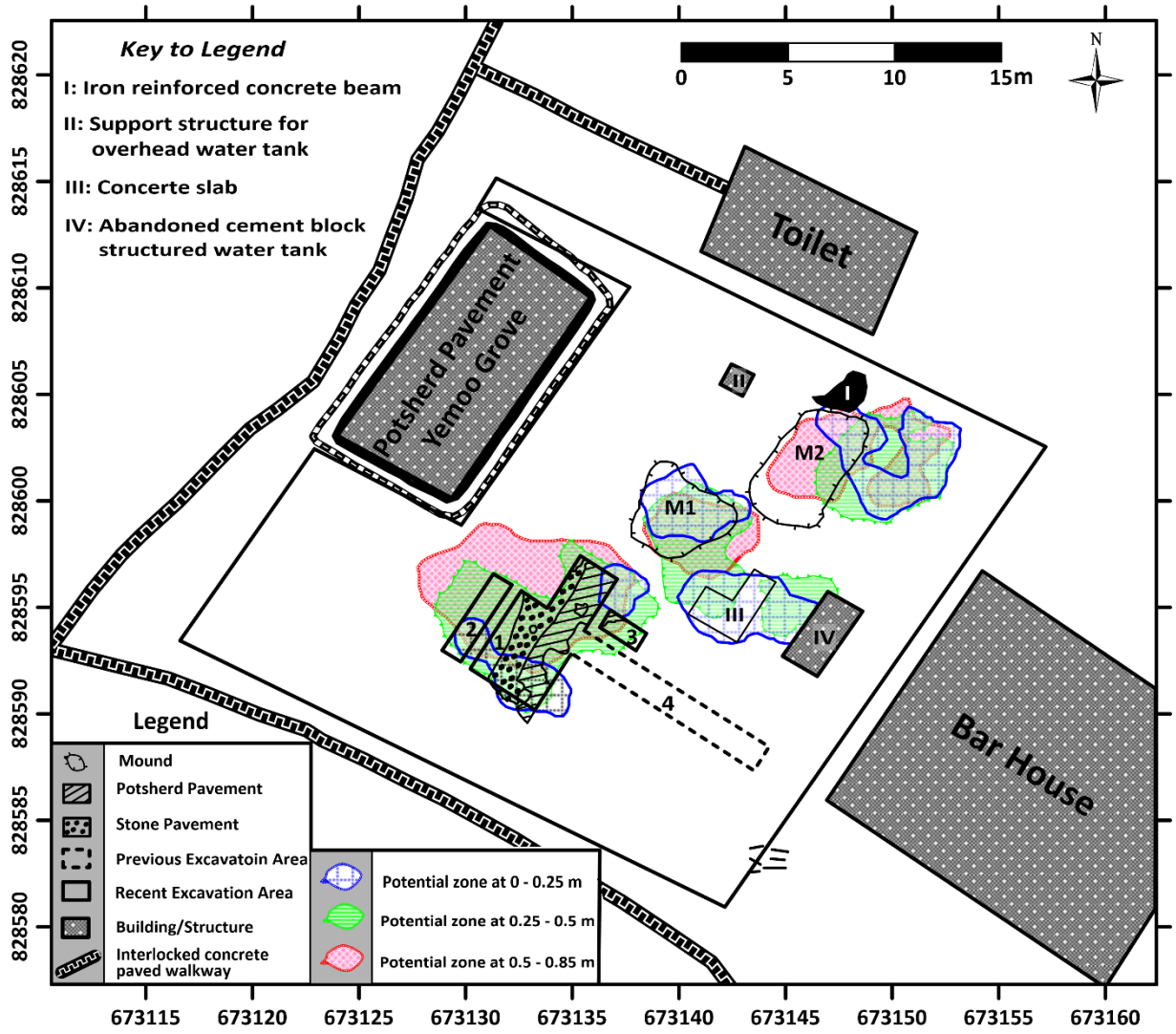

Fig. 34b: Composite GPR thematic map showing archaeological prospective zones at depth ranges of 0-0.25 m, 0.25-0.50 m and 0.50-0.85 m within the study area

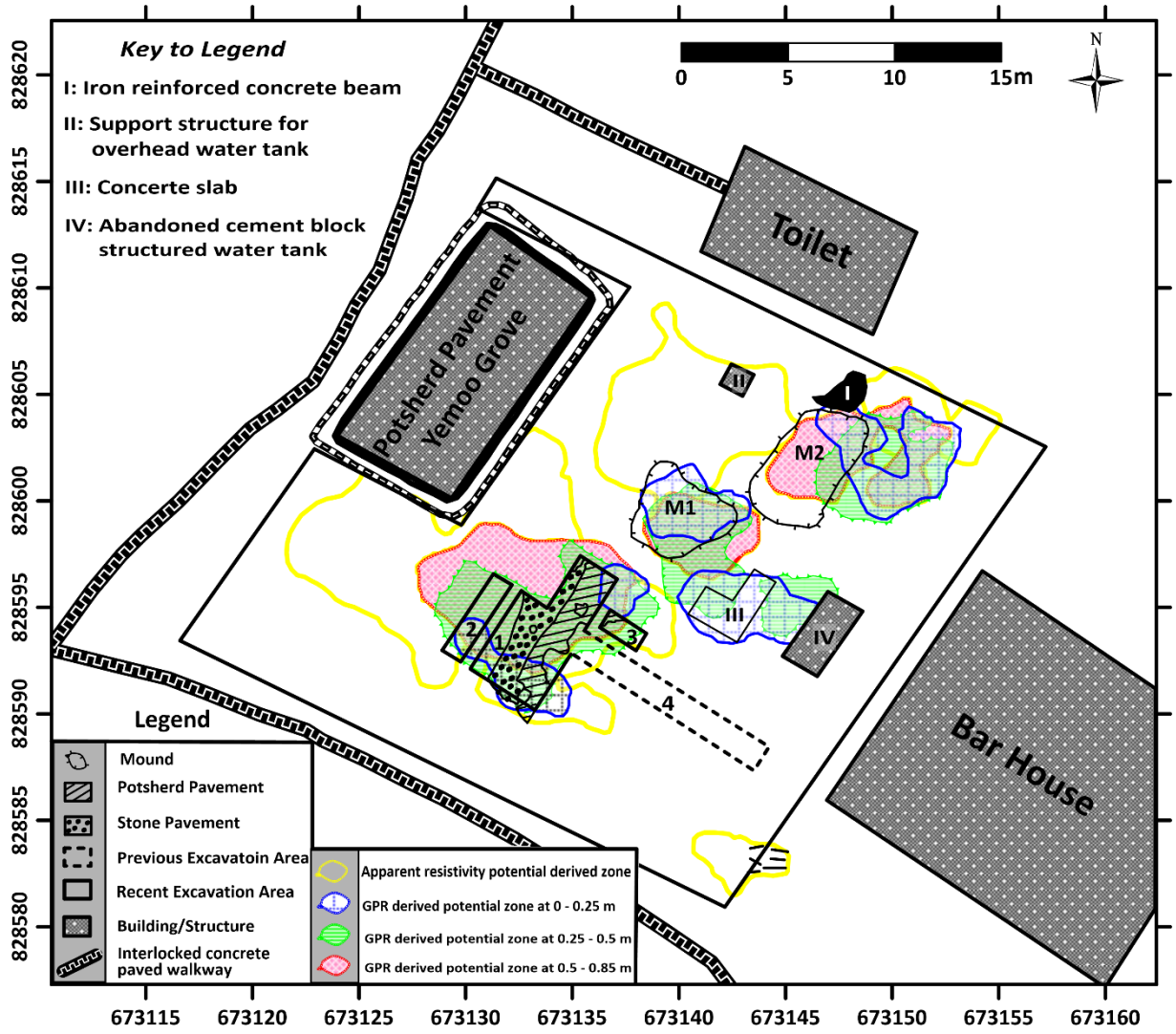

Fig. 35: Superimposed prospective archaeological zones derived from composite GPR and apparent resistivity thematic maps

method in archaeological prospection. Suspected additional archaeological prospective zones were delineated from regions with non-overlapping resistivity using coincident of negative polarity magnetic low zones of the RTE magnetic gradient map (Fig. 13d) (Olorunfemi *et al.*, 2019, Oni *et al.*, 2022 and Olorunfemi *et al.,* 2022) as presented in Figure 36.

Figure 36 shows that prospective archaeological zones are associated with the recently excavated Pits 1-3; the cement concrete slab (III); mounds M1 and M2 and adjoining areas from correlated resistivity and GPR thematic maps. Two other prospective archaeological zones A1 and A2 emerged from correlated coincident resistivity and magnetic thematic maps while zone A3 was developed from correlated resistivity, magnetic and GPR (3D) thematic maps.

The most prominent archaeological zone is associated with the excavated Pits 1-3 with potsherd/stone pavements as the archaeological feature (see Figs. 22a-h). The pavements occur at varying depths from 0 m (ground level) to up to 0.85 m. The presently barren segments of Pit 1 and Pit 2 and Pit 3 with trace of pavement are prospective at deep depths of 0.25 – 0.85 m while the stone pavement extends westward from Pits 1/2.

The prospective zone associated with cement concrete slab (III) displays GPR radargrams with high amplitude radar reflections (see Fig. 22d) typical of pavements. This zone is suspected to host pavements.

The prospective archaeological zones associated with mounds M1 and M2 with its southeastern extension display hyperbolic diffracted radar reflections which are sometimes chaotic (see Figs. 22e; 23a&b). These characteristics are not typical of potsherd/stone pavements but typical of buried archaeological features such as ritual pots, pieces of potsherds, ancient vessels etc. The mounds display relatively high resistivity with coincident negative polarity magnetic intensity which are characteristics of the aforementioned archaeological features.

We are not sure if the referenced mounds are natural or whether they are dumped soil materials excavated from the Yemoo Grove potsherd pavement or excavated soil materials from the old Pit 4. However, the archaeology map (Fig. 36) shows that archaeological features beneath and around the mounds could extend from 0.25 m to about 0.85 m depth level.

Prospective archaeological zones A1 and A2 display no GPR characteristics but show coincident intermediate resistivity and negative polarity magnetic intensity typical of pottery

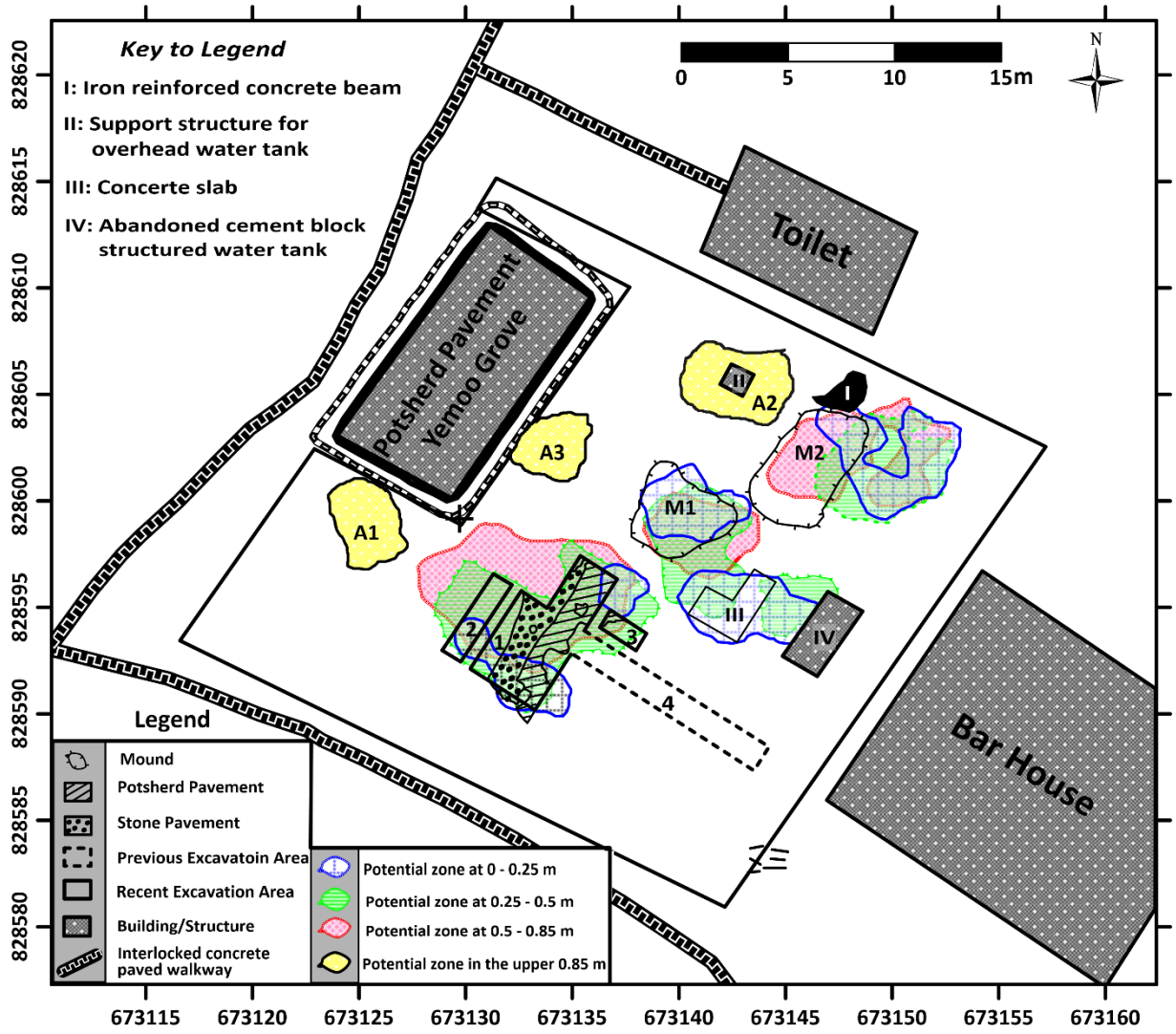

Fig. 36: Archaeological Map of the study area.

related archaeological features. Zone A3 has correlated resistivity, magnetic and GPR attributes which could be indicative of pavement or pottery related artefacts. The depth of archaeological relevance could vary from 0.25 – 0.85 m.

5.0 SUMMARY AND CONCLUSIONS

An integrated geophysical investigation involving the magnetic, electrical resistivity and ground penetrating radar (GPR) methods was carried out within Ita Yemoo archaeological site at Ile-Ife, southwestern Nigeria. This was with a view to assessing the potency of the geophysical methods to individually or collectively identify potsherd/stone pavement and map the spatial distribution of the archaeological feature to guide future excavation and minimize invasiveness. The study area is underlain by pegmatised schist characterised by clay/lateritic clay topsoil overlying a clayey weathered basement.

In order to generate potsherd/stone pavement geophysical characteristics (template) and assess the effectiveness of the geophysical methods adopted to map the archaeological feature and define its geometry, a pilot study was carried out over an outcropping potsherd pavement in front of the Heritage Multipurpose Hall and around a recently excavated portion of the main study area southeast of Yemoo Grove. The outcropping pavement was covered with twenty-one (21) main traverses (with inter-traverse spacing of 1 m) trending in approximately NW-SE direction each 10 m long and four (4) orthogonal traverses to the main traverses each 21 m long with inter-traverse separation of 2 m (Fig. 4). The pilot study at the main survey area engaged nineteen (19) approximately NW-SE trending in-line (main) traverses each 14 m long and fifteen (15) cross-line (orthogonal) traverses each 18 m long with inter-traverse and station interval of 1 m (Fig. 6b). The entire of the main survey area was covered with fourteen (14) main traverses trending NW-SE and ranging in length from 20 - 28 m with inter-traverse spacing of 2 m and station interval of 1 m and six (6) orthogonal traverses with lengths varying from 11-26 m and inter-traverse spacings of 4-6 m with station interval of 1 m. With inter –traverse spacing of 1 m for the GPR survey, the main traverses increased to twenty-seven (27) with orthogonal traverses increasing to seventeen (17) with inter-traverse separation of 2 m (Fig. 6a).

At both the pilot site and the main survey area, total field magnetic data were acquired along all the traverses - main (in-line) and orthogonal (cross-line) at 1 m station interval and at two sensor heights of 2.32 and 1.42 m. The magnetic data sets were corrected for diurnal variation and offset and the magnetic gradient data generated. The magnetic gradient data were subsequently reduced to the magnetic equator (RTE) to center the anomalies on respective causative targets. The RTE map was downward continued to estimate the depth of archaeological significance. The magnetic

data were presented as maps and qualitatively interpreted. The resistivity survey involved 1D and 2D imaging techniques. The 1D Micro Vertical Electrical Sounding (Micro VES) technique adopted the Schlumberger array with half current-current electrode spacing (AB/2) of 0.075 m - 3.0 m and half potential-potential electrode spacing (MN/2) of 0.030 m - 0.25 m. The Micro VES data were presented as VES curves which were quantitatively interpreted and the results presented as geoelectric sections. The 2D imaging, involving the dipole-dipole array, was carried out along main (in-line) and orthogonal (cross-line) traverses with dipole lengths of 0.5 m and 1.0 m and expansion factor (n) varying from 1 to 5. The 2D dipole-dipole data were presented as pseudosections and subsequently inverted into 2D resistivity structures (images) from which true resistivity values were extracted at specific depth range levels for the preparation of resistivity depth slice maps. Apparent resistivity maps were also generated from the raw field data for different expansion factor (n). These maps were interpreted qualitatively for archaeological features. The GPR survey adopted the reflection profiling technique with twin antenna system whose transmitter was operated at 450 MHz and 750 MHz radar frequencies. The GPR data were processed with the MALA Vision GeoGuidline software. The raw data file was imported into the software which in-turn displayed the time-section raw data radargram for each of the profiled lines. Signal enhancing and processing filters including DC offset, De-banding through background (Bg) removal, automatic gain control (AGC) and exponential gain were applied to the raw data. The processed time-section radargrams were analyzed for velocity of propagation of the radar wave to facilitate time-depth radargram conversion. By carrying out interpolation of all the processed 2D radargrams, 3D cube was created from which depth slice maps were generated for spatial delimitation of anomalous radar reflections.

The magnetic method revealed that potsherd/stone pavements are weakly magnetic with intensities overlapping significantly with that of the also weakly magnetic basement derived clayey weathered host materials. The results from the present study show that the pavements are majorly associated with classified intermediate (0 to 15 nT/m (pilot site) and 0 to 40 nT/m (main study area)) magnetic intensities. The archaeological feature was also identified within zones with classified low (0 to -28 nT/m (pilot site) and 0 to -318 nT/m (main study area)) and high (15 to 28 nT/m (pilot site) and 40 to 327 (main study area)) magnetic intensities. In essence, pavements are associated with virtually the entire magnetic spectrum. This limitation does not make the magnetic

method an index geophysical method in pavement mapping. The method however, has its relevance in the estimation of depth of archaeological significance required in field design.

The 1D Micro VES technique of the electrical resistivity method is effective for the mapping of potsherd pavement only at shallow depth, most especially when it outcrops at the surface or located under very thin soil cover when both the layer resistivities (91-244 ohm-m (pilot site)) and thicknesses (0.03-0.04 m (pilot site)) can be effectively estimated. We found estimates of the layer resistivity values useful in the interpretation of 2D resistivity maps. Due to the very thin thicknesses of the pavements, the delineation of the archaeological feature was virtually impossible at depth due to suppression, as experienced at the main study area. This technique has limited application and only where the feature is near-surface or outcropping. The 2D resistivity data were presented as 2D apparent resistivity maps and 2D resistivity depth slice maps. The former are depth specific 2D resistivity maps generated for specific expansion factor (n) and depth while the latter are maps generated for different depth level ranges of the inverted 2D resistivity structures. At the pilot site, the 2D apparent resistivity maps at expansion factors, n=1-3 (at depth levels of 0.29 m, 0.39 m and 0.49 m) delineate the exposed potsherd pavement within resistivity ranges of 80-185 ohm-m, 115-226 ohm-m and 115-220 ohm-m respectively. The equivalent 2D resistivity depth slice maps at depth levels of 0-0.25 m and 0.25-0.50 m delineate the exposed potsherd pavement within resistivity ranges of 55-115 ohm-m and 100-200 ohm-m respectively. These resistivity ranges (most especially those established from the apparent resistivity maps) correlate significantly well with the Micro VES derived resistivity range of 91-244 ohm-m for the exposed pavement. The depth specific 2D apparent resistivity maps were more diagnostic in terms of better definition of the geometry of the exposed potsherd pavement. However, the 2D vertical resistivity images (sections) did not resolve the pavement possibly due to the scale of presentation of the images (the potsherd pavement is very thin – 0.03-0.04 m) or outright suppression.

The GPR radargrams map the planar potsherd/stone pavements as high amplitude, bright coloured (yellow/red) radar reflections and significantly continuous and traceable radar signals characteristic of high dielectric contrasting feature. The radargrams also enabled estimation of pavement depths of occurrence and lateral extent. In this regard, the GPR radargrams are superior to 2D resistivity vertical images (sections). The depth specific 2D GPR depth slice maps were also effective in directly mapping the pavements (within the excavated portion of the main survey area)

and establishing the spatial distribution within and outside the excavated area. The GPR method however, has the limitation of shallow depth of investigation. Strong GPR signals were rarely recorded at depths greater than 1.0 m except for diffracted signals. Resistivity images were still very diagnostic far beyond this threshold depth for the GPR. For this study though, the effective depth of archaeological relevance is about 1 m.

Based on the results from this study, the GPR method is the most potent geophysical method for pavement mapping at relatively shallow depth (of up to 1.0 m or there about) using radargrams and depth slice maps attributes. The electrical resistivity method is next in potency using 2D dipole-dipole data derived and depth specific 2D apparent resistivity maps as diagnostic attributes. This method has the limitation of suppression of the archaeological feature due to its thin nature and overlapping resistivity values with the host materials. The 1D Micro VES has very limited but useful application in the estimation of pavement resistivities and thicknesses of outcropping pavements. These geoelectrical parameters are needed to constrain the interpretation of both 2D resistivity sections and maps. The magnetic method has the least potency because of the overlapping magnetic effects of the weakly magnetic potsherd/stone pavement and the equally weakly magnetic weathered basement derived host materials. The method is however useful in the estimation of depth of archaeological relevance which is needed in field design.

With the benefit of the above, we would also observe as follows that:

(i)The planar nature of the potsherd/stone pavement demands depth specific (not depth range) geophysical attributes for its delineation. The mapping of pavements is essentially an interface problem.

(ii)For potsherd/stone pavement to be effectively mapped, some background information on its characteristic features such as thickness, resistivity range, depth(s) of occurrence, the environment of existence and the subsurface stratigraphy are useful for field design and to constrain interpretation of geophysical attributes.

(iii)While this study rates the GPR method highest in potency followed by the resistivity method and the magnetic method as the least potent in potsherd/stone pavement mapping, there is always the need to integrate several relevant geophysical methods if ambiguities associated with

individual geophysical method are to be minimized or resolved and the quality of results and subsequent prediction are to be enhanced.

An archaeological map (Fig. 36) was developed for the study area from stacked composite apparent resistivity and GPR derived archaeological prospect maps. The composite resistivity thematic map was developed from stacked prospect maps at depth levels of 0.59 m, 0.78 m and 0.98 m while the composite GPR thematic map was generated from stacked prospect maps at depth ranges of 0 – 0.25 m, 0.25 – 0.50 m and 0.50 – 0.85 m.

Prospective archaeological zones are associated with the recently excavated Pits 1-3; the cement concrete slab (III); mounds M1 and M2 and adjoining areas from correlated resistivity and GPR thematic maps. Two other prospective archaeological zones A1 and A2 emerged from correlated coincident resistivity and magnetic thematic maps while zone A3 was developed from correlated resistivity, magnetic and GPR (3D) thematic maps.

The most prominent archaeological zone is associated with the excavated Pits 1-3 with potsherd/stone pavements as the archaeological feature (see Figs. 22a-h). The pavements occur at varying depths from 0 m (ground level) to up to 0.85 m. The presently barren segments of Pit 1 and Pit 2 and Pit 3 with trace of pavement are prospective at deep depths of 0.25 – 0.85 m while the stone pavement extends westward from Pits 1/2.

The prospective zone associated with cement concrete slab (III) displays GPR radargrams with high amplitude radar reflections (see Fig. 22d) typical of pavements. This zone is suspected to host pavements.

The prospective archaeological zones associated with mounds M1 and M2 with its southeastern extension display hyperbolic diffracted radar reflections which are sometimes chaotic (see Figs. 22e; 23a&b). These characteristics are not typical of potsherd/stone pavements but typical of buried archaeological features such as ritual pots, pieces of potsherds, ancient vessels etc. The mounds display relatively high resistivity with coincident negative polarity magnetic intensity which are characteristics of the aforementioned archaeological features.

We are not sure if the referenced mounds are natural or whether they are dumped soil materials excavated from the Yemoo Grove potsherd pavement or excavated soil materials from the old Pit

4. However, the archaeology map (Fig. 36) shows that archaeological features beneath and around the mounds could extend from 0.25 m to about 0.85 m depth level.

Prospective archaeological zones A1 and A2 display no GPR characteristics but show coincident intermediate resistivity and negative polarity magnetic intensity typical of pottery related archaeological features. Zone A3 has correlated resistivity, magnetic and GPR attributes which could be indicative of pavement or pottery related artefacts. The depth of archaeological relevance could vary from 0.25 – 0.85 m.

6.0 LIST OF REFERENCES

Adeyemo, A.A., Ezema, I.C., Adeyemi, E.A. and Anakor, C.A. (2021) Reviewing sustainability, preservation and semiotics of potsherd pavements in southwest Nigerian cultural spaces and built-forms. *IOP Conf. Series: Materials Science and Engineering* 1036012027. Doi: 10. 1088/1757-899 X/1036/1/012027.

Agbaje-Williams, B. (1995) Archaeological investigation of Itagunnodi Potsherd Pavement Site, Ijesaland, Osun State, Nigeria. *1991/92 IFRA Publication*, Institute of African Studies, University of Ibadan, Ibadan.

Aguigah, A. (1995) Pavement et terres damees les regions du Golfe du Benin: enquete archeologique et historique (*Doctoral dissertation, Paris 1)*

Al-Khalidy, A.A. and Kadhum, A.N. (2018) Application of ground penetrating radar to determine the subsurface features of the project of Shams Al-Shmoos hotel building in Al-Najaf Al-Ashraf, Iraq. *Int. Journal of Civil Engineering and Technology (IJCIET),* 9(6), 17-24. http://www.iaeme.com/IJCIET/index.asp

Archie, G.E. (1942) The electrical resistivity log as an aid in determining some reservoir characteristics. *Trans. Am. Inst. Mining Met. Eng*., 146, 54-62.

Chouin, G.L. and Ogunfolakan, A.B. (2015) Ife-Sungbo Archaeological Project. Prelimenary report on excavations at Ita yemoo, Ile Ife, Osun State and on rapid assessment of earthwork sites at Eredo and Ilara-Epe, Lagos State, June – July, 2015. *Technical Report.*

Eyo, E. (1974) Recent excavations at Ife and Owo and their implications for Ife, Owo and Benin studies. *PhD thesis*, University of Ibadan, Ibadan.

Fadare, T.K., Oni, A.G., Olorunfemi, M.O. and Ogunfolakan, B.A. (2020) Geoelectric characterisation of Igbo Oritaa archaeological site, Iwo, southwestern Nigeria. *Pacific Journal of Science and Technology (PJST),* 21(1), 333-344. http//www.akamaiuniversity.us/PJST.htm

Fagan, B.M. and Durrani, N. (2014) In the beginning: *An Introduction to Archaeology* (13th Edition) Routlegde Talyor and Francis Group., pp.141.

Hui, L. and Haitao, M. (2011) Application of ground penetrating radar in dam body detection. Procedia Engineering, 26 (2011), 1820 – 1826.

Ige, O.A. Ogunfolakan, B.A. and Ajayi, E.O.B. (2009) Chemical characterisation of some potsherd pavements from parts of Yorubaland in southwestern Nigeria. *Journal of Archaeological Science* 36(1), 90 – 99. Doi. 10. 1016/j.jas. 2008. 07.014.

Iloeje, N.P. (1981) *A new geography of Nigeria*. New Revised Edition. Academy Press Ltd., Lagos Nigeria.

Jol, H.M. and Bristow, C.S. (2003) GPR in sediments: advice on data collection, basic processing and interpretation, a good practice guide. In Ground penetrating radar in sediments. Bristow, C.S. and Jol, H.M. (eds). *Geological Society: London, Special Publication*. 211, 9-28.

Leute, U (1987) Archaeometry: *An introduction to Physical methods in Archaeology and the history of Art.* Velt Publishers, New York.

Liritzis, I. Laskaris, N. Vafiadou, A. Karapanagiotis, I, Volonakis, P. Papageorgopoulou, C. and Bratitsi, M. (2020) Archaeometry: An overview. *Scientific Culture*, 6(1), 49 – 98. DOI. 10. 5281/zenodo, 3625 220

Ogundiran, A. (2000) Potsherd Pavements in Ilare-Ijesa, Yorubaland: A regional perspective. *NYAME AKUMA*, 53, 35 - 41

Ogunfolakan, B. (1994) Archaeological Survey of Osun North-East Osun State, Nigeria. *M.Sc. Dissertation,* University of Ibadan, Ibadan.

Olorunfemi, M.O., Ogunfolakan, B.A. and Oni, A.G. (2019) Geophysical and archaeology survey in Igbo Oritaa (Iwo), southwest Nigeria. *African Archaeological Review* (Springer Publication), 36(4), 535-552. https://doi.org/10.1007/s10437-019-09357-7.

Olorunfemi, M.O., Oni, A.G. and Fadare T.K. (2022) Geoelectric characterisation of furnace and slag trench structures: case study Obafemi Awolowo University ancient iron smelting site, Ile-Ife, Southwest Nigeria, *NRIAG Journal of Astronomy and Geophysics*, 11:1, 1-20, DOI: 10.1080/20909977.2021.2020999.

Oni, A.G., Olorunfemi, M.O., Ogunfolakan, B.A. and Okunnubi, M.O. (2022) Archaeo-geophysical investigation of Ife City Ground Resort Iron Smelting Site at Ile-Ife, Southwest Nigeria. *Journal of African Archaeology* (2022), 1-15. DOI:10.1163/21915784 – BJA10010.

Orijemie, E.A. and Ogiogwa, J.M.I. (2016) Potsherd Pavements in Ope-Odu, Ibadan. Autochthonous or migrant phenomenon? NYAME *AKUMA*, 85, 104 – 113.

Powell, A.J., McDonnell, J.G., Batt, C.M., and Vernon, R.W. (2002) An assessment of the magnetic response of an iron-smelting site. Department of Archaeological Sciences, University of Bradford, Bradford BD7 1DP, UK. *Archaeometry* 44(4), 651-665.

Reynolds, J. M. (1997) *An introduction to applied and environmental geophysics*. John Wiley & sons, New York.

Robson, M., Bristoco, C., Mc Kinley, J. and Ruffell, A. (2013) Ground penetrating radar. *Geomorphological Techniques, Part 1,* sec. 5.5 (2013), 1-26 (British Society for Geomorphology) ISSN 2047 – 0327.

Roth, L., Chouin, G. and Ogunfolakan, A. (2011) Lost in Space? Reconstructing Frank Willet's excavations at Ita-Yemoo, Ile-Ife, Nigeria: Rescue Excavation (1957-1958) and Trench XIV (1962-1963) *Afrique Archaeologic Arts*, Vol 17/2021 pp. 77-114. https:/doi.org/10.4000/aaa.3328

Roy, A. and Apparao, A. (1971) Depth of investigation of direct current methods. *Geophysics,* 36, 943-959.

Sharma, P.V. (1997) *Environmental and Engineering geophysics* Cambridge University Press

Siyanbola, A. (1988) Archaeological investigation of Imesi-Ile, Obokun Local Government Area, Ijesaland. *B.A. Thesis*, Obafemi Awolowo University, Ile-Ife.

Szalai, S., Novak, A. and Szarka, L. (2014) Depth of investigation and vertical resolution of surface geoelectric arrays. *Journal of Environmental and Engineering Geophysics*. https://www.researchgate.net/publication /250377643

Telford, M.W., Geldart, L.P., Sheriff, R.E and Keys, D.A. (1990) *Applied Geophysics*. 2nd Edition, Cambridge University Press. 214.

Turner, D.C. (1989) Upper Protozoic schist belts in the Nigerian sector of the Pan-African Province of west Africa. *In Geology of Nigeria*. Edited by C.A. Kogbe (Second Edition). Rock View (Nig.) Ltd., Jos Nigeria. Pp 93-109.

Willett, F. (1959) Bronze and Terra-cotta Sculptures from Ita-Yemoo, Ife. The South African *Archaeological Bulletin,* 14 (56): 135-137

Willett, F. (1967) *Ife in the History of West African Sculpture*, London. Thames and Hudson.

Willett., (2004) The Art of Ife: A descriptive catalogue and database. *COROM,* University of Glasgow.

Zeng., X. and Mc Mechan, G. A. (1997) GPR Characterisation of buried tanks and pipes. *Geophysics*, 62 (3), 797-806